

X-625-65-47

NASA TM X-55479

# TRAVELING WAVE TUBE DEVELOPMENT FOR A SERRODYNE RE-ENTRANT AMPLIFIER

N66 26851

FACILITY FORM 602

(ACCESSION NUMBER)

74

(PAGES)

TMX-55479

(NASA CR OR TMX OR AD NUMBER)

(THRU)

1

(CODE)

09

(CATEGORY)

APRIL 1965

GPO PRICE \$ \_\_\_\_\_

CFSTI PRICE(S) \$ \_\_\_\_\_

Hard copy (HC) 3.00

Microfiche (MF) .75

FF 653 July 65



GODDARD SPACE FLIGHT CENTER  
GREENBELT, MARYLAND

207-38810

X-625-65-47

TRAVELING WAVE TUBE DEVELOPMENT  
FOR A SERRODYNE RE-ENTRANT AMPLIFIER

by

Louis J. Ippolito  
Walter K. Allen  
Clay Prillaman

April 1965

Goddard Space Flight Center  
Greenbelt, Maryland

TRAVELING WAVE TUBE DEVELOPMENT  
FOR A SERRODYNE RE-ENTRANT AMPLIFIER

PREFACE

A NASA/Goddard Space Flight Center supporting research task entitled, "Direct RF to RF Converters for Communications Satellites" required the study of various transponder schemes for directly converting one microwave frequency to another in connection with providing the necessary signal amplification. Re-entrant traveling wave tube amplifier schemes can be used to effect the frequency conversion and amplification. In one scheme by driving the helix of the traveling wave tube (TWT) with a sawtooth wave form a frequency shift of the input signal can be effected along with amplification. The amount of frequency shift is equivalent to the sawtooth wave frequency. This is known as "serrodyning." By coupling the output signal back through the TWT additional shift and gain can be had. This document presents the results of a contractual endeavor with the Microwave Electronics Corporation (MEC), Palo Alto, California, to study and develop an optimum TWT for use in a serrodyne re-entrant amplifier. Enclosed in this document is the text of the final report of work done under this contract, NAS 5-3443. The final report was prepared by MEC and covers work done by them from June 26, 1963 to November 31, 1964. The final report is presented in its entirety and includes corrections and clarification where found necessary.

The final section of this document includes comments by the sponsoring GSFC personnel on the test of the MEC report and on the results of the investigation.

This document concludes the serrodyne amplifier phase of the GSFC Direct RF to RF study program.

# CONTENTS

	<u>Page</u>
SECTION I – TEXT OF MEC FINAL REPORT .....	1
1.1 INTRODUCTION .....	1
1.1.1 Purpose .....	1
1.1.2 Original Serrodyne TWT Specifications .....	1
1.1.3 Serrodyne Techniques .....	2
1.1.4 Sideband Suppression Analyses .....	3
1.1.5 TWT Mixer Frequency Shifter .....	4
1.2 SERRODYNE TWT .....	5
1.2.1 Serrodyne Modulation of the TWT .....	5
1.2.2 Basic Serrodyne Drift-Tube TWT Approach .....	5
1.2.3 Modes of Serrodyne Action .....	7
1.2.4 Traveling-Wave Tube Parameters .....	8
1.2.5 Design Parameters of the Drift Tube Serrodyne TWT .....	8
1.2.6 Vacuum Envelope .....	9
1.2.7 Package Approach .....	11
1.2.8 Serrodyne TWT RF Characteristics .....	13
1.2.9 Sawtooth-Wave Synthesis by Harmonic Summation .....	16
1.2.10 Experimental Tests: Two Frequencies to Gun .....	18
1.2.11 Experimental Tests: Three Frequencies to Gun .....	24
1.2.12 Experimental Tests: Three Frequencies to Helices and Drift Tube .....	24
1.2.13 Experimental Tests: Re-entrant Circuit .....	24
1.3 TWT MIXER FOR WIDE RANGE FREQUENCY SHIFTS .....	32
1.3.1 Introduction .....	32
1.3.2 The Mixer TWT .....	35
1.3.3 Experimental Tests: 6 to 4 Gc Mixer .....	36
1.3.4 General Aspect of Mixer Operation .....	42

Contents (Continued)

	<u>Page</u>
1.4 APPENDIX I – THEORETICAL STUDIES – TWO-FREQUENCY MODULATOR . . . . .	43
1.5 APPENDIX II – TRAVELING WAVE AMPLIFIER TEST METHODS . . . . .	58
1.6 APPENDIX III – RE-ENTRANT AMPLIFIER TEST METHODS . . . . .	63
SECTION 2 – GSFC COMMENTS . . . . .	67
2.1 NOTES ON TEXT OF THE MEC REPORT . . . . .	67
2.2 SUMMARY OF RESULTS OF MEC STUDY PROGRAM . . . . .	68
2.3 REVIEW OF THE RE-ENTRANT SERRODYNE TWT COMMUNICATIONS SATELLITE TRANSPONDER . . . . .	70
2.4 REFERENCES . . . . .	74

## LIST OF ILLUSTRATIONS

<u>Figure</u>		<u>Page</u>
1	Traveling wave phase modulator amplifier . . . . .	6
2	Typical MEC metal-ceramic vacuum envelope . . . . .	9
3	Serrodyne traveling-wave tube . . . . .	10
4	Helix assembly with continuous wrap tie-wires . . . . .	11
5	Basic mechanical configuration . . . . .	12
6	Traveling-wave tube/vacuum envelope . . . . .	13
7	TWT package and serrodyne circuit console . . . . .	14
8	Input VSWR versus frequency . . . . .	15
9	Output VSWR versus frequency . . . . .	16
10	Small-signal gain versus frequency . . . . .	17
11	Saturated output power versus frequency . . . . .	17
12	Change in phase versus helix voltage . . . . .	18
13	Change in phase versus input power . . . . .	19
14	Block diagram of multiple frequency modulator with independent control over signal levels . . . . .	19
15	Output waveform of three-frequency modulator . . . . .	20
16	Amplitude of $M_1$ as a function of the fundamental modula- tion voltage amplitude with no second harmonic present . . . . .	20
17	Amplitude of $M_1$ as a function of the fundamental modula- tion voltage amplitude with 5.1 volts of the second harmonic present . . . . .	21
18	Amplitude of $M_1$ as a function of the fundamental modula- tion voltage amplitude with 10.2 volts of the second harmonic present . . . . .	21
19	Spectral display of sidebands when TWT is modulated with 30 Mc waveform . . . . .	23

List of Illustrations (Continued)

<u>Figure</u>		<u>Page</u>
20	Spectrum display of TWT output; (a) modulated TWT output and (b) serrodyne TWT output showing the $f_0$ , $f_{-1}$ and $f_{-2}$ sidebands . . . . .	25
21	Alternate modulation system . . . . .	26
22	Carrier and 2nd sideband suppression versus input power . .	27
23	Spectral display of sidebands where $f_0 = 6$ Gc and $f_1$ and $f_2$ are 6030 and 6060 Gc, respectively . . . . .	28
24	Sideband and carrier output versus carrier input with open loop and optimized for equal sideband and carrier rejection VE D, Serial 7 . . . . .	29
25	Re-entrant amplifier test setup . . . . .	30
26	Sideband and carrier output versus carrier input with closed loop . . . . .	31
27	Output power at 6 Gc versus input power at 5.94 Gc using 3 filters . . . . .	32
28	Output pulse of re-entrant amplifier with re-entrant loop open and closed . . . . .	33
29	Trailing and leading edge of pulse on an expanded scale . . .	34
30	Detail of electron gun and helix structure of the three-helix mixer . . . . .	35
31	TWT mixer tube test setup . . . . .	37
32	Mixer output power (@ 4 Gc) as a function of LO power (@ 10 Gc) for a signal input power (@ 6 Gc) of -30 dbm . . . .	37
33	Output power at 4 Gc for input of 6 Gc . . . . .	38
34	Output power at 3.9 Gc for input of 6.5 Gc . . . . .	39
35	Output power at 5.5 Gc for input of 4.5 Gc . . . . .	40
36	Output power at 4.5 Gc for input of 5.5 Gc . . . . .	41

List of Illustrations (Continued)

<u>Figure</u>		<u>Page</u>
I-1	Zeros of $M_0$ and $M_2$ as a function of R with A as a parameter, and the value of A leading to a maximum value for $M_1$ at each value of R . . . . .	50
I-2	Expanded plot of $M_0$ , $M_2$ and the maximum values of $M_1$ . . .	51
I-3	Zeros of $M_0$ and $M_2$ as a function of R and A with $B = -2$ , and the maximum value of $M_1$ for each value of R and A . . . .	52
I-4	Zeros of $M_0$ and $M_2$ as a function of R and A with $B = -1$ , and the maximum value of $M_1$ for each value of R and A . . . .	53
I-5	Zeros of $M_0$ and $M_2$ as a function of R and A with $B = 0$ and the maximum value of $M_1$ for each value of R and A . . . . .	54
I-6	Zeros of $M_0$ and $M_2$ as a function of R and A with $B = 1$ and the maximum value of $M_1$ for each value of R and A . . . . .	55
I-7	Zeros of $M_0$ and $M_2$ as a function of R and A with $B = 2$ and the maximum value of $M_1$ for each value of R and A . . . . .	56
I-8	Computed values of $M_1$ for values of R and A with $B = 2.0$ . .	57
I-9	Computed values of $M_1$ for values of R and A with $B = -2.0$ . .	57
II-1	VSWR test setup . . . . .	59
II-2	Saturated power output test setup . . . . .	59
II-3	Test setup for measuring small-signal gain . . . . .	59
II-4	Setup for measuring TWT phase characteristics . . . . .	60
II-5	Setup for measuring noise figure (automatic) . . . . .	60
II-6	Noise figure measurement setup ("Y factor" method) . . . . .	61
II-7	Gain and suppression test setup . . . . .	62
III-1	Re-entrant amplifier gain measurement setup . . . . .	63
III-2	Setup for measuring echo effects . . . . .	64
III-3	FM to AM distortion measurement block diagram . . . . .	64
III-4	Test setup to measure noise figure . . . . .	65
III-5	Intermodulation distortion test setup . . . . .	66



List of Illustrations (Continued)

<u>Figure</u>		<u>Page</u>
2.2.1	Summary of serrodyne techniques . . . . .	69
2.2.2	Performance characteristics of delivered serrodyne traveling wave tube . . . . .	70
2.2.3	Serrodyne output versus input characteristics for delivered TWT serrodyne system . . . . .	71
2.3.1	Frequency translation satellite transponder . . . . .	72
2.3.2	Serrodyned re-entrant TWT amplifier . . . . .	73

TRAVELING WAVE TUBE DEVELOPMENT  
FOR A SERRODYNE RE-ENTRANT AMPLIFIER

ABSTRACT

Program objectives were to study serrodyne techniques and determine TWT characteristics to incorporate in serrodyne re-entrant amplifiers. Investigations included the upper limit of serrodyning, optimum modulation methods and the necessary sawtooth generator circuits. Tube properties studied were amplifier intermodulation, noise figure, and over-all design for optimum re-entrant amplifier characteristics.

Sawtooth generation and use for TWT modulation is difficult at rf frequencies. Instead, the fundamental and the second and third harmonics of a sawtooth waveform may be combined and used to modulate the TWT drift tube.<sup>G1</sup> This simplifies the generation problem but modulation becomes difficult due to drift-tube pole-piece capacitance. While this capacitance can be reduced by a factor of four, waveform amplitude is decreased when coupled to the TWT. Also, waveform distortion is encountered when its amplitude is varied after initial tuning.

The most practical technique is to modulate the input and output helices and the drift tube separately. This uses the TWT as a mixer for all three harmonic frequencies with the input signal. By properly adjusting modulation-frequency amplitude and phase, frequency shift is obtained with carrier and sidebands down 16 db with respect to the desired output frequency.

Theoretical studies show that infinite carrier and sideband suppression may be obtained with three modulation-voltage amplitudes having approximately 7:1:1 ratios, the first number denoting the fundamental and the second and third representing second and third harmonic amplitudes. Translation loss is about 5.4 db, indicating the presence of other sidebands not considered. Other ratios give superior suppression, but translation loss always exceeds 5.4 db.

In practical experiments, three-frequency modulation was applied as described, the fundamental (30 Mc) to the drift tube and 60 Mc and 90 Mc to the input and output helix. Three-element modulation was necessary due to waveform distortion and amplitude reduction that arose when trying to modulate the

---

G1—See Section 2.1, Notes on Text of MEC Report.

drift tube along with the three frequencies combined. Carrier and second-sideband suppression below the desired sideband were measured at 18 and 20 db, respectively. Modulation-voltage amplitudes were 34:5:5, close to those determined theoretically. When the re-entrant loop was closed, the desired sideband was translated and underwent 14 db of gain. Analysis showed that lower conversion loss would be obtained with three-than with two-frequency modulation, the decrease in loss being calculated at 4 db, and this was verified experimentally.

Finally, a TWT mixer was fabricated to achieve larger frequency translations, consisting of an input helix centered at 6 Gc, an intermediate helix with local-oscillator input at 10 Gc, and an output helix optimized for operation at the cross-product frequency of 4 Gc. Data are given for different combinations of frequency, to determine bandwidth and output linearity. At the optimum operating point, input-signal gain was 10 db at the new output frequency. This is another approach to achieving large frequency shifts.

**SECTION I**

**Text of the Final Report of a Study Entitled**

**A TRAVELING-WAVE TUBE FOR A SERRODYNE  
RE-ENTRANT AMPLIFIER**

**Submitted December 1964**

**to**

**Goddard Space Flight Center**

**Covering work done June 26, 1963 to November 30, 1964**

**under contract NAS 5-3443**

**by**

**Microwave Electronics Corporation**

**3165 Porter Drive**

**Palo Alto, California**

**The contents of the MEC final report were prepared by Messrs. N. Berger, R. DeGrasse, G. Foggiato, J. Hansen, and J. Tangney and approved by C. L. Cussia, Director of Research and Engineering.**

# TRAVELING WAVE TUBE DEVELOPMENT FOR A SERRODYNE RE-ENTRANT AMPLIFIER

## 1.1 INTRODUCTION

### 1.1.1 Purpose

The purpose of this program is to investigate methods of using the traveling-wave tube for frequency translation, with particular emphasis upon serrodyning, pointed toward applications in re-entrant amplifier systems.

The scope of the investigation has included investigating serrodyning the traveling-wave tube from many avenues including:

- drift tube phase modulation in the TWT
- sawtooth excitation of the electron gun structure
- forming a quasi-sawtooth wave by a number of harmonically related frequencies, and
- modulating different TWT sections with harmonics of the serrodyning voltage.

In the final program phase, a traveling-wave tube mixer, using three helix sections for input, local oscillator and output frequency signals respectively, demonstrated the feasibility of frequency shifts of 2000 Mc without attendant spurious signals and amplitude modulation.

### 1.1.2 Original Serrodyne TWT Specifications

The serrodyne TWT effort on this program has been directed toward the following specifications:

1. The TWT was to be serrodyne modulated with a linear sawtooth drive adjustable to obtain approximately  $360^\circ$  change of phase in the transit time delay of the TWT.
2. Optimized input carrier signal rejection – at least 30 db plus the tube gain.

3. Intermodulation distortion was to be minimized for an intelligence bandwidth of 20 Mc.
4. The contractor was to determine
  - The optimum method of driving the TWT's (helix or electron gun)
  - The upper frequency at which linear serrodyne is practical.
5. The contractor was to consider the following criteria for the serrodyne amplifier and TWT.
  - Frequency: The amplifier was to operate at a frequency near 6 Gc.
  - Bandwidth: The optimum intelligence bandwidth was to be determined by the contractor with a minimum of 20 Mc.
  - Gain: The gain was to be the maximum practical, with a minimum of 30 db.
  - Noise: The noise figure was to be optimum.

#### 1.1.3 Serrodyne Techniques

Serrodyne techniques included establishing the upper frequency limit of linear serrodyne mode, optimum modulation methods and sawtooth generator circuits. The TWT properties to be investigated were intermodulation in the amplifier, noise figure and design required to give optimum re-entrant amplifier characteristics.

The generation of a sawtooth, and using it to modulate a TWT, is difficult at RF frequencies. Problems associated with the generator were reduction of flyback time and obtaining a linear sawtooth slope. Since at 30 Mc, external capacitances of common vacuum tubes increase the flyback time, a very high power modulator would be required to produce the sawtooth wave; however, the problem of building the modulator would probably exceed that of the TWT. A Fourier Synthesis approach was taken which combined the fundamental 30 Mc wave with the second (60 Mc) and third (90 Mc) harmonics to form a sawtooth waveform to modulate the TWT's drift tube. With the correct amplitude and phase relationships, a reasonably linear sawtooth could be generated, but the flyback time was approximately 30 percent. Difficulties were encountered in acquiring the optimum phase relationships since the phase change was accomplished by detuning a tuned circuit with a consequential amplitude change.

The three harmonic approach simplified the generation problem, but modulating the TWT became difficult due to drift-tube pole piece capacitance. Distortion was introduced in the wave form shape and the amplitude was reduced. Flyback time was increased, but with proper retuning, it could be reduced to 30 percent.

To reduce the sawtooth flyback time, an approach was discussed whereby a Gaussian pulse would be applied to the TWT grid. By synchronizing the pulse with the trailing edge of a positive slope sawtooth, the TWT beam current would be cut off, thus reducing sawtooth flyback time.

Other pulse shapes; i.e., rectangular and delta; will contribute many sideband components. In the Gaussian pulse spectrum, however, the sidebands are reduced by  $\exp - (f/f_1)^2$  as compared, for example, to the reduction as the inverse of frequency which is characteristic of a rectangular pulse.

Due to the difficulties encountered in modulating the TWT drift tube with the sawtooth, a new technique was devised whereby each TWT element, i.e., the input helix, output helix and drift tube, would be modulated by one sawtooth harmonic. The method incorporates the TWT as a mixer for all three harmonics of the serrodyne frequencies with the input signal. By proper adjustment of amplitude and phase of the modulation frequencies, a frequency shift was obtained, resulting with the sidebands and carrier down 16 db in intensity with respect to the desired output frequency.

#### 1.1.4 Sideband Suppression Analysis

Theoretical studies described in Appendix I indicated that infinite carrier and sideband suppression may be obtained with three modulation voltages whose amplitudes were in the approximate ratio of 7:1:1; the first number denoting the fundamental, and the second and third representing the amplitudes of the second and third harmonic. Translation loss was approximately 5.4 db, thus indicating that some other sidebands may be present that were not considered. Other amplitude ratios gave large carrier and sideband suppressions, but the translation loss in each case exceeded 5.4 db. Analysis showed that less conversion loss could be obtained with three-frequency than with two-frequency modulation, the decrease in loss being 4 db.

The two-frequency theoretical analysis was verified with experimental data obtained when operating the TWT in the serrodyne mode. Agreement within 3 db was found. This was considered acceptable, considering that the analysis did not

take into account generation of lower and upper sidebands. "Nulls" and "peaks" occurred almost exactly as theory predicted, some discrepancies occurring due to measurements and test equipment instability.

Three-frequency modulation was investigated by applying the fundamental (30 Mc) to the drift tube and 60 Mc and 90 Mc to the input and output helix respectively. Modulating the three elements was necessary due to the difficulties of waveform distortion and amplitude reduction encountered when trying to modulate the drift tube alone with a combination of the three frequencies. Carrier suppression of 18 db was experienced with the second sideband 20 db below the desired sideband. Respective modulation voltage amplitudes were 34 volts for the fundamental and 5 volts for both first and second harmonic. These amplitudes agreed closely with those predicted theoretically. In order to utilize the TWT to obtain twice the small-signal gain, a re-entrant loop may be utilized. In this application, the input signal is amplified and shifted in frequency and then re-directed into the TWT for further amplification and another frequency shift. Preliminary tests, with an open loop, were made to optimize sideband suppression and shifted carrier amplitude. When the re-entrant loop was closed, the desired sideband was translated again and underwent a 14-db gain, this being the calculated system gain.

Limitations imposed by modulation techniques and RF sawtooth generation were found to restrict serrodyning the TWT to small frequency shifts. Sideband and carrier suppression are insufficient with this method of frequency shift for practical utilization in a re-entrant amplifier system. However, better modulation techniques and further study in coupling the modulation waveforms to the TWT could yield a practical system where translation losses are approximately 8 to 10 db and carrier and sideband suppression is 30 db or more.

#### 1.1.5 TWT Mixer Frequency Shifter

As a final experiment, a TWT mixer tube was fabricated to achieve larger frequency translations. The TWT mixer included an input helix centered at 6 Gc, an intermediate helix with a local oscillator input at 10 Gc and an output helix optimized for operation at the cross-product frequency of 4 Gc.

Significant characteristics noted were output linearity with respect to the input signal, and the wide bandwidth obtained. With the one tube fabricated, gains of 10 db were achieved. Optimum helix design could increase the gain to at least 30 db, the gain being a function of the output helix length, depending on the manner in which mixing takes place. This mixer seems a very feasible method of frequency translation both from the standpoint of large frequency shifts and wide bandwidth available.



## 1.2 SERRODYNE TWT

### 1.2.1 Serrodyne Modulation of the TWT

The transit time delay of a TWT is nearly a linear function of the voltage impressed on the helix. If the helix dc voltage is modulated with a signal, the TWT effectively phase modulates the RF signal carrier. When the modulating signal is a sine wave, the resultant RF signal has many sidebands—both positive and negative. When the modulation amplitude is adjusted for a phase deviation of  $2.4$  radians, the carrier disappears and all of the energy is in the sidebands. This technique is called synchrodying.

If the modulating signal is a linear sawtooth adjusted to deviate the phase  $2\pi$  radians, all the sidebands and the carrier are suppressed except one of the first sidebands. The sawtooth slope determines which sideband (+ or -) remains. This is serrodyning and is effectively termed single sideband, suppressed carrier. Sideband deviation equals the fundamental frequency of the modulating sawtooth signal. If the modulating sawtooth amplitude were increased so as to increase the phase deviation to  $4\pi$  radians, the sideband deviation would be twice the fundamental of the modulating sawtooth. In general terms, if the modulation deviates the phase by  $2N\pi$  radians, then the sideband is displaced  $N$  times the fundamental modulation frequency.

The degree of carrier and unwanted sideband suppression is affected by the flyback time and linearity of the sawtooth, as well as certain helix characteristics.

One problem that arises from this type of modulation is intermodulation distortion. Intermodulation distortion is due to nonlinear TWT gain which to some extent is a function of the helix voltage. The greater the helix voltage deviation, the greater will be the nonlinearity and therefore the greater will be the intermodulation distortion. For this reason, a serrodyne system limited to  $2\pi$  radians of phase deviation only will be considered throughout the remainder of this technical discussion.

### 1.2.2 Basic Serrodyne Drift-Tube TWT Approach

The basic structure of the traveling-wave tube developed on this program for serrodyne action is shown in Figure 1. The traveling-wave amplifier shown includes an electron gun projecting an electron beam through an input helix. The RF signal applied to this helix is transferred to the beam and is amplified to a prescribed level.

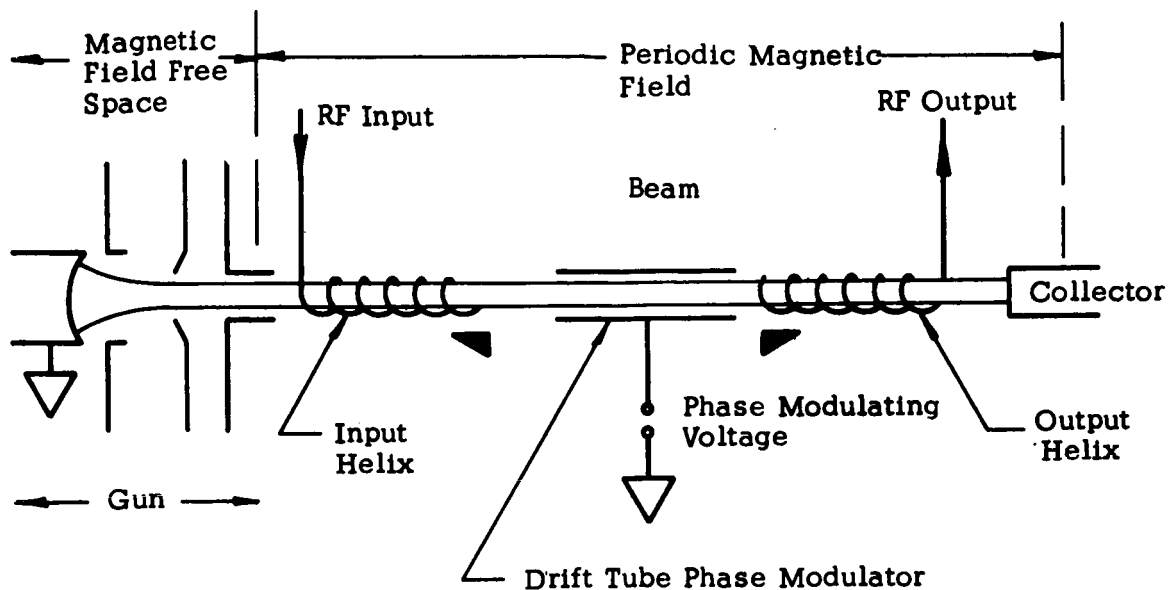


Figure 1—Traveling wave phase modulator amplifier.

The beam is then passed through the drift tube wherein it is either accelerated or slowed depending upon the drift-tube voltage, resulting in phase or transit time beam control. The beam, upon leaving the drift tube, is passed through the output helix where the amplified and the phase controlled signal is amplified to its final gain level. The amplified signal then passes through the RF output region. The beam then passes to the collector. A convergent-flow gun, compatible with required power levels, is shown.

Since the TWT gain is proportional to the inverse of helix voltage, modulation of the helix introduces AM. Thus, the advantages of a traveling-wave phase shifter using drift-tube modulation, as compared with a helix-voltage serrodyne TWT which undergoes changes in power output, are listed as follows:

- Small size, high efficiency capability
- Phase shift easily obtained using a nonintegrating electrode
- Broadband modulation
- Phase modulation anywhere in octave frequency band without any device readjustment or tuning
- Negligible amplitude modulation during phase modulation
- Power output capability
- Excellent crosstalk suppression

The approximate relationship between the phase shift  $\Delta\phi$ , produced by a drift tube voltage change  $\Delta V$ , is given by

$$1 + \frac{\Delta V}{\phi_d} = \left(1 + \frac{\Delta V}{V_d}\right)^{-1/2} \quad (1)$$

where  $\phi_d$  is the static phase through the drift tube at the static drift tube voltage  $V_d$ .

That is,

$$\phi_d = \frac{2\pi fL}{\sqrt{2\eta V_d}} \text{ radians,} \quad (2)$$

where  $f$  is the operating frequency,  $L$  is the drift tube length, and  $\eta$  is the electron charge-to-mass ratio.

The phase shift is seen to be a linear function of length and frequency and to vary inversely as the square root of the drift-tube voltage. The drift-tube voltage variation required to produce a given phase shift is, of course, smaller as the drift-tube length is increased. Maximum allowable voltage swing will be limited by beam defocusing. The drift-tube diameter can be made much larger than the helix diameter so that no beam current is intercepted by the drift tube. The modulation power required is then only that necessary to drive the capacitance between the drift tube and the TWT magnetic focusing structure.

### 1.2.3 Modes of Serrodyne Action

Three modes of serrodyning employed included:

- Sawtooth modulation of the gun structure including cathode, grid and anode.
- Sawtooth modulation of the drift tube— the sawtooth voltage formed by the summation of a 30 Mc sinusoidal signal and properly phased harmonics.
- Quasi-sawtooth modulation of the slow-wave structure by the simultaneous application of a 30-Mc sinusoidal signal to the drift tube a second harmonic 60 Mc signal to the input helix and the third harmonic 90 Mc signal to the output helix.

These modes, the experimental apparatus, and experimental results will conclude the discussion of this section.

#### 1.2.4 Traveling-Wave Tube Parameters

Two basic parameters dictated the TWT design as follows. The system defined by NASA required the TWT gain to be 30 db (re-entrant gain at 60 db) and the output of the serrodyne TWT to drive a power amplifier having 30-db gain and 33-dbm output, thereby defining the power output of the serrodyne TWT at the desired sideband at 1 milliwatt. <sup>G2</sup>

Tests on an MEC M2203 C-band 10-milliwatt serrodyne TWT have shown the translation loss to the desired sideband to be around 5 to 7 db, and for 25-Mc bandwidth and a frequency shift of 30 Mc, the level of suppression of the undesired second sideband, as compared to the desired first sideband, is 55 db. The degree of carrier and sideband rejection is independent of TWT output power when the input power is less than  $P_s$  minus 20 db ( $P_s$  being defined as the input power where the relation  $G_{ss} P_s = P_{o(sat)}$  is true;  $G_{ss}$  is the small-signal gain and  $P_{o(sat)}$  is output power at saturation).

For a 1-milliwatt output at the desired sideband, and a second-sideband suppression of 55 db, and a tube gain of 30 db the TWT saturated output power should be 33 dbm. Anticipating a 3-db increase in conversion gain with the improvement of modulation techniques, a tube with a minimum of 1-watt output is identified.

#### 1.2.5 Design Parameters of the Drift Tube Serrodyne TWT

The following operating parameters were chosen for the serrodyne TWT.

Helix Voltage	1200 volts
Cathode Current	6 ma
Saturated Power Output	1 watt
Anode Voltage	500 volts (approximately)
Peak-to-Peak Modulation Voltage	±20 volts for ±180 degrees

By applying conventional traveling-wave-tube design formulation to the input and output helices and the drift tube, the following design parameters were established based on the above basic operating parameters.

Input Helix:	Length	2.1 inches
	Diameter	0.056 inch
	TPI	113
	$\gamma a$	1.3 at 6 Gc
	$d\phi_{H1}/dV$	2.35 degrees/volt
Drift Tube:	Length	8.5 inches
	Hole Diameter	0.056 inch
	$d\phi_d/dV$	6.25 degrees/volt
Output Helix:	Length	3.5 inches
	Diameter	0.056 inch
	TPI	113
	$\gamma a$	1.3 at 6 Gc
	$d\phi_{H2}/dV$	3.9 degrees/volt

### 1.2.6 Vacuum Envelope

Microwave Electronics Corporation's metal-ceramic approach to vacuum envelope construction lends itself to constructing a tube having, as the slow-wave structure, the input helix, drift tube, and output helix in cascade, each element operable at a different dc voltage, and with direct connection RF connections through the vacuum envelope to the two sections, through metal-ceramic windows.

Figure 2 shows a cutaway of a typical MEC vacuum envelope whose constructional principals are applied to the vacuum envelopes built in this program. Figure 3 shows the external constructional features of the vacuum envelope of the drift tube serrodyne TWT indicating the various sections involved and the isolating ceramics.

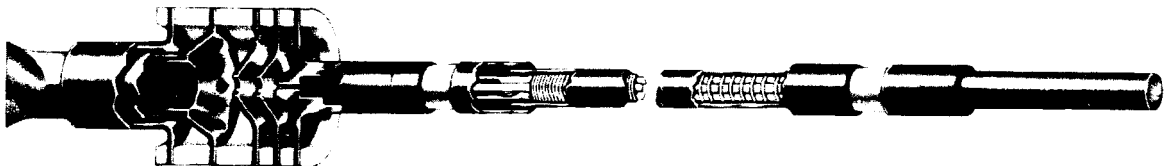


Figure 2—Typical MEC metal-ceramic vacuum envelope.

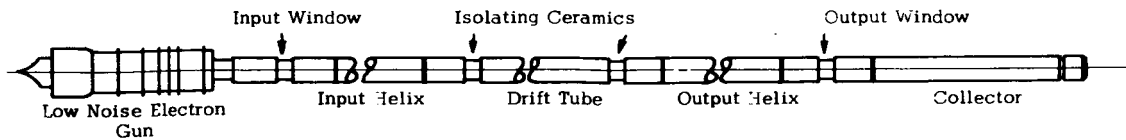


Figure 3—Serrodyne traveling-wave tube.

High-alumina ceramic, stainless steel, monel, and copper are used in the vacuum envelope of Figure 2. Use of metal and high-temperature ceramic yields parts and assemblies reproducible to critical mechanical tolerances. These materials provide a rugged TWT that can be processed at high temperature and that can operate in high-ambient-temperature environments with minimum performance degradation. Use of stacked metal-ceramic construction makes inclusion of the drift tube a relatively simple helix barrel modification.

Stacked gun construction shown in Figure 2 provides a very rugged assembly. No gun elements are mounted on leads from a stem, where they could move under vibration or shock. Connecting leads to the gun are spot-welded to the electrode discs and potted to the gun to prevent movement. All gun parts are vacuum fired before stacking and brazing. The stacked-gun braze is performed in a vacuum atmosphere so that all gun subassembly parts have been subjected to two complete 1000°C vacuum outgassing cycles.

RF energy is coupled to the helix by way of pins installed in cylindrical ceramic windows. This gives minimum parts and maximum design simplicity within the vacuum envelope and permits a highly reliable, non-critical vacuum seal to be used.

The helix sections involve helices supported by three ceramic rods which in turn are installed in tight tie-wire wrap as shown in Figure 4. This construction gives excellent pitch accuracy and freedom from movement under vibration and shock. The helix and ceramic-rod assembly are handled as a unit before installation in the metal envelope, are measured optically and electrically, are vacuum and hydrogen processed, and have pyrolytic carbon attenuation applied before installation in the tube.

A magnetically shielded, convergent-flow gun is used to provide the required 6 ma with reduced emission density at low cathode temperature and low heater power. A passive cathode base nickel is carefully processed in hydrogen and vacuum to eliminate impurities. Cathode processing on exhaust, with the tube body at high temperature, is used to effectively eliminate thermal design of the cathode support structure, suitable heat shielding, and a cathode operating temperature below 750°C was used to minimize heater power and assure good tube life.



**Figure 4—Helix assembly with continuous wrap tie-wires.**

Preprocessing and bakeout used on the vacuum envelope are similar to those employed in high-power microwave tubes. All parts within the vacuum envelope were vacuum baked at 1000°C at least once before assembly and exhaust. Finished tubes were baked under vacuum at 625°C, and the cathodes activated while at this temperature. Ion pumping at exhaust eliminated oil-vapor contamination and, in combination with high temperature processing, contributed stable emission, reduction of spurious modulation and satisfactory operating life.

#### **1.2.7 Package Approach**

The vacuum envelope of Figure 3 was installed with periodic field permanent magnet focus structure over the helix and drift tube sections and a magnetic shield over the electron gun, in a package 18.5 inches long and 1 inch in diameter. Figure 5 is a cross-sectional diagram showing focus structure detail, vacuum envelope installation and the RF and DC connections to the vacuum envelope.

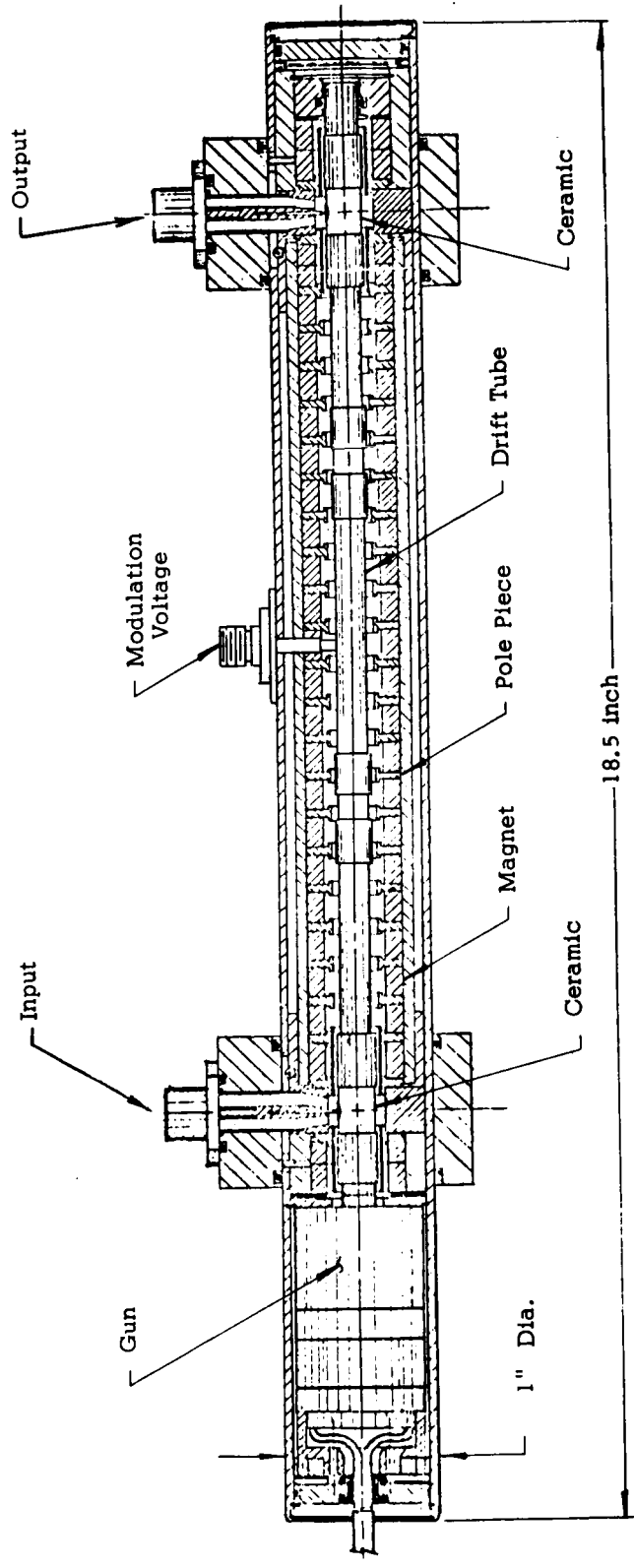


Figure 5—Basic mechanical configuration.



Figure 6 shows the completed TWT package, and Figure 7 shows the TWT package and serrodyne circuit console.

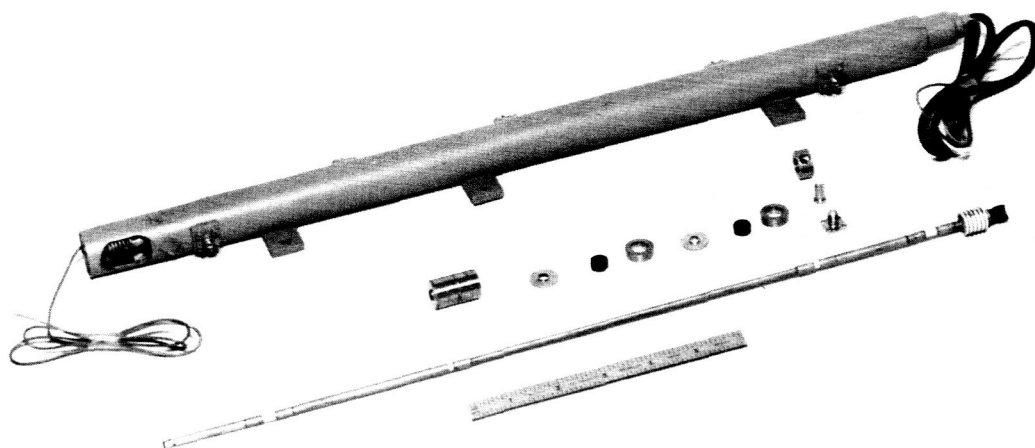


Figure 6—Traveling-wave tube/vacuum envelope.

Problems encountered with the TWT were associated with focusing such a long tube. Being a PPM-focusing structure, the input helix magnetic field has to be tapered properly since a convergent flow electron gun was used. Also, drift tube current interception was very sensitive to helix voltage since the beam tends to scallop. This was due to the multiple IF couplers used to couple the IF modulation frequencies on the respective TWT elements. These introduced transverse magnetic fields causing the electron beam to deviate from a linear path.

The TWT package and circuit console of Figure 7 are the units delivered to NASA at the end of the program; this system employs the serrodyne mode whereby the fundamental, second and third harmonics of the serrodyne frequency (30 Mc) are applied respectively to the drift tube, input helix, and output helix.

#### 1.2.8 Serrodyne TWT RF Characteristics

Four tubes designated A, B, C, and D were fabricated in RF tests made using the techniques identified in Appendix I. The first tube, A, had limited saturated output power because the output helix was short; thus, the second tube, B, had a longer output helix to increase saturated output power. Two tubes, vacuum envelopes C and D, were fabricated using the drift tube designed to reduce the capsule-to-drift tube capacitance. Match and gain characteristics of vacuum envelope C showed an output VSWR of 3.0:1 and gain variation of 4 db from 5.5 Gc to 6.5 Gc. Vacuum Envelope D was chosen as the delivery tube since its over-all characteristics were the best.

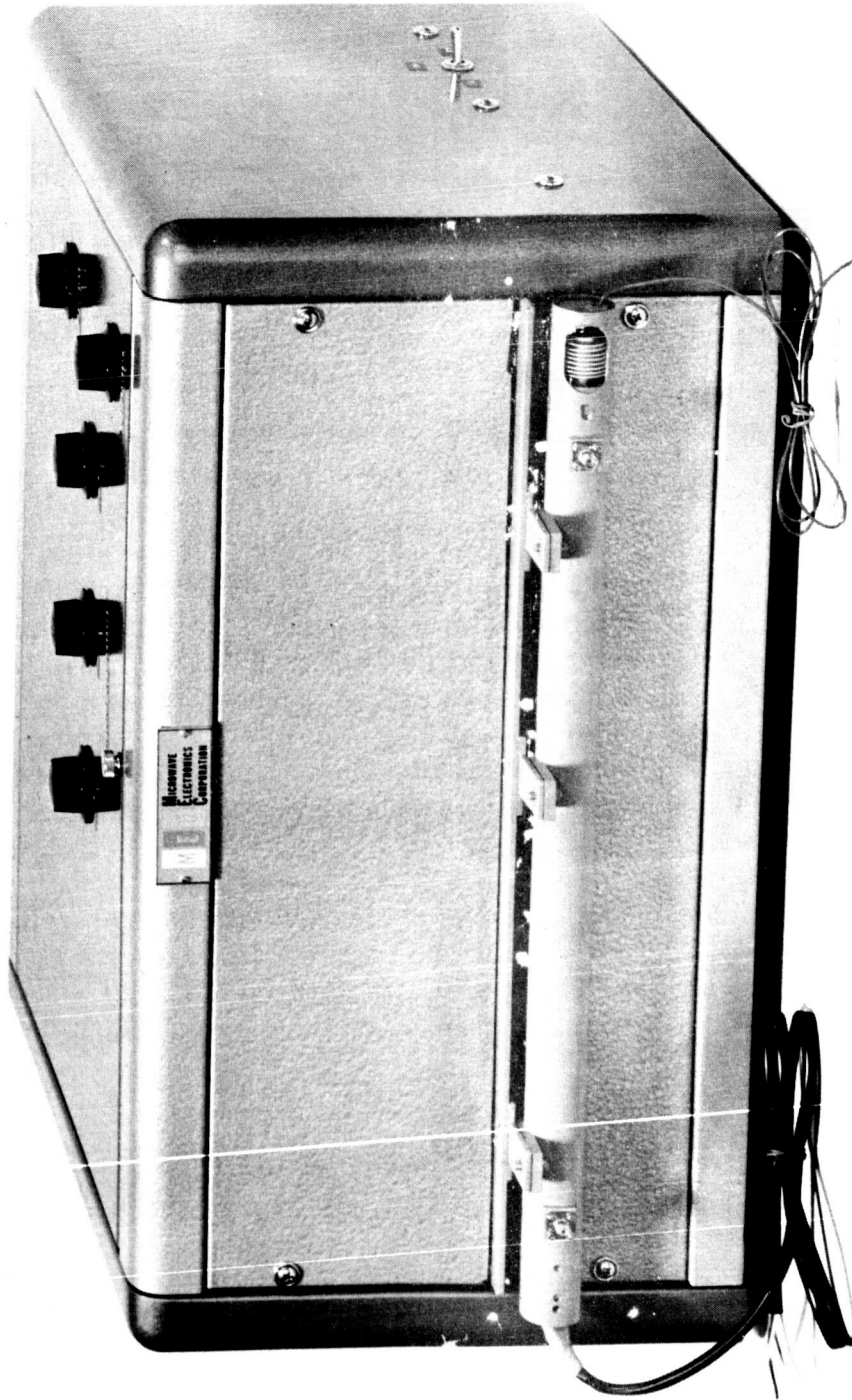


Figure 7 - TWT package and serrodyne circuit console.

Input and output VSWR versus frequency for Envelope C are shown in Figures 8 and 9, respectively. The output match is good and does not exceed 1.5:1 over the band of interest. Small-signal gain characteristics are shown in Figure 10, the gain at 6.0 Gc being 29 db. Note the gradual slope at 6.0 Gc, indicating slight FM to AM distortion; a frequency deviation of 145 Mc results in an amplitude change of 2 db, thus giving distortion of 0.41 db per 30 Mc. The saturated power output versus frequency characteristics are shown in Figure 11. Saturated power output has a 2-db variation from 5.5 to 6.5 Gc.

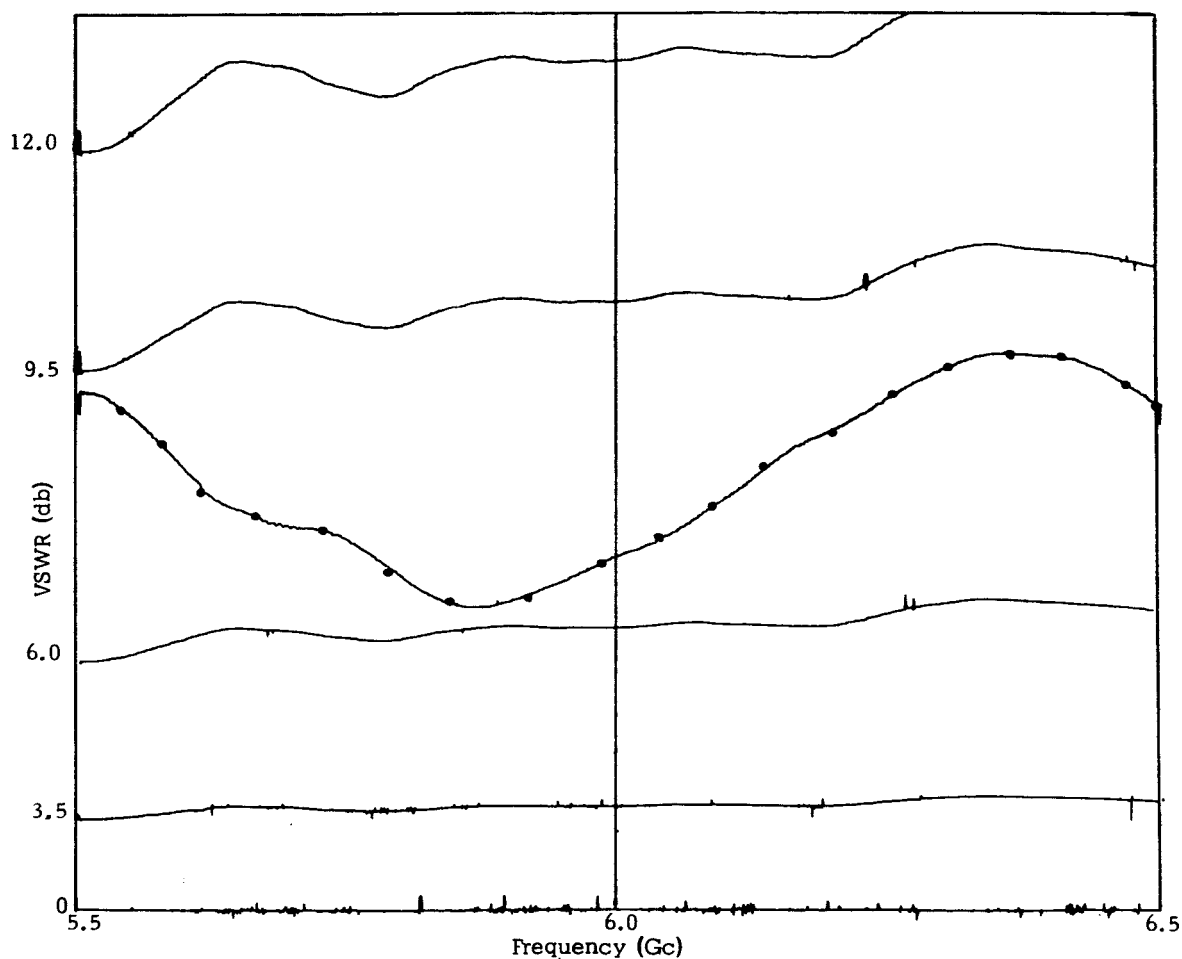


Figure 8—Input VSWR versus frequency.

Other data were taken to determine the TWT phase characteristics and the AM to FM distortion. Figure 12 shows phase change versus helix voltage change, the voltage change being referenced to the synchronous voltage. The slope of the

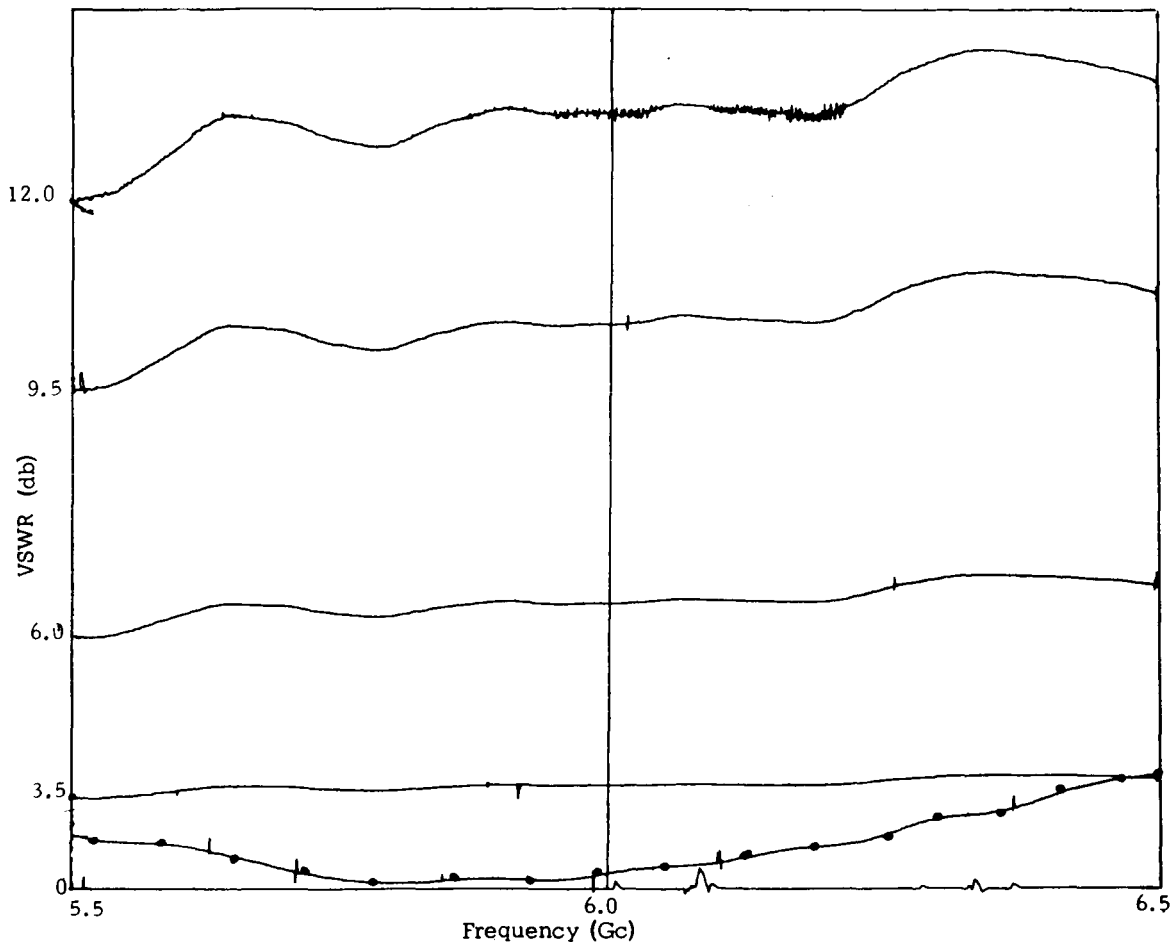


Figure 9—Output VSWR versus frequency.

curve is 14.6 degrees per volt, indicating a large phase shift with an incremental change in voltage. The incremental phase shift versus input power is plotted in Figure 13. The tube was driven beyond saturation, the saturation point at  $P_{in}$  being 1.3 dbm. Note the large phase change beyond the saturation point.

### 1.2.9 Sawtooth-Wave Synthesis by Harmonic Summation

A nearly linear sawtooth, with freedom from ringing, was synthesized by summing voltages of proper phase and amplitude at 30, 60, and 90 Mc. Flyback time was approximately 35 percent. A block diagram of the circuit is shown in Figure 14. This circuit provides a separate amplifier for each of the frequency components so that the amplitude of each may be independently controlled. Figure 15 is a display of the circuit output waveform illustrating the nearly "sawtooth" waveform.

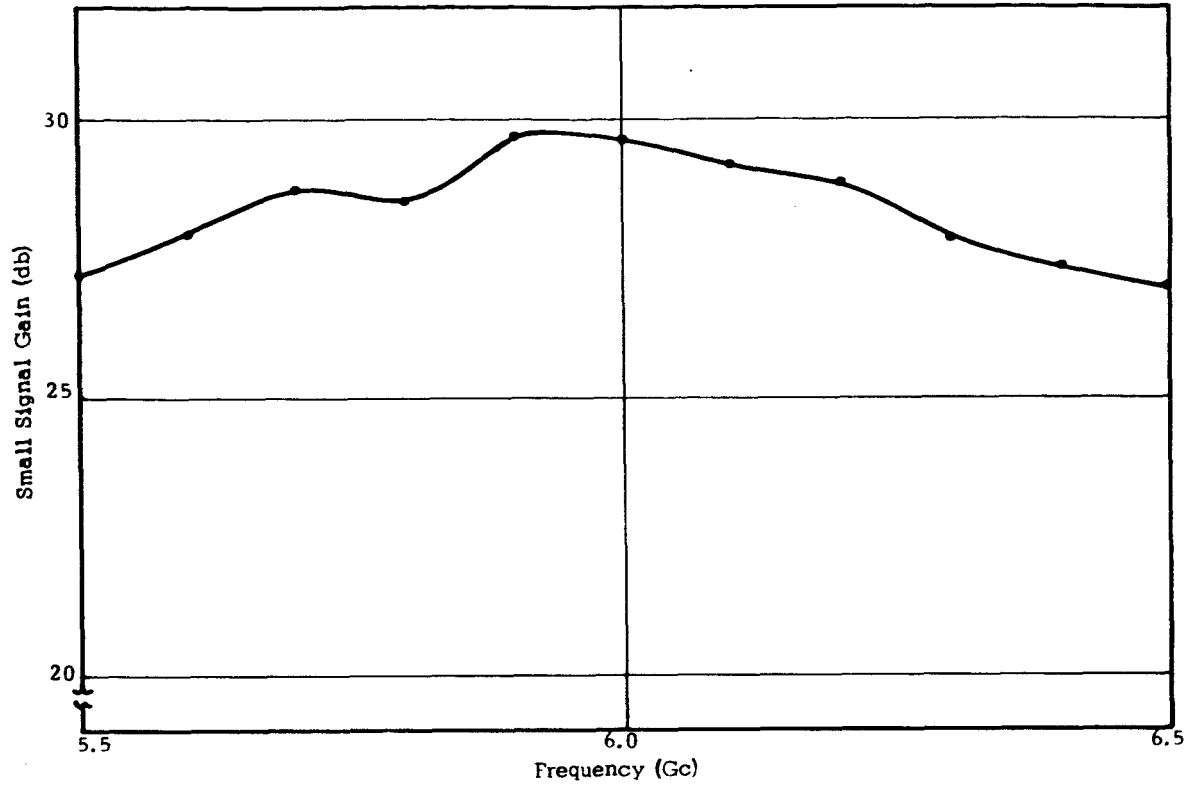


Figure 10—Small-signal gain versus frequency.

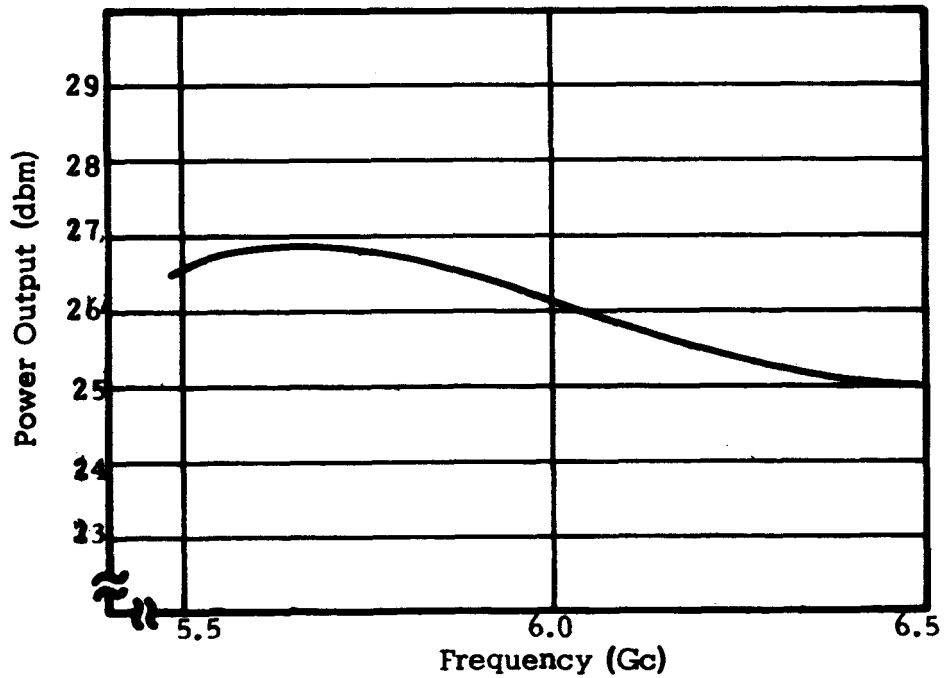


Figure 11—Saturated output power versus frequency.

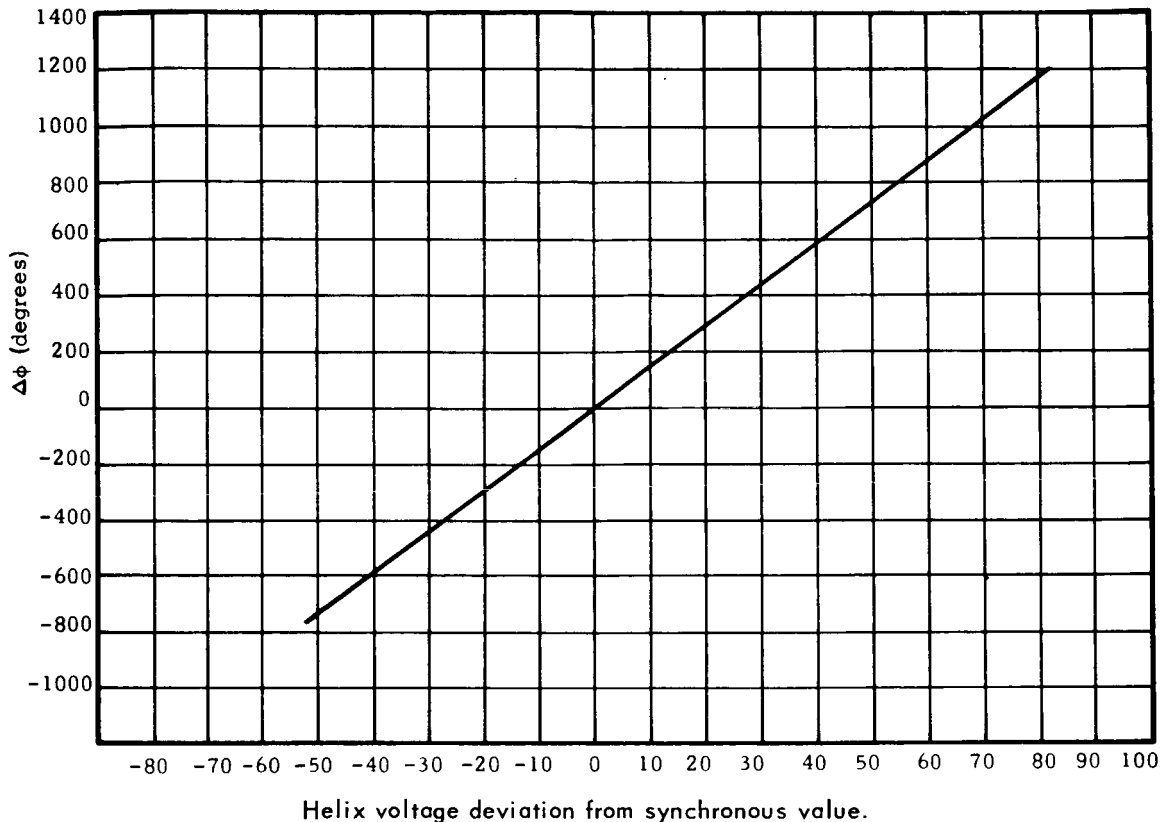


Figure 12--Change in phase versus helix voltage.

Some difficulty was encountered in the summing network which imposed a limitation on the sawtooth waveform amplitude, since the drive to the final amplifier was low. Some interaction between amplifier stages was present and problems were encountered when varying the phase of each component. The phase of each component was varied by detuning the output tuned circuit of the respective amplifier, which also resulted in an amplitude change. Some change in waveform was encountered when the waveform was coupled to the TWT drift tube; the high capacitance and low impedance distorted the waveform and decreased its amplitude appreciably.

#### 1.2.10 Experimental Tests: Two Frequencies to Gun

The summed 30 Mc and 60 Mc components were applied to the serrodyne tube gun (cathode, anode, and grid) to obtain data to compare the theoretical results of two-frequency modulation presented in Appendix I. The results are shown in Figures 16 through 18 for the desired M, this being the first upper sideband.<sup>G3</sup> The carrier and second sideband suppression points are shown to occur at the amplitudes of the modulation frequencies (as predicted by theory).

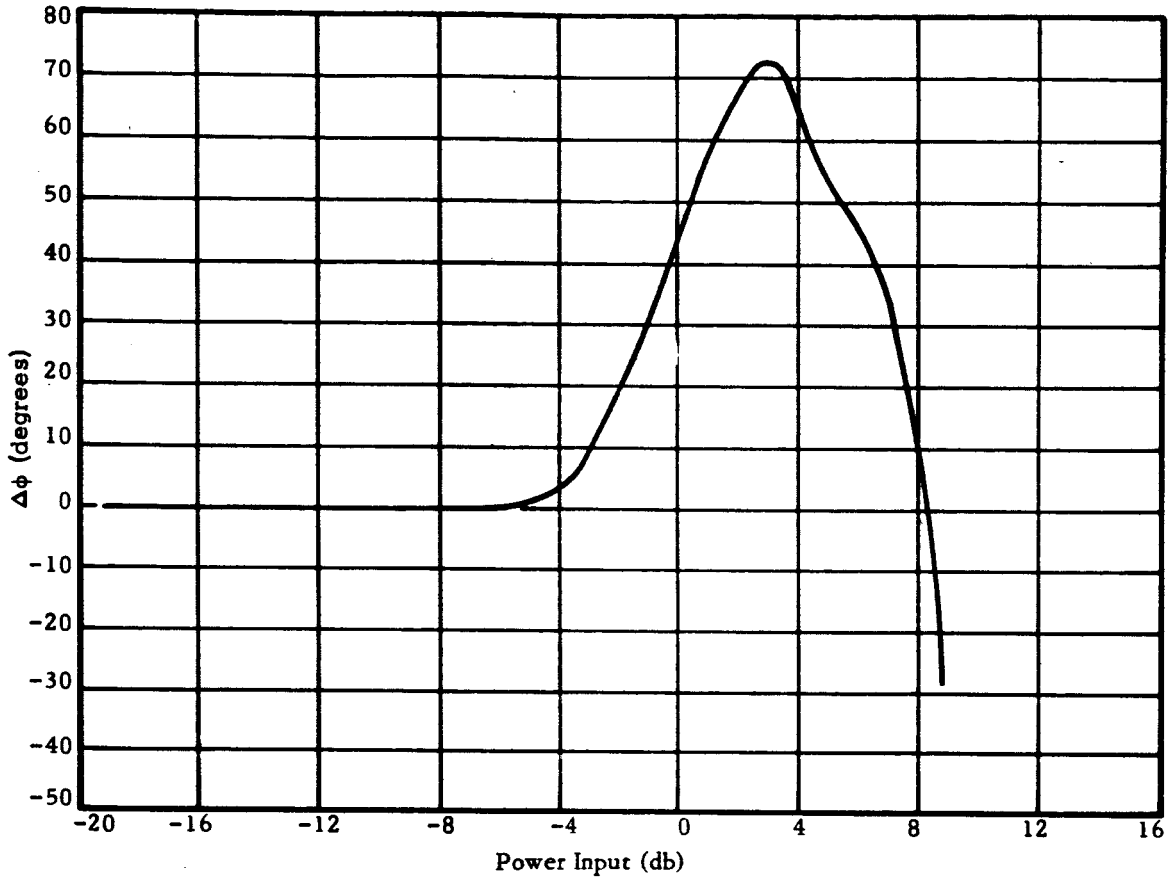


Figure 13—Change in phase versus input power.

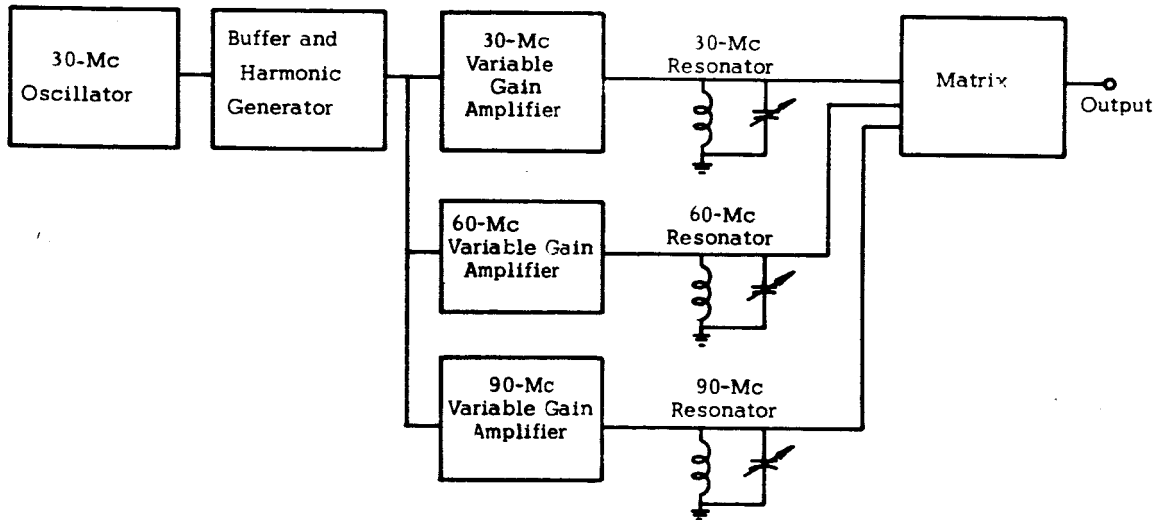


Figure 14—Block diagram of multiple frequency modulator with independent control over signal levels.

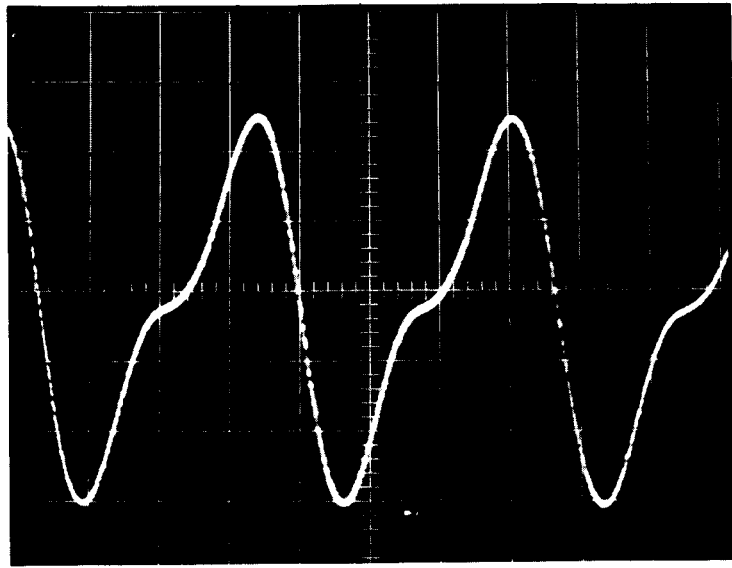


Figure 15—Output waveform of three-frequency modulator.

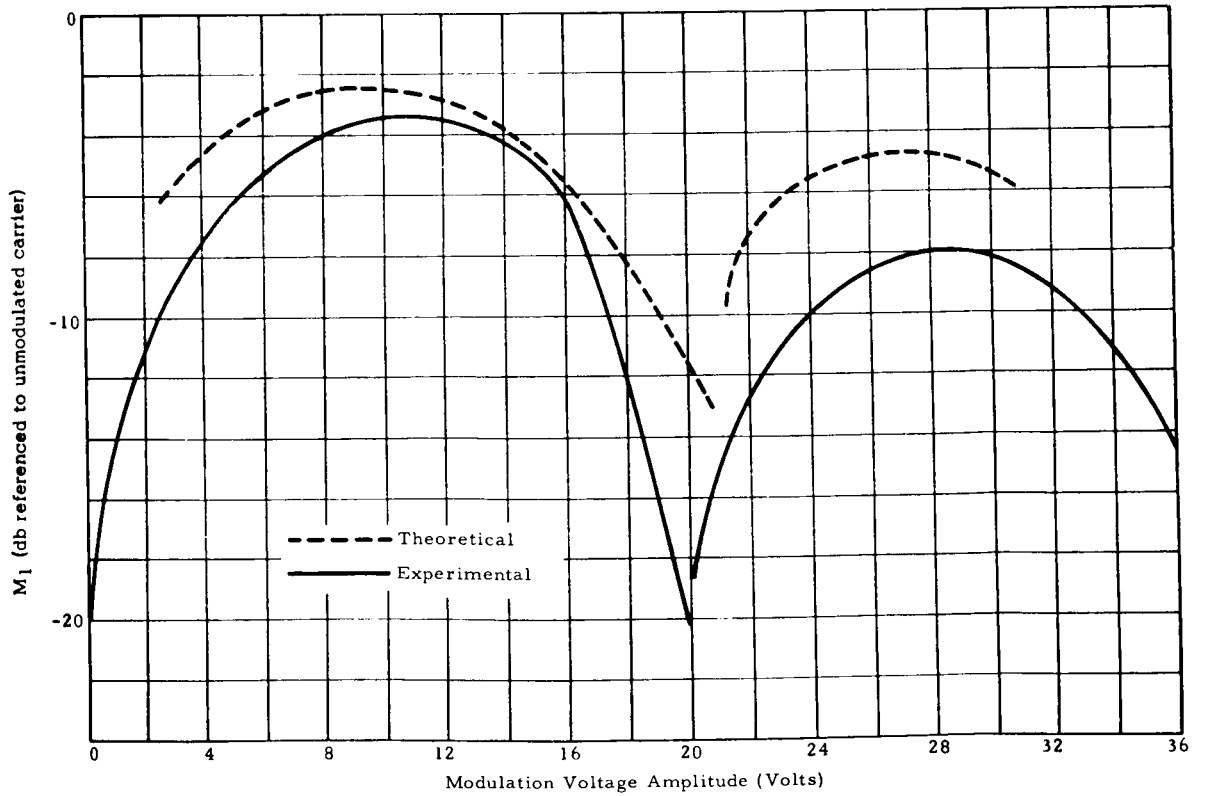


Figure 16—Amplitude of  $M_1$  as a function of the fundamental modulation voltage amplitude with no second harmonic present.



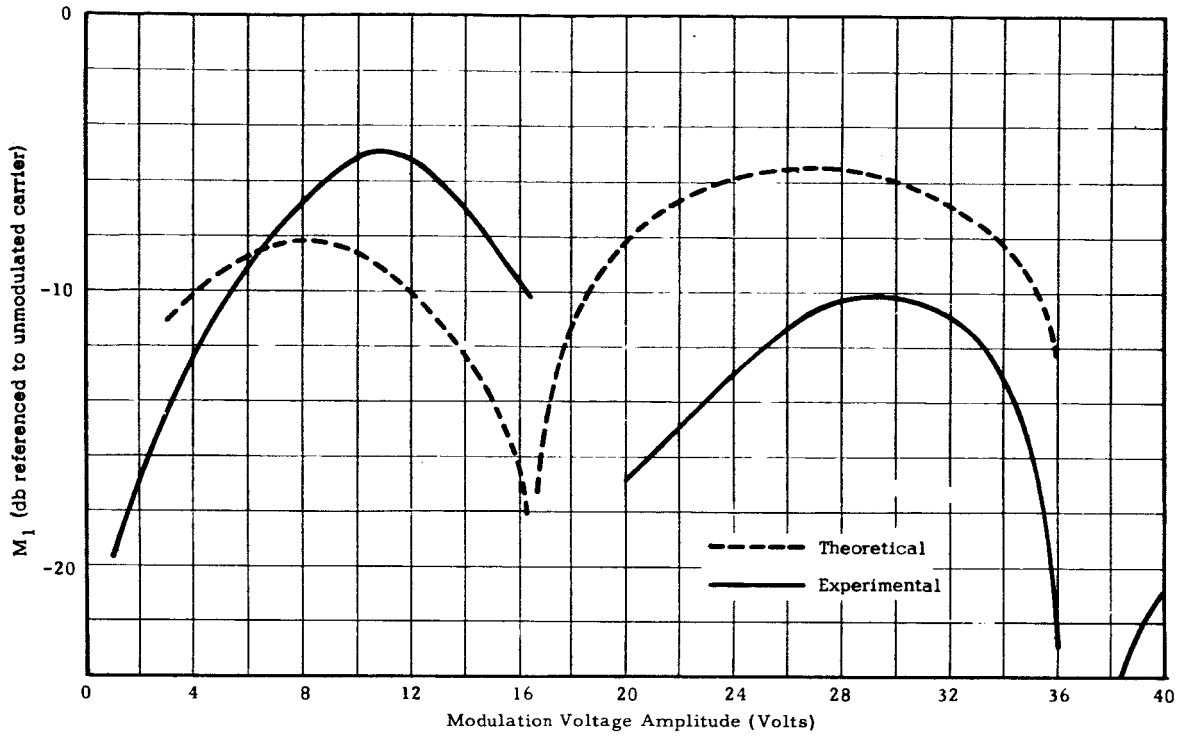


Figure 17—Amplitude of  $M_1$  as a function of the fundamental modulation voltage amplitude with 5.1 volts of the second harmonic present.

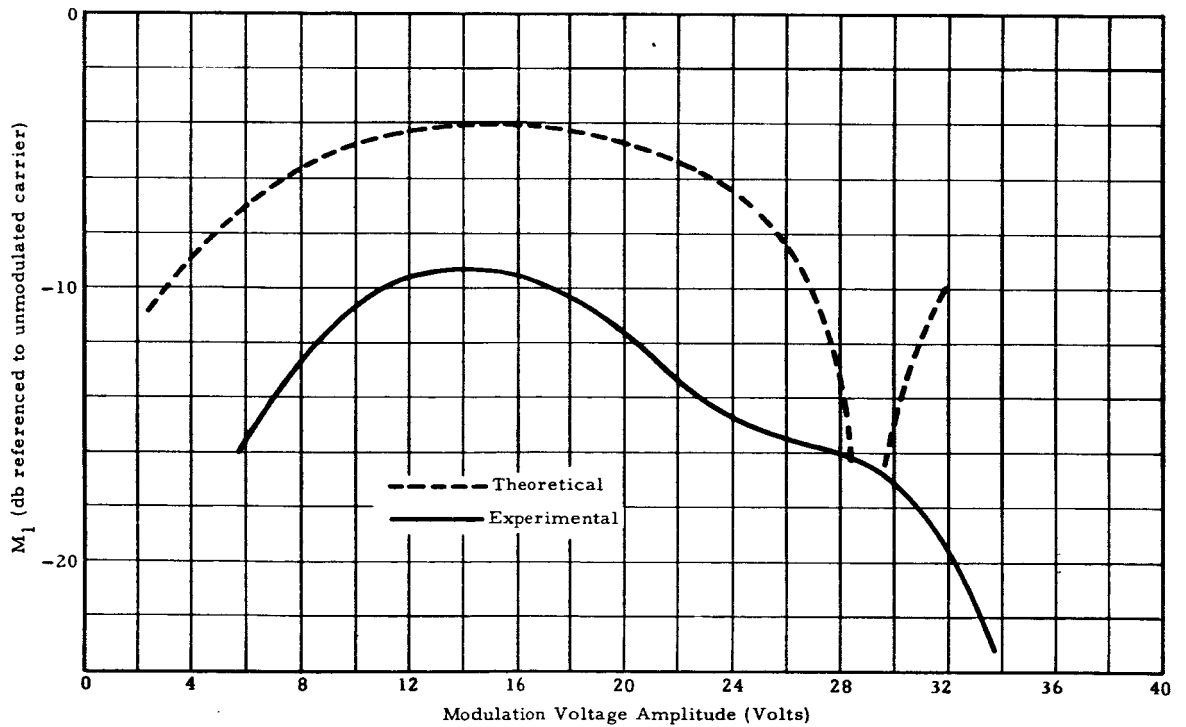


Figure 18—Amplitude of  $M_1$  as a function of the fundamental modulation voltage amplitude with 10.2 volts of the second harmonic present.

Tests indicated that the frequencies of significant amplitude are the carrier and four sidebands (two upper and two lower). The first lower sideband power approximately equals the upper sideband. The same holds for the second sideband, the difference being 3 to 5 db. Thus, almost as much power is shifted to the lower as to the upper sidebands, resulting in a higher translation loss. This result tends to substantiate the difference between the theoretical and experimental results.

Test results indicated that about 25 percent peak-to-peak AM is present when modulating the TWT electron gun. The incidental AM reduces the carrier and sideband suppression and introduces other sidebands. One advantage of drift tube modulation is the reduction in incidental AM present.

Tests were made to correlate further the two-frequency modulation results presented in Appendix I and the experimental data. Sideband and carrier suppression of 26 db was obtained compared to infinite suppression as predicted by the theory. The experimental data showed a 12-db translation loss, which is 3 db more than the theoretical results indicated. Much of this loss was attributed to the additional sidebands present and the discrepancy in carrier and sideband suppression. Both upper and lower sidebands were present, but one set could be maximized.

A spectral display of the output sidebands is presented in Figure 19. Figure 19a shows the carrier (6000 Mc) and second sideband (6060 Mc) suppressed below the first sideband (6030 Mc). The suppression (about 26 db maximum) was very sensitive to modulation amplitude and phase, and the helix voltage. Figure 19b shows the lower sideband levels for the same 30 Mc waveform.

Since sideband suppression was low, using two-frequency modulation, tests with the re-entrant loop were not performed. Instead, the third modulation frequency was introduced and preliminary tests were made. A carrier suppression of 42 db was experienced with the second sideband being 36 db below the desired sideband. The translation loss was 12 db, which is 7 db more than that predicted by the theory. Again, this is due to the other sidebands present and the incomplete suppression of the carrier and second sideband.

In general, it can be stated that the gun-modulation approach on this program gave the best sideband suppression even though a 25 percent peak-to-peak AM was introduced.

Vertical scale for both displays is 4.3 db/cm.

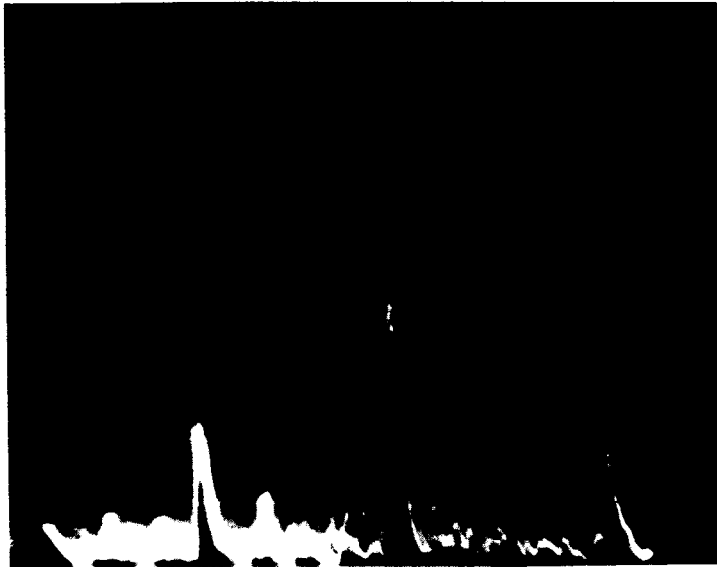


Figure 19a—Upper sidebands (frequency in Mc).

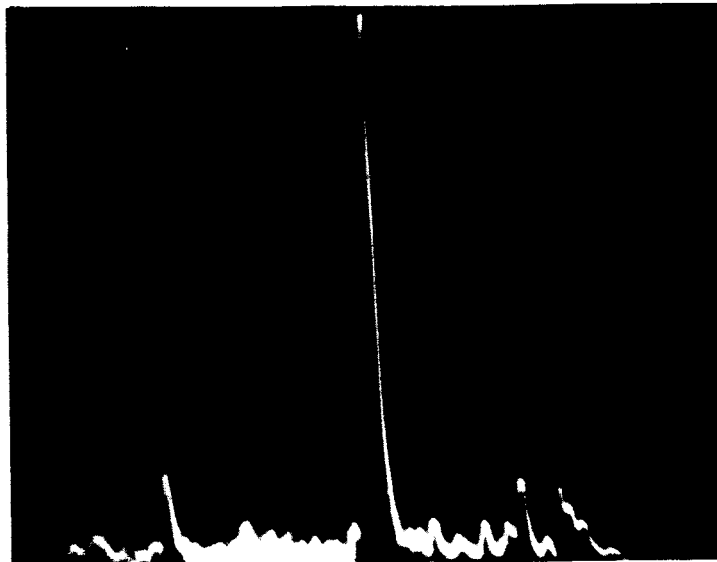


Figure 19b—Lower sidebands (frequency in Mc)

Figure 19—Spectral display of sidebands when TWT is modulated with 30 Mc waveform.

### 1.2.11 Experimental Tests: Three Frequencies to Gun

The three-frequency modulation technique was used to apply all three components to the electron gun of the serrodyne tube. Figure 20 shows a spectral display of the unmodulated and modulated TWT outputs. Fine adjustment of the modulator and TWT voltages made it possible to suppress  $f_0$  40 db below the  $f_{-1}$  sideband<sup>G4</sup> in amplitude, and the  $f_{-2}$  sideband was 27 db below  $f_{-1}$ . A 5-db translation loss was experienced.

Independent control of each modulation frequency for both amplitude and phase was found to result in better carrier ( $f_0$ ) and sideband ( $f_{-2}$ ) suppression. Preliminary theoretical studies indicate that two variables (amplitude of two modulation frequencies) will suffice to provide the simultaneous suppression of two sidebands, and the addition of a third modulation frequency will maximize the desired sideband output.

### 1.2.12 Experimental Tests: Three Frequencies to Helices and Drift Tube

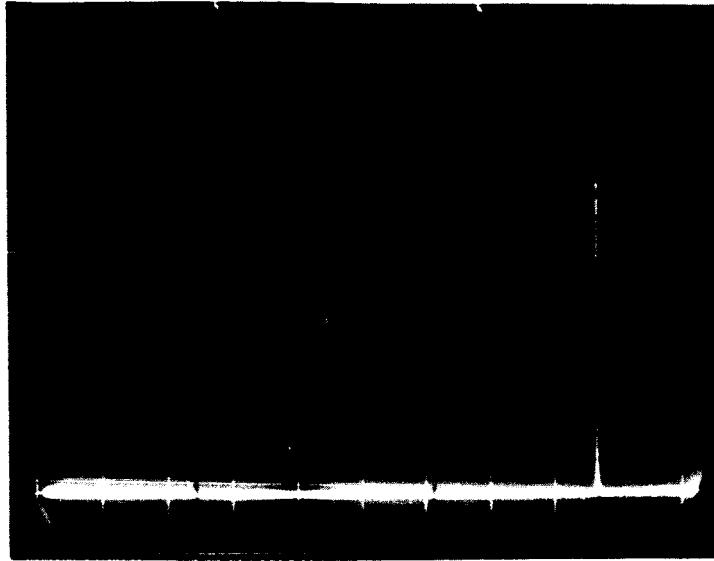
The buffer-amplifier outputs were link-coupled to resonant circuits connected directly to the TWT; 30 Mc was connected to the delay tube; 60 Mc was connected to the input; 90 Mc was connected to the output helix. With this method, it was possible to deliver over twice the required modulation voltage of each component. The coupling scheme is shown in Figure 21.

Two TWT models were designed and fabricated for tests with this modulation system, using a smaller outside diameter drift tube to reduce the capacitance between the PPM stack and the drift tube.

Figure 22 shows the carrier and second sideband level referenced to the first sideband. Note the increased carrier level as input power is increased. Figure 23 is a spectral display of the sidebands when  $P_{in}$  was 40 db down from the reference, the reference in this case being the input power at saturation. A plot of output versus input power for each sideband is shown in Figure 24. Note the linearity up to an input power level of -12 dbm. Beyond this point the tube becomes nonlinear because the electron beam begins to saturate. In general, this modulation network can be summarized as being most successful in minimizing amplitude modulation; however, the suppression of 18 to 20 db was not as great as that afforded by the gun modulation approach.

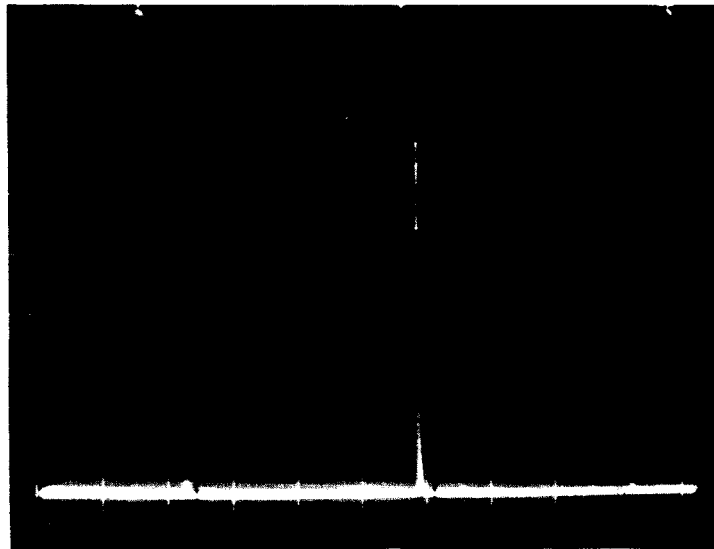
### 1.2.13 Experimental Tests: Re-entrant Circuit

A serrodyne TWT with the synthesized sawtooth applied to the gun was tested with the re-entrant loop shown in Figure 25, using the test methods of Appendix III.



$f_0$   
6000 Mc

(a)



$f_-$                        $f_{-1}$                        $f_0$   
5940                      5970                      6000

(b)

Figure 20—Spectrum display of TWT output; (a) modulated TWT output, and (b) serrodyned TWT output showing the  $f_0$ ,  $f_{-1}$  and  $f_{-2}$  sidebands.

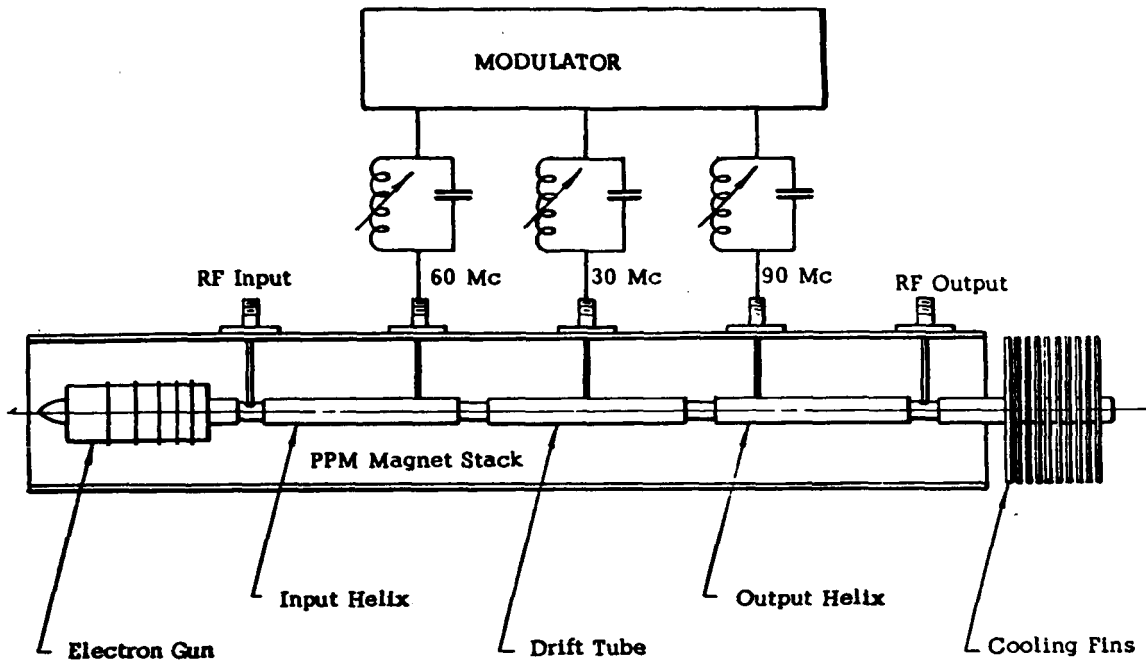


Figure 21—Alternate modulation system.

The input to the TWT was a CW signal at 5970 Mc. In passing through the TWT the signal was shifted to 6000 Mc with a minimum carrier and sideband suppression of 36 db. With the re-entrant loop bandpass filter centered at 6000 Mc, the shifted signal was returned to the TWT input. In passing through the TWT, the TWT signal was again shifted by 30 Mc, the frequency now being 6030 Mc. For two passes through the TWT, the net gain was 26 db for the desired sideband. A lower sideband, originally at 5940 Mc, was also shifted upward and appeared at the carrier frequency. Due to this sideband shift, the carrier level was increased by 20 db.<sup>G5</sup>

In an experiment with the 30-, 60-, and 90-Mc modulating voltages applied to the drift tube, first and second helices respectively, the re-entrant loop was closed and another set of data of each sideband level was taken. These data are shown in Figure 26. Of interest in this case is the increase of the second sideband beyond the saturation point of the TWT. Linearity is obtained up to approximately -15 dbm input power.

Figure 27 plots output versus input power. The total loss through the filter system was 38.5 db. This included cable and attenuator losses. The serrodyne tube gain may be found from

$$P_{out} - P_{in} = 2G_{serro} - 38.5$$

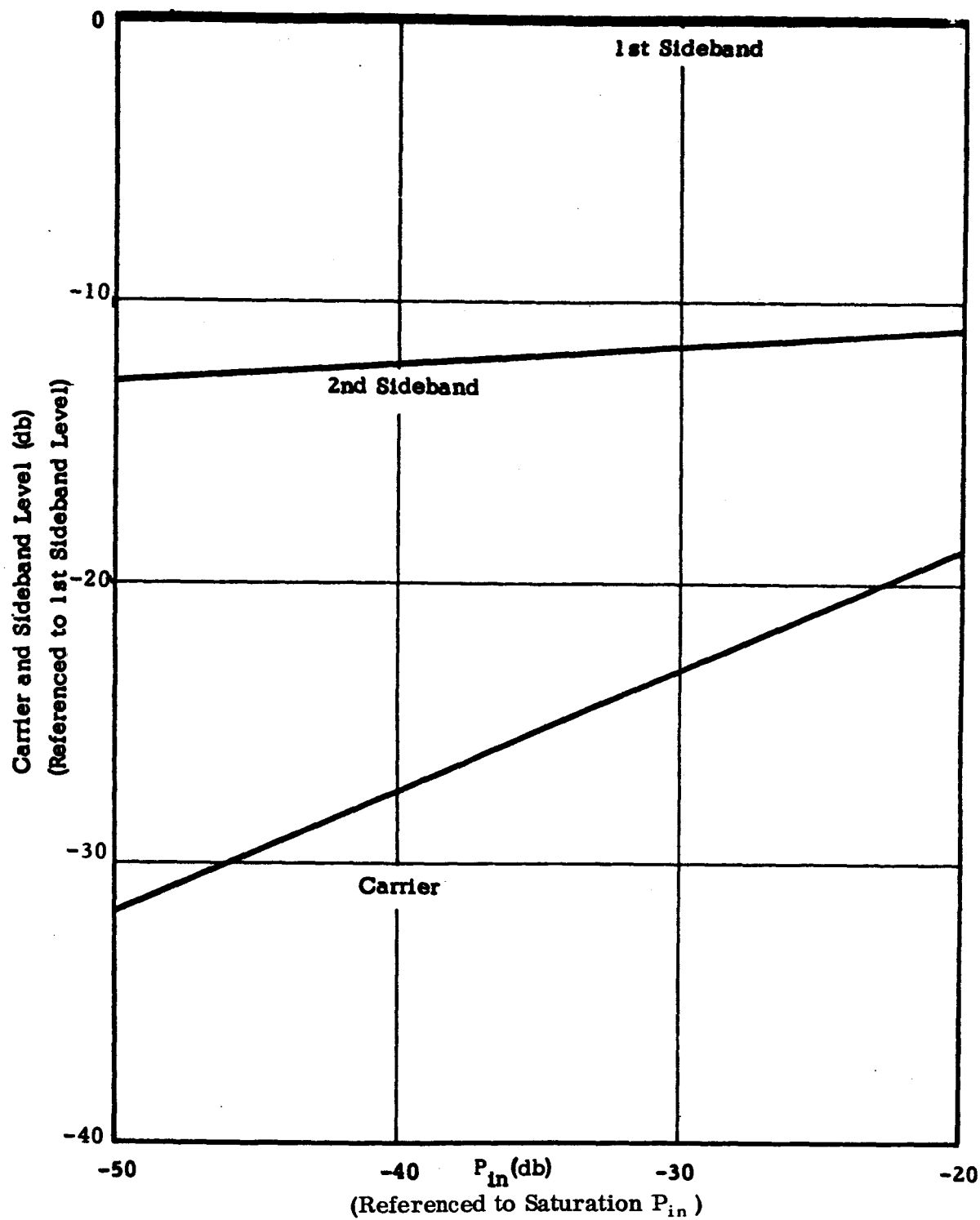
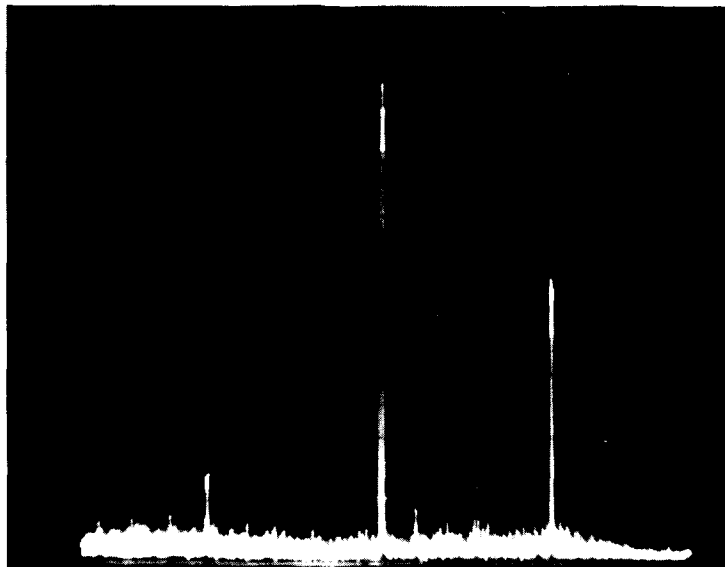


Figure 22—Carrier and 2nd sideband suppression versus input power.



$f_0$                    $f_1$                    $f_2$   
 6000                  6030                  6060

Figure 23—Spectral display of sidebands where  $f_0 = 6$  Gc and  $f_1$  and  $f_2$  are 6030 and 6060 Gc respectively.

A typical point is at the input power equal to -10 dbm.  $P_0 - P_{in}$  in this case is -11 db. So  $-11 = 2G_{\text{erro}} - 38.5$

$$G_{\text{erro}} = 13.75 \text{ db.}$$

The TWT gain, when the tube is modulated, is 13.8 db for the desired sideband. The other sidebands are significant since they are not suppressed sufficiently. Gain suppression due to two signals being amplified at the same time is also significant since the "return loop" signal is near the saturation input power of the TWT.

Echo effects due to insufficient suppression of the undesired sidebands were observed. A 5-microsecond pulse was used and a delay line was inserted between the loop filter and the TWT output. This increased the loop delay time to 120 nanoseconds, thus delaying the desired frequency pulse which returned through the loop.

Figure 28 shows the desired frequency pulse at the output with the loop open and in a re-entrant mode. The trailing edge of the pulse shows the undesired sideband amplitude which was 5.6 db below the desired frequency level. This echo represents insufficient suppression of the carrier. In Figure 29 the time scales have been expanded to illustrate the echo effect more clearly.



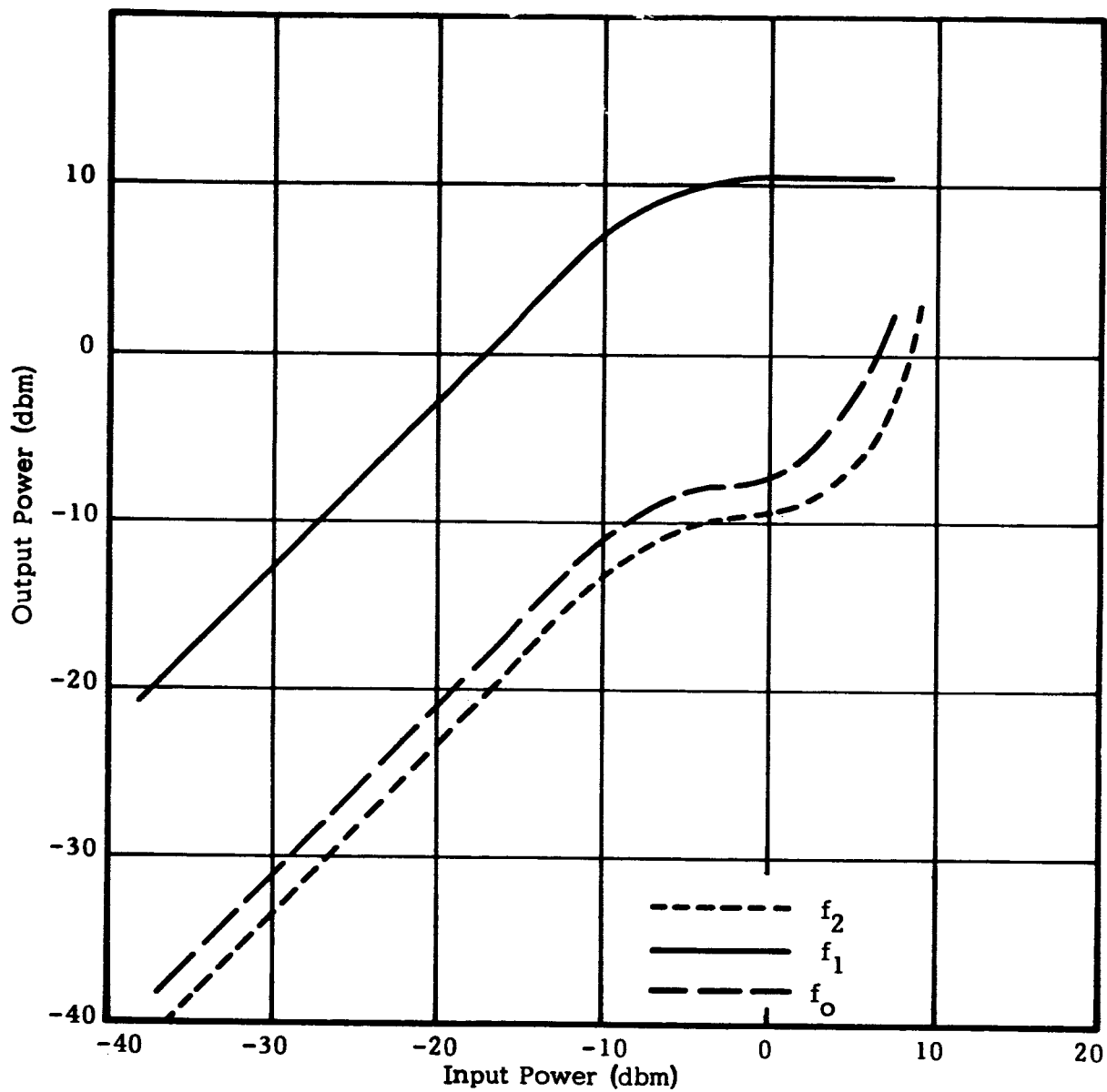


Figure 24—Sideband and carrier output versus carrier input with open loop and optimized for equal sideband and carrier rejection VE D, Serial 7.

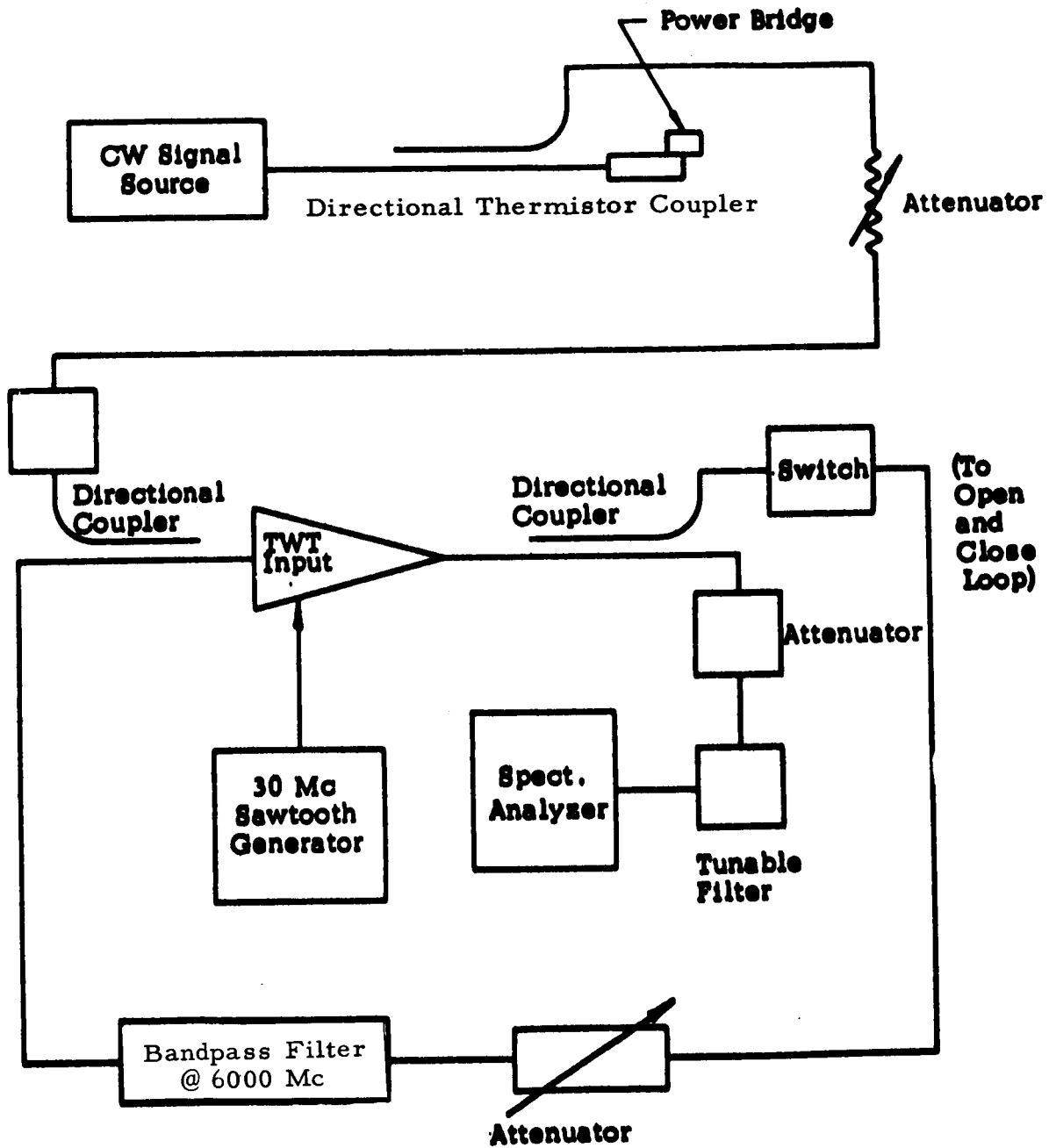


Figure 25—Re-entrant amplifier test setup.

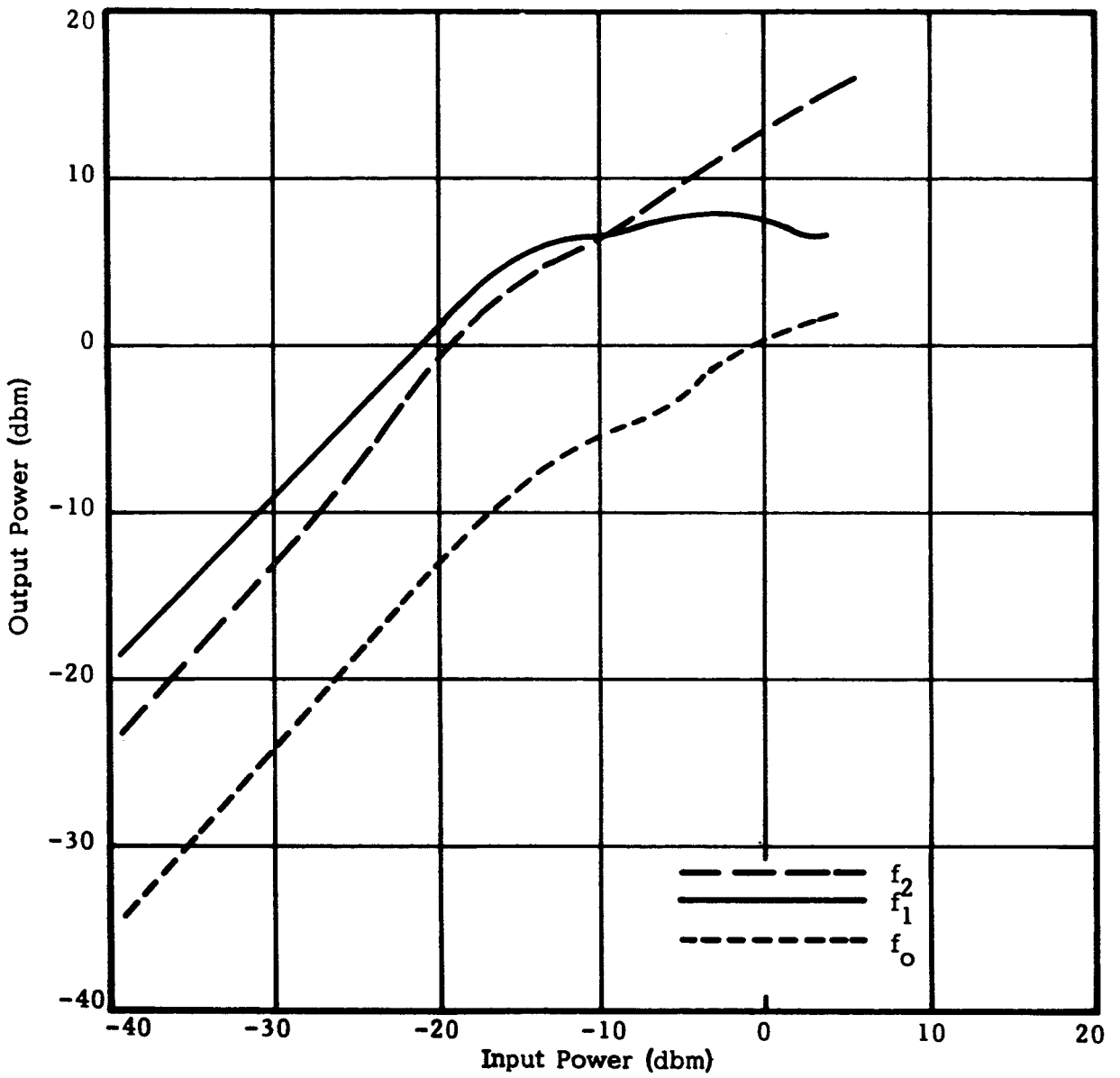


Figure 26—Sideband and carrier output versus carrier input with closed loop.

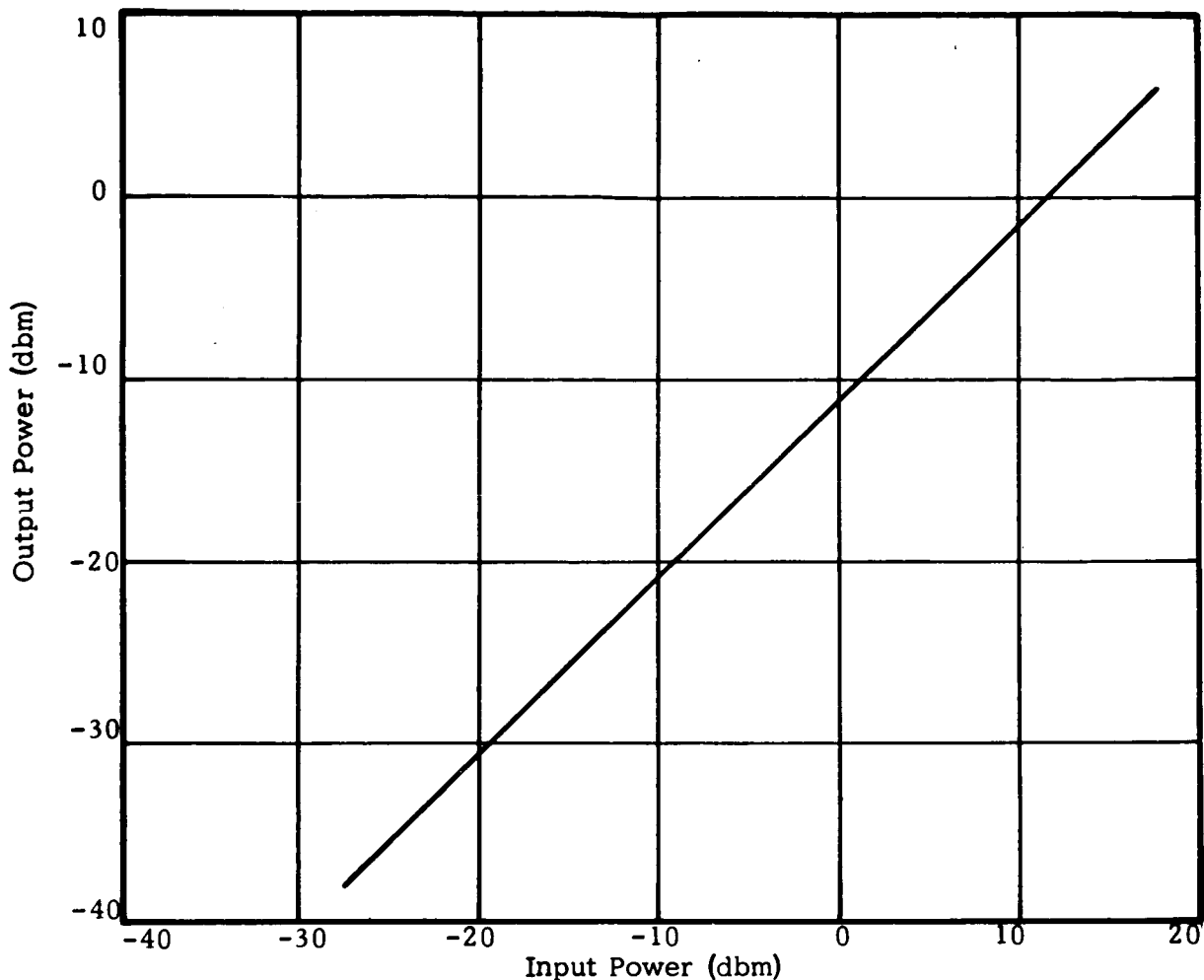
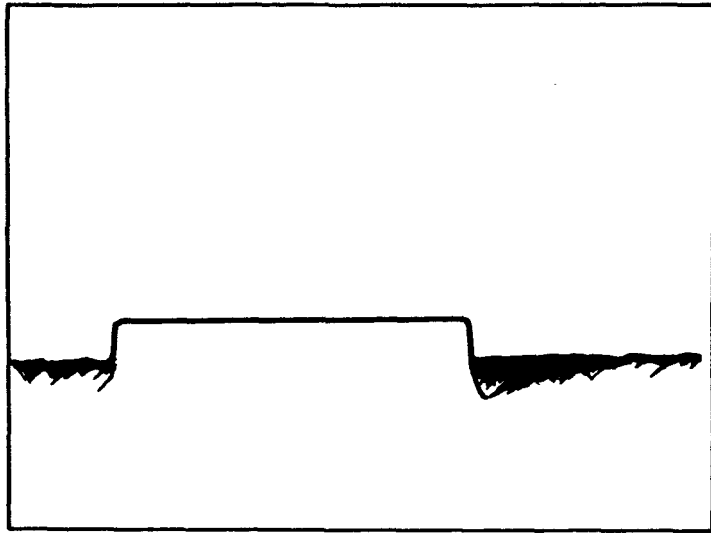


Figure 27—Output power at 6 Gc versus input power at 5.94 Gc using 3 filters.

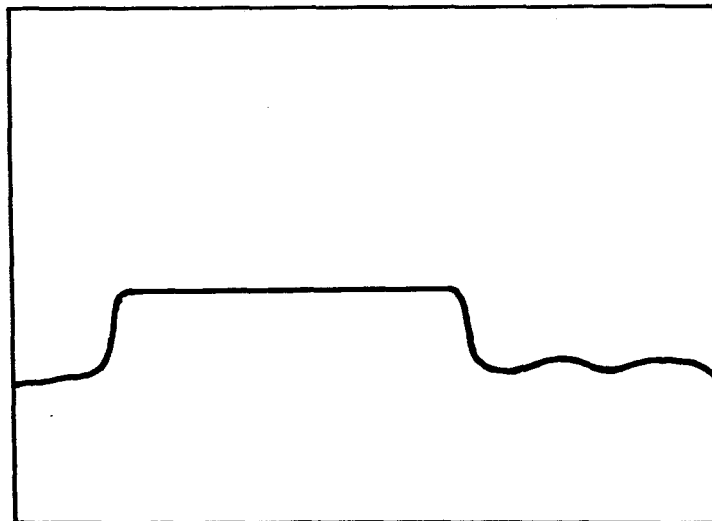
### 1.3 TWT MIXER FOR WIDE RANGE FREQUENCY SHIFTS

#### 1.3.1 Introduction

Another method of obtaining a large frequency shift is the technique of mixing in a TWT. In the serrodyne system, the beam is modulated by a sawtooth waveform and the output frequency will be the input frequency, plus or minus multiples of the sawtooth frequency. With an ideal waveform, translation loss will be zero; thus the total tube gain is used to amplify the desired signal. The mixing technique differs from the serrodyne technique in that it employs the nonlinear properties of the electron beam to mix the input signal with the local oscillator. By incorporating a large difference in local-oscillator and input frequencies, a large frequency shift may be obtained without significant sidebands.

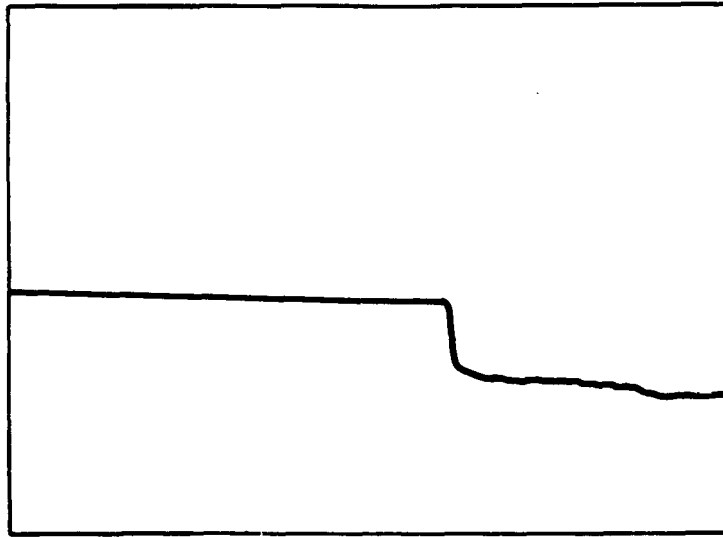


(a) Output pulse with open re-entrant loop.

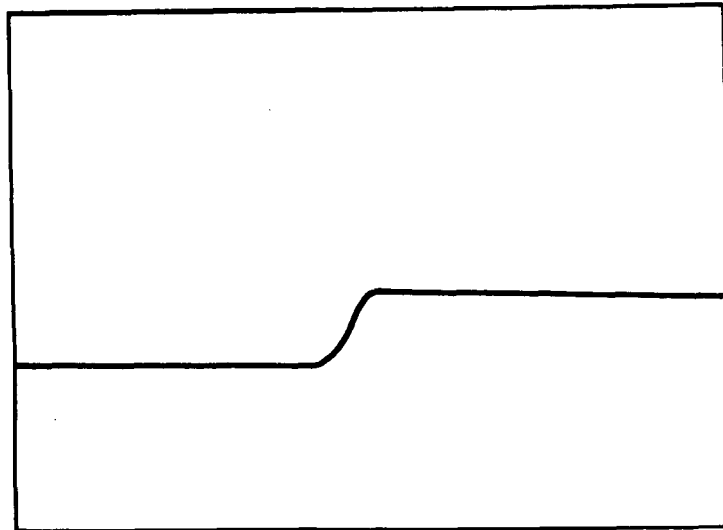


(b) Output pulse with loop in re-entrant mode.

Figure 28—Output pulse of re-entrant amplifier with re-entrant loop open and closed.



(a) Trailing edge of pulse.



(b) Leading edge of pulse.

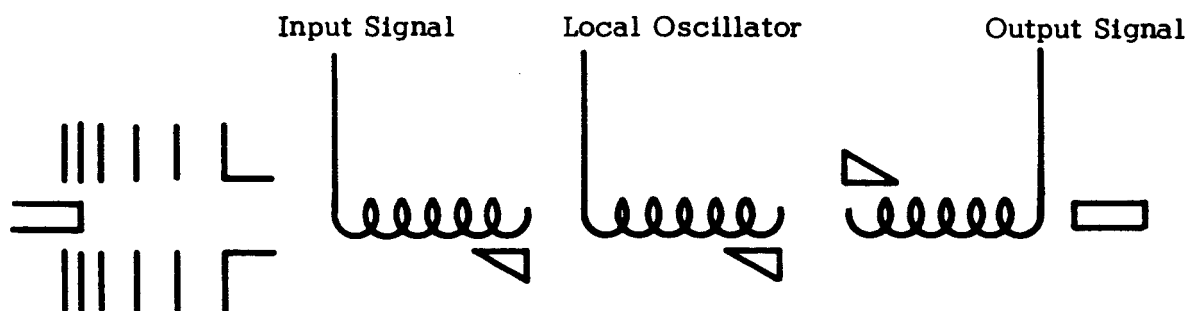
Figure 29—Trailing and leading edge of pulse on an expanded scale.

In the experiment to be described, a signal was shifted from 6 Gc to 4 Gc. This experiment demonstrated that

- Frequency shifts of 2000 Mc can be achieved without the generation of significant spurious signals,
- The process involved is capable of significant gain and power output,
- TWT miniaturization and circuit simplification can be employed,
- The TWT mixer is stable and very broadband.

### 1.3.2 The Mixer TWT

To obtain mixing in a TWT, three circuits are embodied into the vacuum envelope as shown in Figure 30. One circuit – the input helix – must couple the input signal to the electron beam. A center helix, optimized for operating at the local-oscillator frequency, will couple the local-oscillator signal to the beam and mixing will begin. The output helix, optimized for operation at the desired output frequency, will enhance mixing and amplify the desired sideband.



	<u>Nominal Values</u>		
Helix Voltage	1100	1100	1100
Beam Current	6 ma	6 ma	6 ma
$\gamma_a$	1.3	1.7	1.5
Helix ID	0.060	0.060	0.060
Frequency	6 Gc	10 Gc	4 Gc

Figure 30—Detail of electron gun and helix structure of the three-helix mixer.

One tube, incorporating all three circuits, was fabricated and tested in the final program phases. The tube consisted of an input helix centered at 6.0 Gc, a center helix optimized to operate at 10 Gc and an output helix which was designed to operate as an amplifier from 3.0 to 5.0 Gc. All three sections operated at different helix voltages, these being optimized for the best possible mixing with the same helix diameter.<sup>1</sup>

Using a multiplicity of helix sections is made practical by the techniques presently used by MEC in its metal-ceramic TWT construction using metal barrels and ceramic windows. As shown by the cutaway drawing of a MEC envelope (Figure 2), the stacking process is used to assemble MEC vacuum envelopes and the present tube can be assembled easily using this same stacking or assembly process with techniques already evolved in the M5144.

### 1.3.3 Experimental Tests: 6 to 4 Gc Mixer

The data presented in Figures 32 through 36, using the test setup shown in Figure 31, were taken with a local oscillator level of 7.5 dbm. The local oscillator output versus input power at 4 Gc is plotted in Figure 32. The input signal in this case was at 6.0 Gc with the local oscillator at 10.0 Gc. An X-band klystron was used as the local oscillator to give stable operation. From Figure 32 it is seen that the local oscillator input power should be approximately 15 dbm before saturation of the X-band helix occurs, which sets the operating point for the local oscillator level to the TWT. All the data presented in Figures 33 through 36 were taken with a local oscillator level of 7.5 dbm.

Figures 32 through 36 also show output versus input power up to the mixer saturation point. Small-signal gain was 6 db at an input frequency of 6.1 Gc, the resulting output being at 3.9 Gc. Upon changing the input frequency to 5.5 Gc and optimizing the operating conditions, the small-signal gain achieved was 10 db. Higher gain could easily be had by increasing the output-helix length since it is in this region where most of the mixing takes place and the desired sideband is amplified. Of particular interest is the linearity and slope of the curves.

This experiment conclusively demonstrates the capability of the mixer TWT to obtain large frequency shifts. Filters may be used in the output to eliminate undesired sidebands. However, these sidebands will be at a low level since the output helix may be designed for optimum operation at the desired output frequency. The linearity indicates that intermodulation effects would not be a serious problem.

---

<sup>1</sup>R. W. DeGrasse, "Frequency Mixing in Microwave Beam-Type Devices," TR No. 386-2, Stanford University, July 28, 1959.



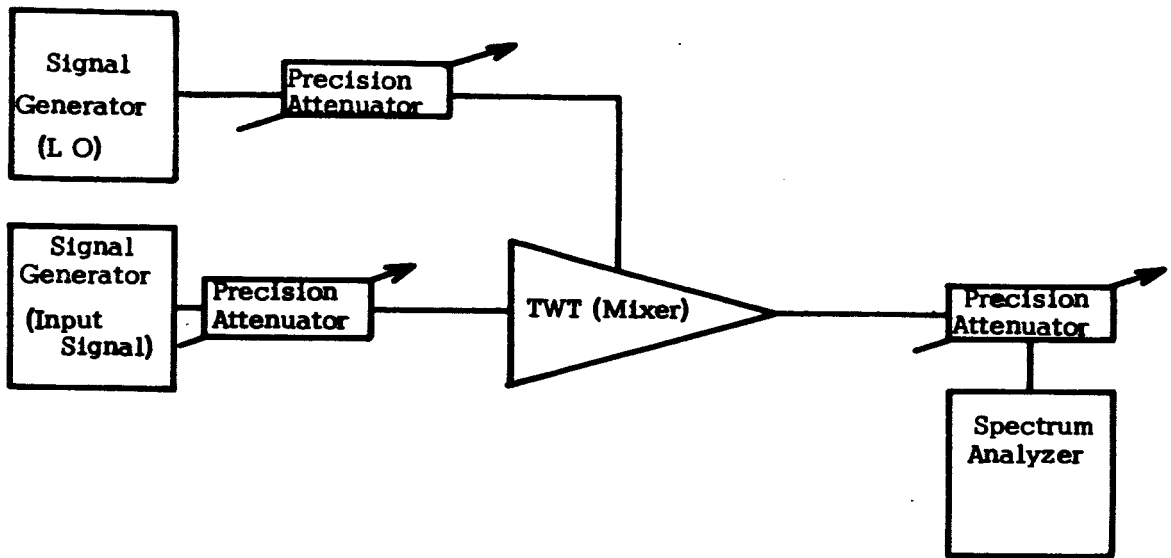


Figure 31—TWT mixer tube test setup.

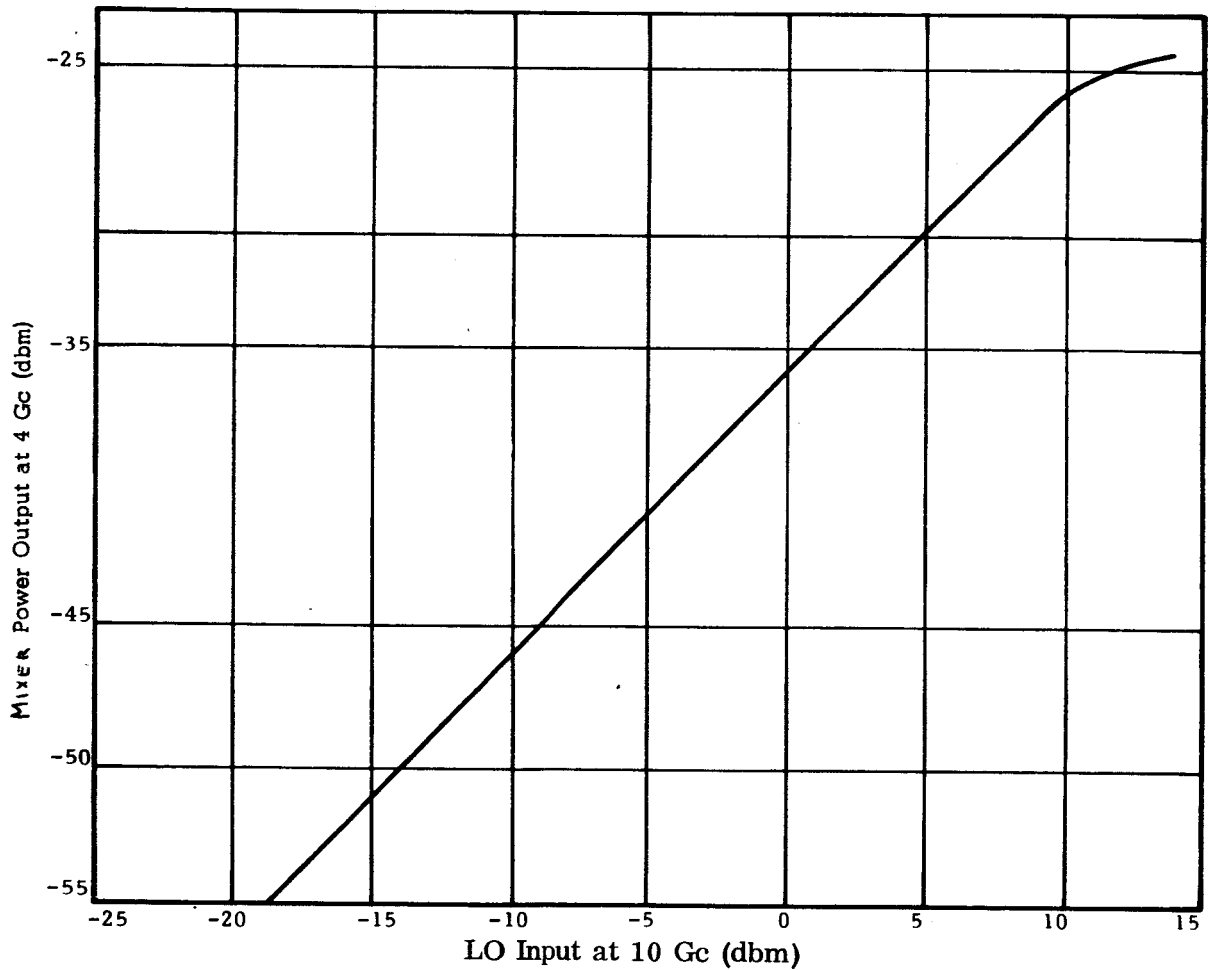


Figure 32—Mixer output Power (@ 4 Gc) as a function of L0 Power (@ 10 Gc) for a signal input power (@ 6 Gc) of -30 dbm.

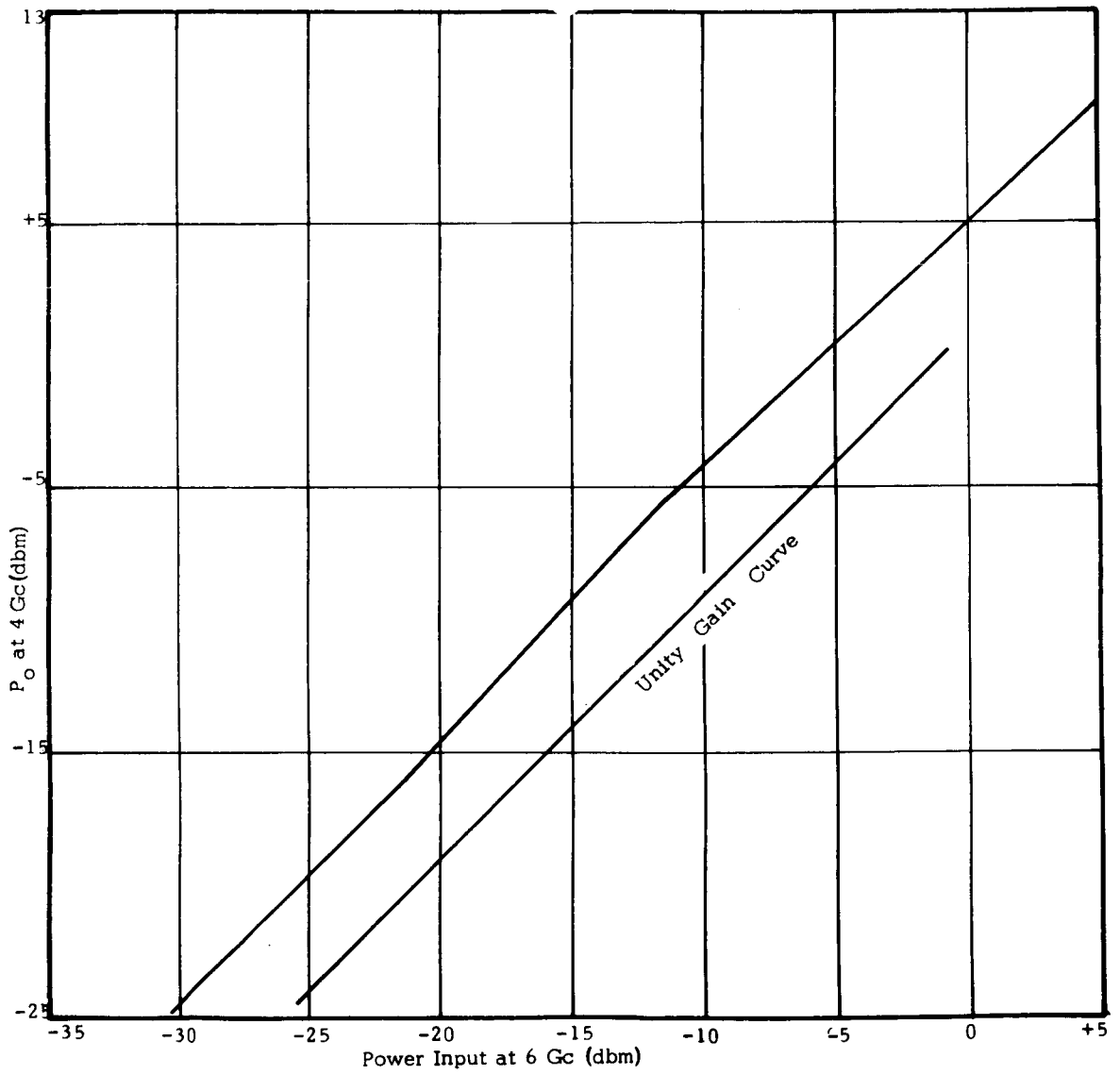


Figure 33—Output Power at 4 Gc for input of 6 Gc.

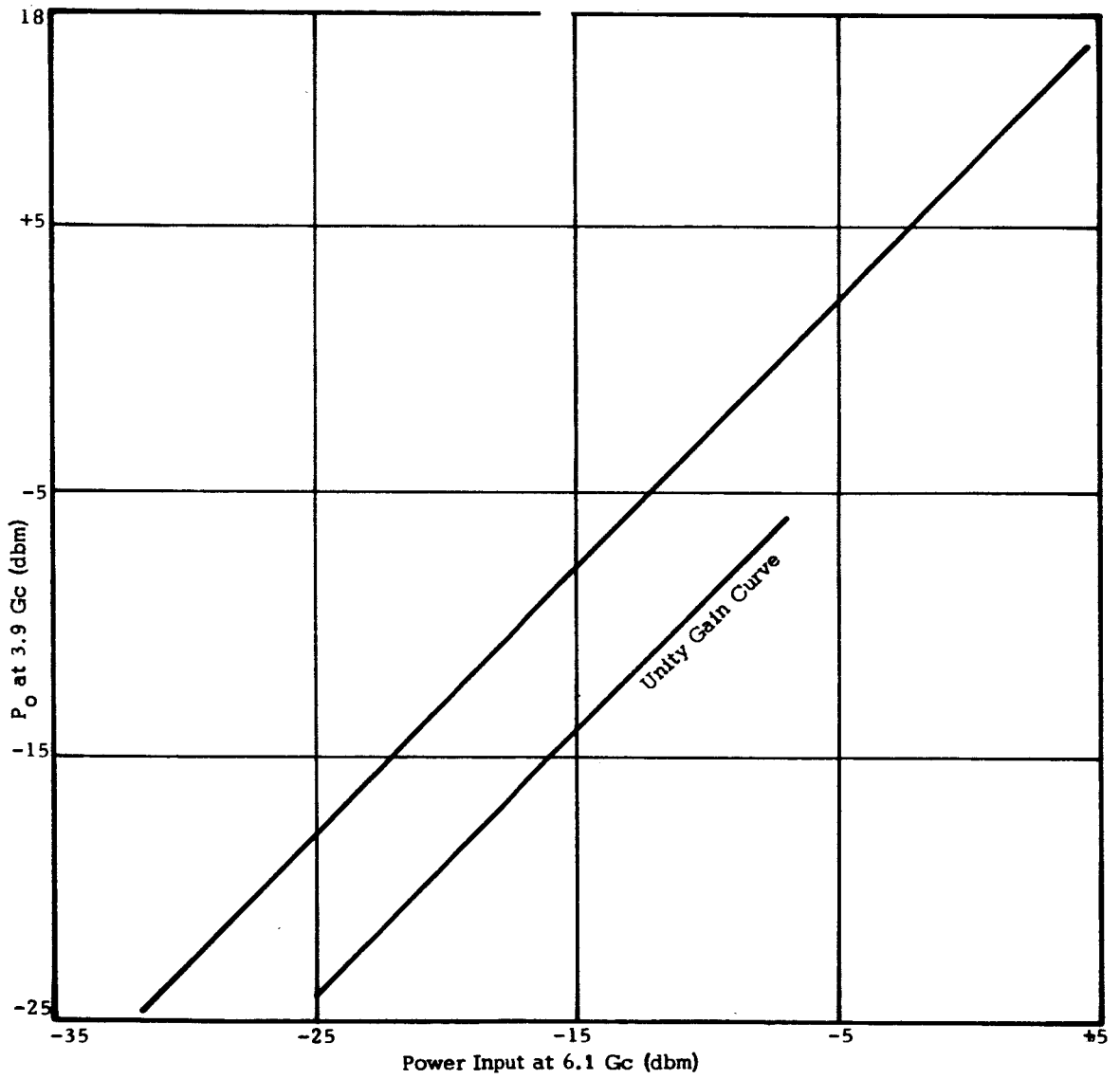


Figure 34—Output Power at 3.9 Gc for input of 6.1 Gc.

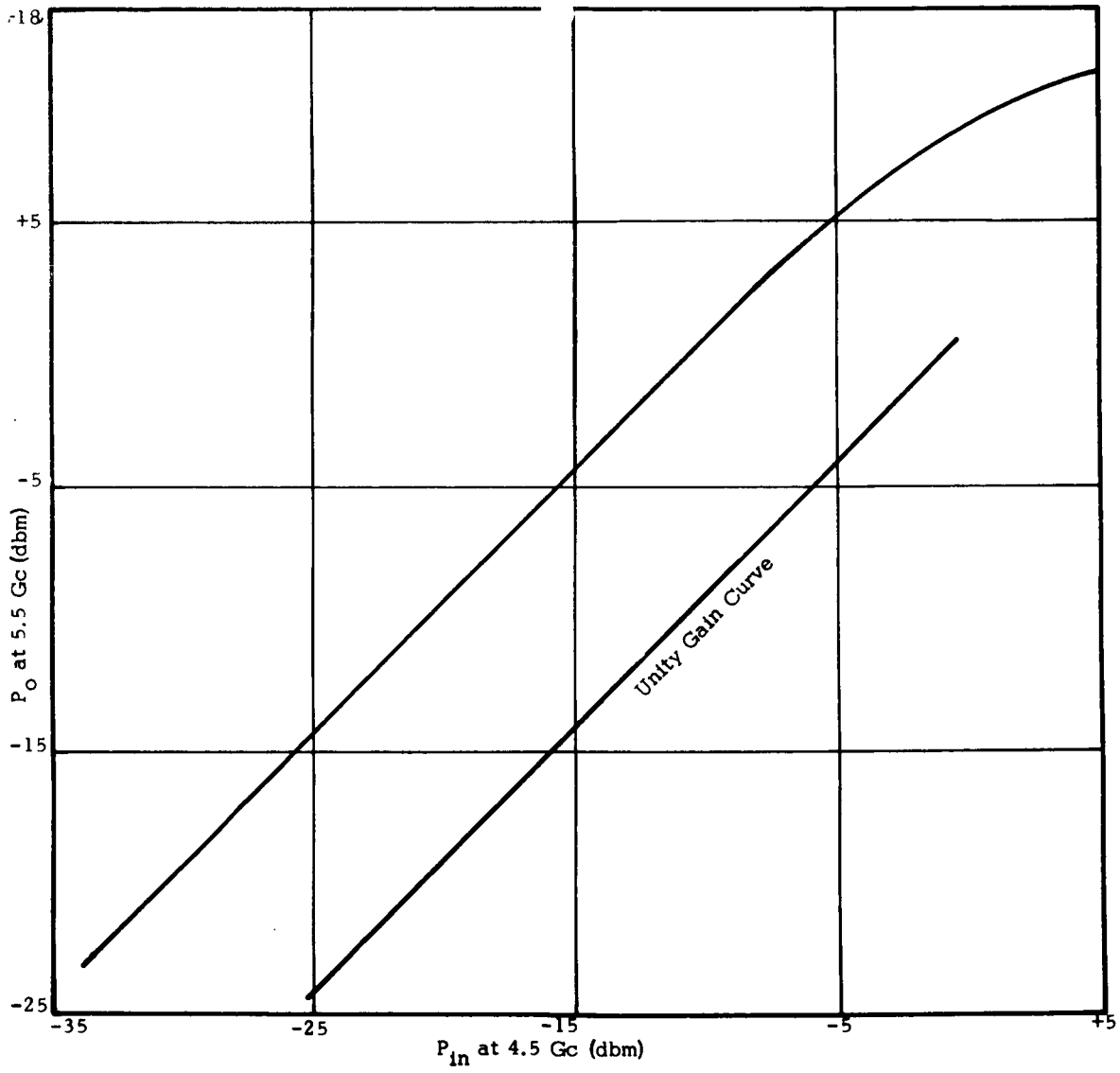


Figure 35—Output power at 5.5 Gc for input of 4.5 Gc.

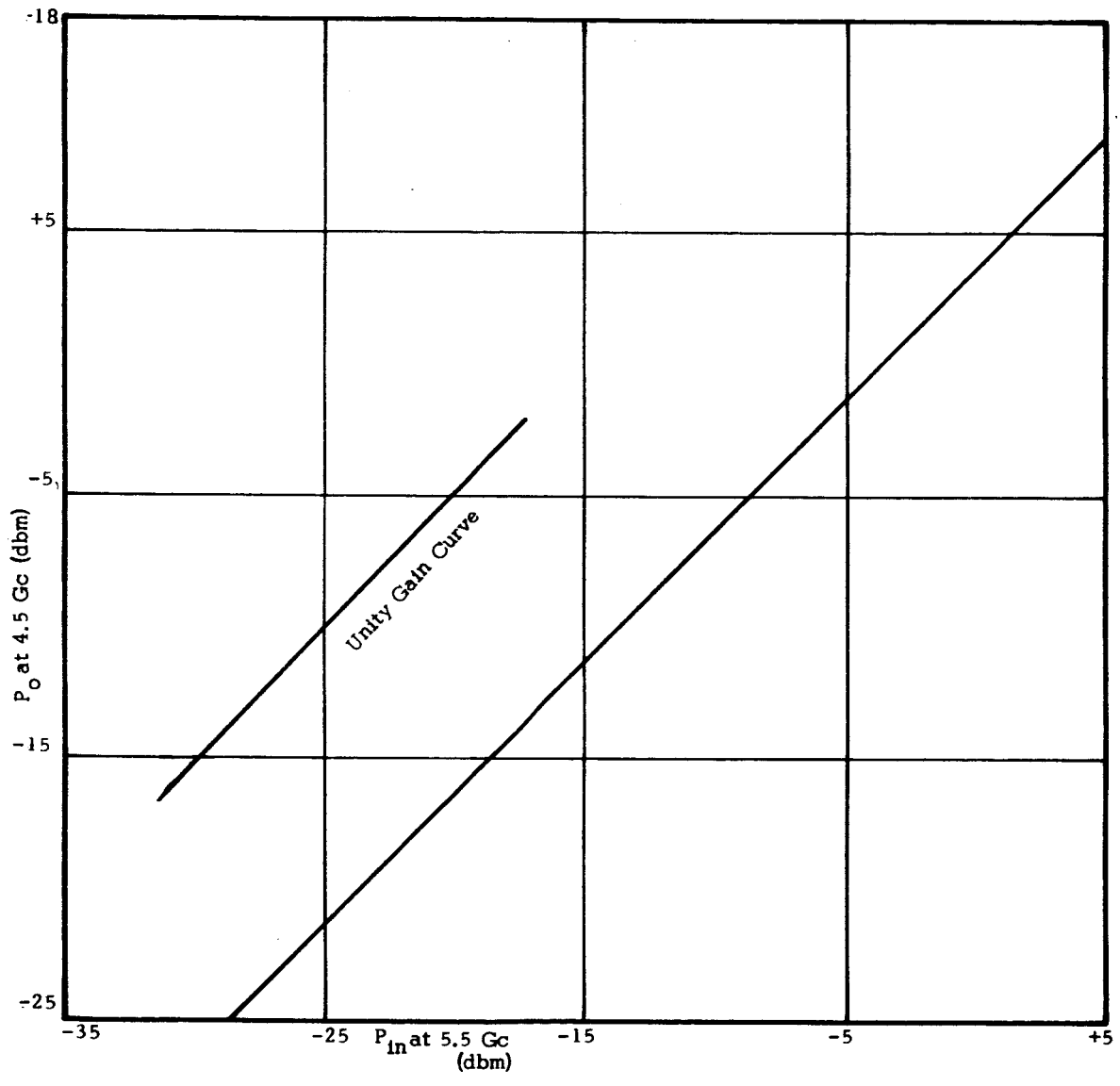


Figure 36—Output power at 4.5 Gc for input of 5.5 Gc.

#### 1.3.4 General Aspect of Mixer Operation

DeGrasse and Wade<sup>2</sup> have shown that the output mixer power for constant input power is related to the square of the difference frequency. It follows therefore that while the TWT mixer presents definite advantages for very wideband frequency shifting, it will also perform well for narrow band frequency shifting; i.e., 7900 Mc to 7500 Mc, with reduced conversion gain, which can be compensated for by increasing the gain in the output helix.

---

<sup>2</sup>R. W. DeGrasse and G. Wade, "Microwave Mixing and Frequency Dividing," Proc IRE; July 1957.

## 1.4 APPENDIX I – THEORETICAL STUDIES – TWO-FREQUENCY MODULATOR

Some theoretical considerations were investigated to determine the simplest modulation scheme consistent with the requirements of the serrodyne re-entrant amplifier. As pointed out by Cumming<sup>1</sup> the sawtooth waveform is the optimum transit-time modulation useable to suppress all undesired sidebands. For transit-time modulation with no incidental AM, the sideband level referenced to the output with no serrodyne is given by:

$$M_n(0, r) = \frac{1}{2\pi} \int_{-\pi}^{\pi} e^{-j[rS(\Phi) + n\Phi]} d\Phi \quad (1)$$

where  $S(\Phi)$  is the waveform applied, and  $M_n$  is the relative level of the  $n^{\text{th}}$  sideband.

For the sawtooth waveform:

$$S(\Phi) = -\Phi/\pi \quad (2)$$

and

$$M_n(0, r) = \frac{1}{2\pi} \int_{-\pi}^{\pi} e^{j[r - n\pi]\Phi/\pi} d\Phi = \frac{\sin(r - n\pi)}{r - n\pi} \quad (3)$$

For the ideal case, the desired sideband  $M_1(0, r)$  is unity and  $M_n(0, r)$  is zero for all other values of  $n$ . This represents an optimum translation with infinite rejection to all the undesired frequencies.

At rf frequencies an ideal sawtooth waveform would be difficult to generate. Also, for re-entrant-serrodyne operation, suppression of only the original ( $n = 0$ ) and the output frequency ( $n = 2$ ) is important.

<sup>1</sup>Cumming, Raymond C., "The Serrodyne Frequency Translator," Proceedings of the IRE, pp. 175-186; February 1957.

Consider a waveform consisting of the first three Fourier components of an ideal sawtooth waveform. For this case  $S(\Phi)$  becomes:

$$S(\Phi) = \frac{2}{\pi} \left[ -\sin \Phi + \frac{1}{2} \sin 2\Phi - \frac{1}{3} \sin 3\Phi \right] \quad (4)$$

Substituting this into Eq. (1), for  $r = \pi$  as in the ideal sawtooth, yielded suppression of the original signal ( $n = 0$ ) and of the second sideband ( $n = 2$ ) by a factor of 5, or only about 7 db.

Since only two frequencies must be suppressed, it appears that this could be accomplished by using the fundamental modulation frequency and the second harmonic, adjusting their amplitudes arbitrarily to produce nulls for  $M_0(0, r)$  and  $M_2(0, r)$ . Thus, the two important sidebands may be infinitely suppressed and the translated output frequency is given by  $M_1(0, r)$ ; however, all other components would remain finite. Since only two restrictions are imposed to accomplish this condition, adjusting the amplitudes alone should suffice. The phases will be allowed to remain the same as in the ideal sawtooth waveform. Thus,

$$M_n(0, r, a) = \frac{1}{2\pi} \int_{-\pi}^{\pi} e^{j \left[ \frac{2r}{\pi} (\sin \Phi - a \sin 2\Phi) - n\Phi \right]} d\Phi \quad (5)$$

is the expression for the various sideband amplitudes with respect to the unmodulated output obtained. To satisfy the conditions required for re-entrant amplifier operation, one must further impose the restrictions that

$$M_0(0, r, a) = 0 \quad (6)$$

and

$$M_2(0, r, a) = 0 \quad (7)$$

Evidently, for both  $M_0(0, r, a)$  and  $M_2(0, r, a)$  to pass through zero, the parameter  $a$  must be adjusted to some optimum value. While the existence of this optimum value is not necessarily proven, it seems reasonable that a curve, for which the conditions in Eq. (6) are satisfied, can be plotted giving the parameter  $r$  as a function of  $a$ . Likewise, the condition in Eq. (7) can be plotted. If these curves cross, the intersection represents a point at which both conditions are satisfied.



As a first step, only the fundamental and its second harmonic can be considered. There exists an optimum amplitude at which the fundamental and second harmonic frequencies will completely suppress the undesired sidebands of the output frequency.

Equation (5) shows that the amplitude of the  $n^{\text{th}}$  sideband referenced to the unmodulated output is given by

$$M_n(o, r, a) = \frac{1}{2\pi} \int_{-\pi}^{\pi} e^{j \left[ \frac{2r}{\pi} (\sin \Phi - a \sin 2\Phi) - n\Phi \right]} d\Phi \quad (8)$$

where it is understood that the real part is to be taken. Rewriting and taking the real part, Eq. (8) becomes

$$M_n(o, r, a) = \frac{1}{2\pi} \int_{-\pi}^{\pi} \cos \left[ \frac{2r}{\pi} (\sin \Phi - a \sin 2\Phi) - n\Phi \right] d\Phi \quad (9)$$

Modifying Eq. (9) to simplify interpretation of results, yields

$$M_n(O, R, A) = \frac{1}{2\pi} \int_{-\pi}^{\pi} \cos [R \sin \omega t + A \sin 2\omega t - n\omega t] d\omega t \quad (10)$$

For calculating the sideband levels by computer, the integral in Eq. (10) is replaced by a summation over finite increments. Rewriting Eq. (10) as a summation provides the following expressions for the undesired sidebands:

$$M_0(O, R, A) = \frac{1}{60} \sum_{n=1}^{60} \cos \left[ R \sin \frac{n\pi}{30} + A \sin \frac{n\pi}{15} \right] \quad (11)$$

and

$$M_2(O, R, A) = \frac{1}{60} \sum_{n=1}^{60} \cos \left[ R \sin \frac{n\pi}{30} + A \sin \frac{n\pi}{15} - \frac{n\pi}{15} \right] \quad (12)$$

The desired frequency is given by

$$M_1(O, R, A) = \frac{1}{60} \sum_{n=1}^{60} \cos \left[ R \sin \frac{n\pi}{30} + A \sin \frac{n\pi}{15} - \frac{n\pi}{30} \right] \quad (13)$$

For either A or R equal to zero, the expression in Eq. (10) becomes Bessel's equation.

$M_0$ ,  $M_1$ , and  $M_2$  of equations 11, 12, and 13 were calculated with the computer. The results were plotted to determine the zeros of  $M_0$  and  $M_2$  and the maximum values of  $M_1$ .

The curves plotted in Fig. I-1 are the zeros of  $M_0$  and  $M_2$  as a function of A and R, and the maximum values of  $M_1$  as a function of A and R. Fig. I-1 shows that simultaneous zeros of  $M_0$  and  $M_2$  occur near the point  $R = 5.4$  and  $A = 0.45$ . An enlarged plot of this crossover point is presented in Fig. I-2 in which it may be seen that a maximum value of  $M_1$  does not occur at the crossover of the zeros of  $M_0$  and  $M_2$ . It was anticipated that the addition of a third modulation frequency would permit a maximum of  $M_1$  to coincide with simultaneous zeros of  $M_0$  and  $M_2$ .

It may be seen that the value of  $M_1$ , at the point giving simultaneous zeros of  $M_0$  and  $M_2$ , is approximately 0.339. Converting to decibels points out the fact that the conversion gain of the tube is degraded by 9.4 db under the modulation process. This indicated the importance of considering three-frequency modulation to increase the value of  $M_1$ .

The amplitude of the  $n^{\text{th}}$  sideband with respect to the unmodulated output is given by Eq. (5). For three-frequency modulation this equation becomes

$$M_n(o, r, a, b) = \frac{1}{2\pi} \int_{-\pi}^{\pi} e^{j \left[ \frac{2r}{\pi} (\sin \Phi - a \sin 2\Phi + b \sin 3\Phi - n\Phi) \right]} d\Phi \quad (14)$$

where the real part is to be taken. Equation (14) may be written to explicitly form the real part as

$$M_n(o, r, a, b) = \frac{1}{2\pi} \int_{-\pi}^{\pi} \cos \left[ \frac{2r}{\pi} (\sin \Phi - a \sin 2\Phi + b \sin 3\Phi - n\Phi) \right] d\Phi \quad (15)$$

To calculate the sideband levels by computer, a summation over finite increments is formed to perform the integration. Equation (15) for the undesired sidebands becomes

$$M_0(O, R, A, B) = \frac{1}{60} \sum_{n=1}^{60} \cos \left[ R \sin \frac{n\pi}{30} + A \sin \frac{n\pi}{15} + B \sin \frac{n\pi}{10} \right] \quad (16a)$$

and

$$M_2(O, R, A, B) = \frac{1}{60} \sum_{n=1}^{60} \cos \left[ R \sin \frac{n\pi}{30} + A \sin \frac{n\pi}{15} + B \sin \frac{n\pi}{10} - \frac{n\pi}{15} \right] \quad (16b)$$

The desired sideband is given by

$$M_1(O, R, A, B) = \frac{1}{60} \sum_{n=1}^{60} \cos \left[ R \sin \frac{n\pi}{30} + A \sin \frac{n\pi}{15} + B \sin \frac{n\pi}{10} - \frac{n\pi}{30} \right] \quad (16c)$$

Equations 16a, b, and c were programmed for the computer and  $M_0$ ,  $M_1$  and  $M_2$  were calculated. Seven points of interest were found where the desired sideband is large, and it appears that the carrier and undesired sideband simultaneously go through a zero or minimum. These points were expanded to find the approximate amplitude of the fundamental modulation frequency and the second and third harmonic.

Results of the three-frequency modulation analysis are plotted in Figs. I-3 through I-7. The curves present the zeros of  $M_0$  (amplitude of carrier) and  $M_2$  (amplitude of second sideband) as a function of R and A, with B a parameter, and the values of A giving maximum values of  $M_1$  (amplitude of first sideband) for each value of R are plotted with B as a parameter. R is the amplitude of the fundamental modulation frequency and A and B are the second and third harmonic amplitudes, respectively.

It may be seen that a maximum value of  $M_1$  does not occur at the crossover of the zeros of  $M_0$  and  $M_2$  for any of the curves shown. Points may be chosen where the crossover nearly occurs, and an expansion of the data may be performed. Seven points of interest are found which could yield a solution of  $M_0 = 0$  and  $M_2 = 0$  with a maximum value of  $M_1$ .

From the data presented in Figs. I-3 through I-7 the following five points are of particular interest:

	<u>R (Fundamental Amplitude)</u>	<u>A (Second Harmonic Amplitude)</u>	<u>B (Third Harmonic Amplitude)</u>	<u>M<sub>1</sub> (max)</u>
(1)	1.75	-1.85	-1.00	0.15
(2)	2.00	0.75	2.00	0.10
(3)	2.80	-2.10	-2.00	0.28
(4)	5.30	2.00	1.50	0.14 to 0.38
(5)	5.60	-0.50	0.50	0.33 to 0.35

In addition, two points may be found from the plots of M<sub>1</sub> versus R, A, and B. Figs. I-8 and I-9 yield solutions for R near zero:

	<u>R</u>	<u>A</u>	<u>B</u>	<u>M<sub>1</sub></u>
(6)	0.10	2.00	2.00	0.55
(7)	0.25	2.20	-2.00	0.50

The latter two points are of most interest since the values of M<sub>1</sub> are larger than any of the ones given above.

All seven of the points above were expanded to determine the crossing point of the zeros of M<sub>0</sub> and M<sub>2</sub>, and the maximum of M<sub>1</sub>. Expansion of the latter two points, (6) and (7), showed that simultaneous zeros of M<sub>0</sub> and M<sub>2</sub> do not occur in this region. For the first of the two, the carrier and sideband suppression is 20 db and 24 db, respectively, with a conversion loss of 12 db. This occurs when the respective modulation frequency amplitudes are R = 0.30, A = 1.8, and B = 2.2. For the second point, complete carrier suppression is obtained, but the second sideband is only 8 to 12 db below the unmodulated carrier level.

The greatest suppression, 12.2 db, is obtained near R = 0.05, A = 2.2, and B = -2.2.

Since the values of M<sub>1</sub> are smaller than those of the other points, the first two points (1) and (2) were not probed in detail. Expansion of point (3) indicates complete suppression of M<sub>2</sub> is obtained and M<sub>0</sub> is partially suppressed. Maximum rejection of M<sub>0</sub> and M<sub>2</sub> is obtained at the point R = 5.53, A = 2.2, and

$B = 1.4$ . The conversion loss at this point is 12.4 db, indicating that unless the conversion gain is upgraded, this is not a practical operating point. The fourth point of interest was expanded and a simultaneous maximum of  $M_1$  occurs at the crossover point of  $M_0 = 0$  and  $M_2 = 0$ . The value of  $M_1$  is approximately 0.260 which represents a conversion loss of 11.6 db.

Expansion of the fifth point indicates that it is the most practical operating point. Other points have shown larger values of  $M_1$ , but less suppression of either the carrier or second sideband. This is the analogous point shown in the expansion of the two-frequency modulation analysis. Comparing the values of  $M_1$  with the results of the two-frequency case shows that the desired sideband is enhanced by approximately 4.0 db with the addition of the third modulation frequency.

The exact intersection of the  $M_0 = 0$ ,  $M_2 = 0$ , and maximum  $M_1$  curves occurs for more than one value of  $B$  which indicates that the maximum of  $M_1$  fluctuates through the simultaneous zeros of  $M_0$  and  $M_2$ . The largest value of  $M_1$  is 0.53 which represents a conversion loss of 5.4 db. The respective values of  $R$ ,  $A$ , and  $B$  at this point are  $R = 5.73$ ,  $A = 1.0$ , and  $B = 0.76$ . Clearly, this is the most practical operating point.

The values given above show that the respective phase of the second harmonic is 180 degrees out of phase with the fundamental and third harmonic modulation frequencies. This was anticipated from the first three terms of the Fourier series representation of the sawtooth waveform which is given by:

$$f(\omega t) = A \left[ \cos \omega t - \frac{1}{2} \cos 2\omega t + \frac{1}{3} \cos 3\omega t + \dots \right]$$

In comparison, the amplitudes of the respective frequencies are unlike those given by the equation above.

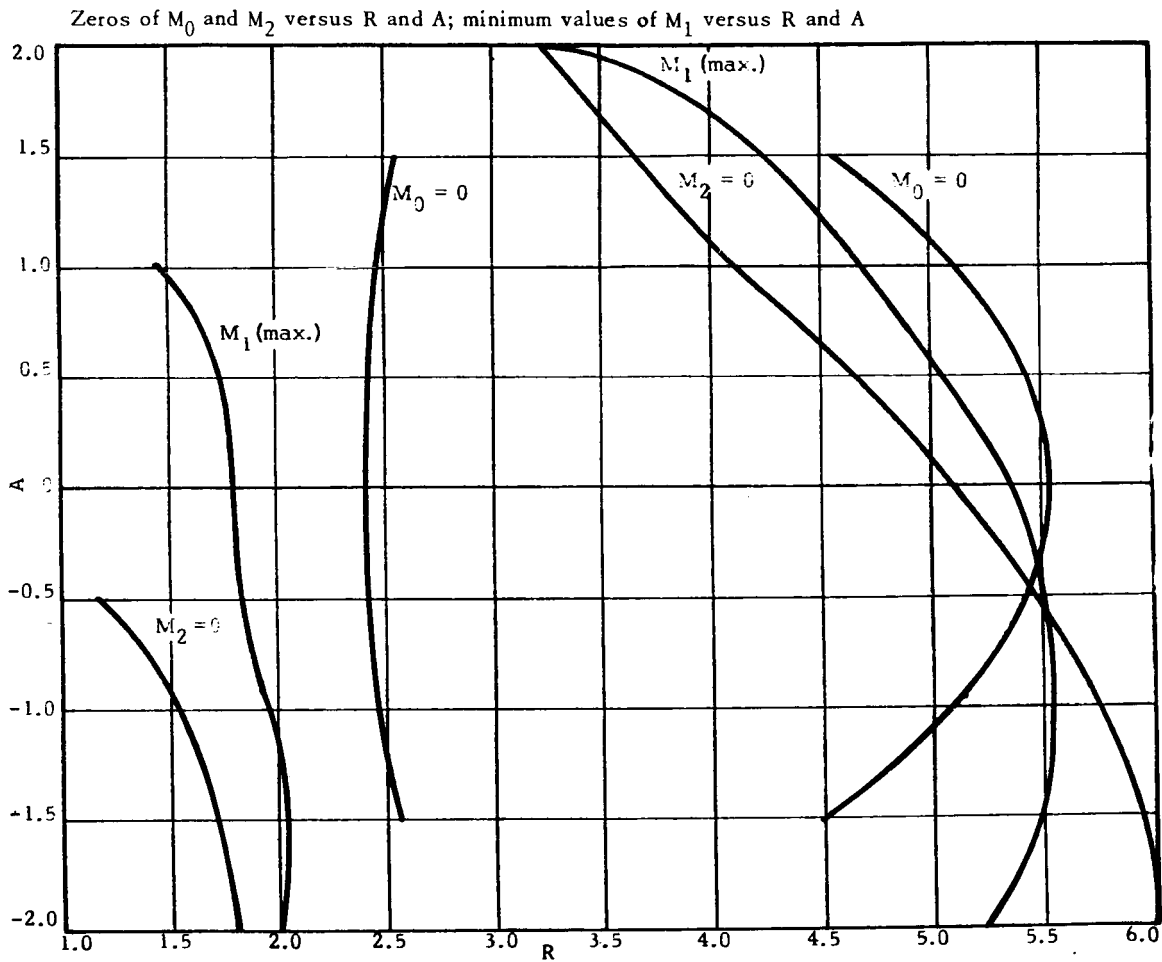


Figure 1-1—Zeros of  $M_0$  and  $M_2$  as a function of R with A as a parameter, and the value of A leading to a maximum value for  $M_1$  at each value of R.

Zeros of  $M_0$  and  $M_2$  and maximum values of  $M_1$  versus R and A

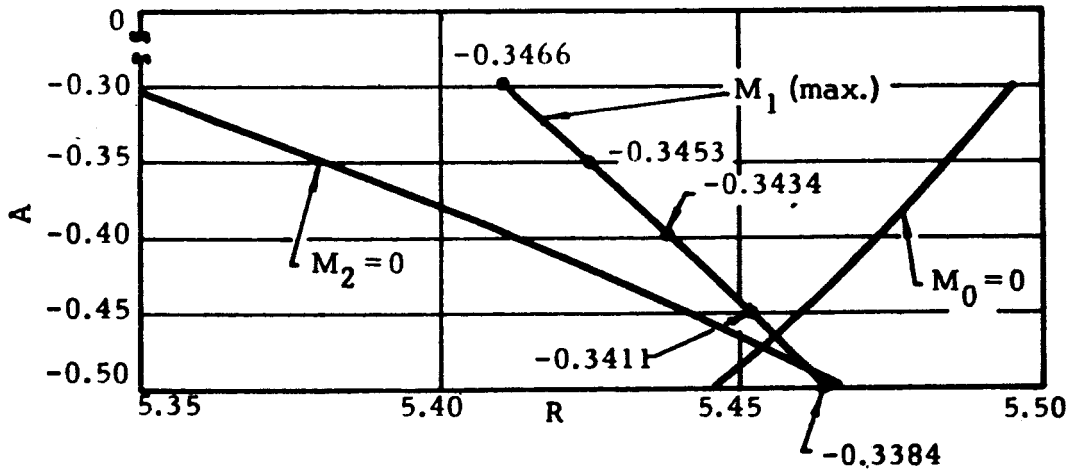


Figure 1-2—Expanded plot of  $M_0$ ,  $M_2$  and the maximum values of  $M_1$ .

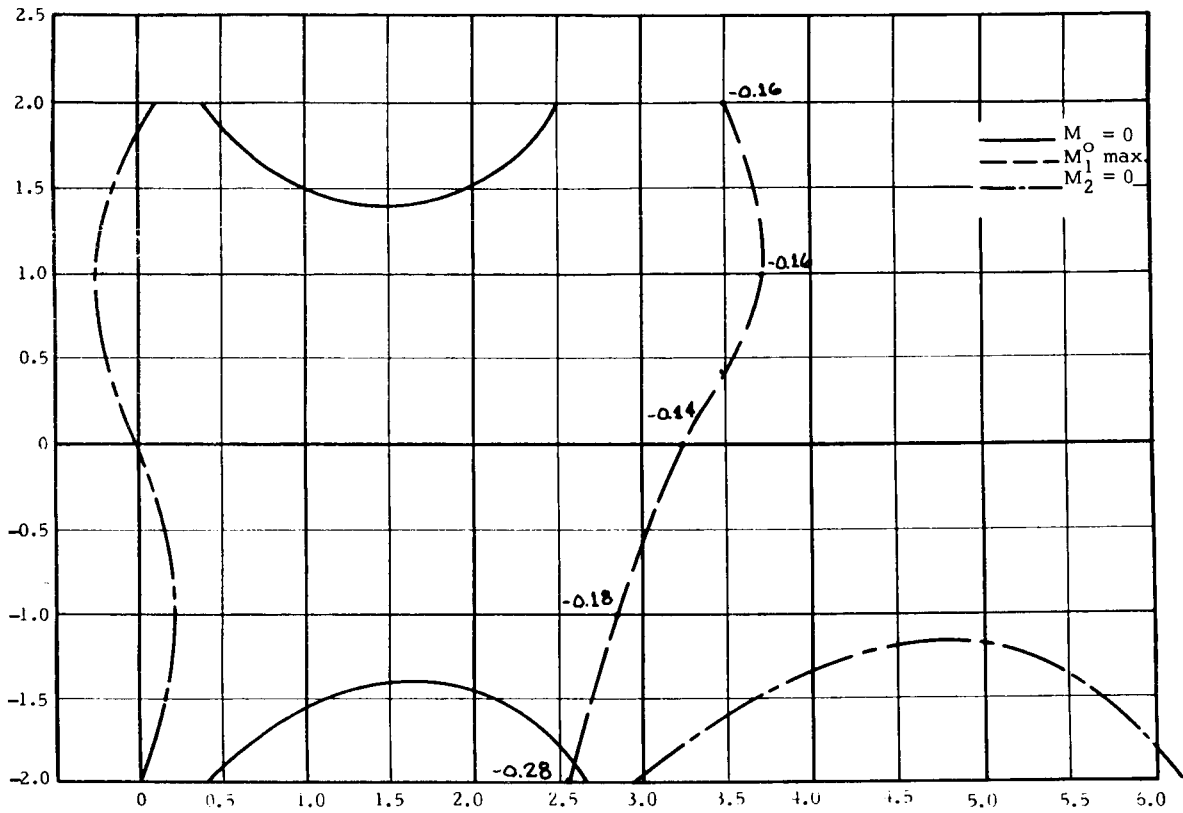


Figure I-3—Zeros of  $M_0$  and  $M_2$  as a function of  $R$  and  $A$  with  $B = -2$ , and the maximum value of  $M_1$  for each value of  $R$  and  $A$ .



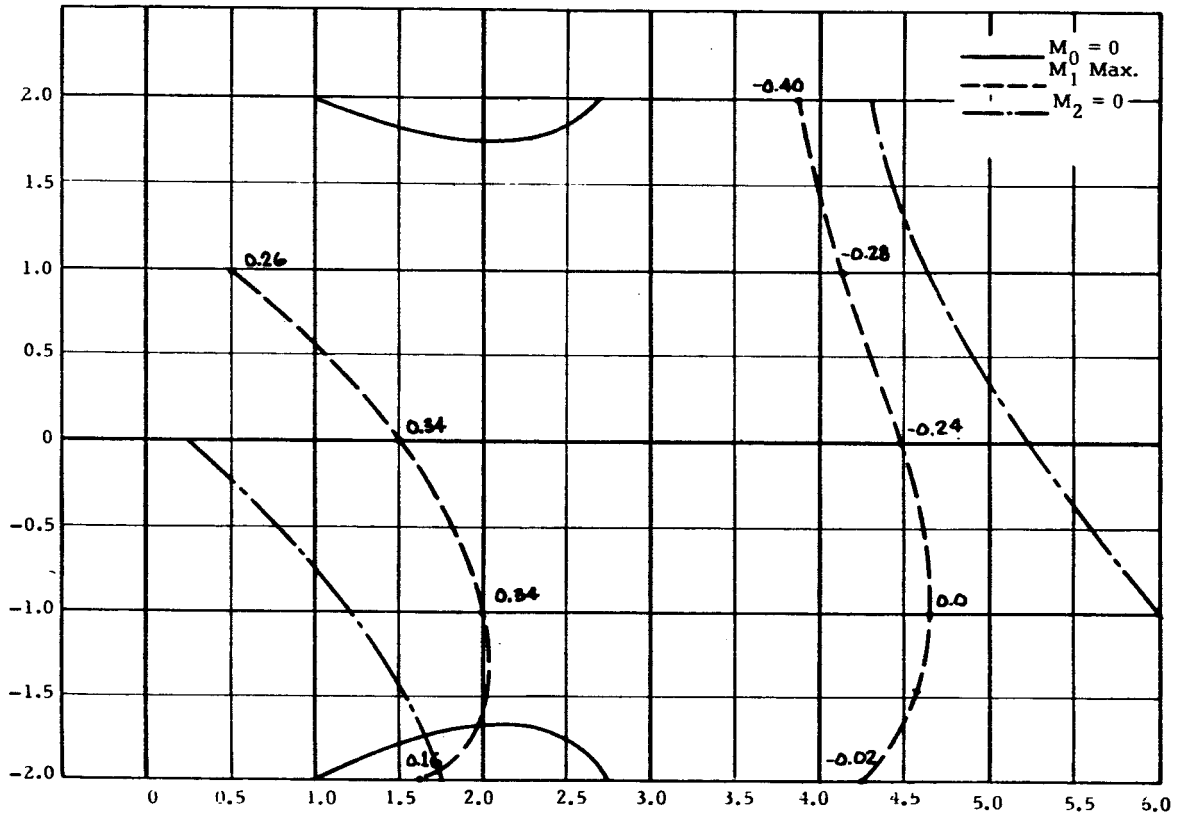


Figure I-4—Zeros of  $M_0$  and  $M_2$  as a function of  $R$  and  $A$  with  $B = -1$  and the maximum value of  $M_1$  for each value of  $R$  and  $A$ .

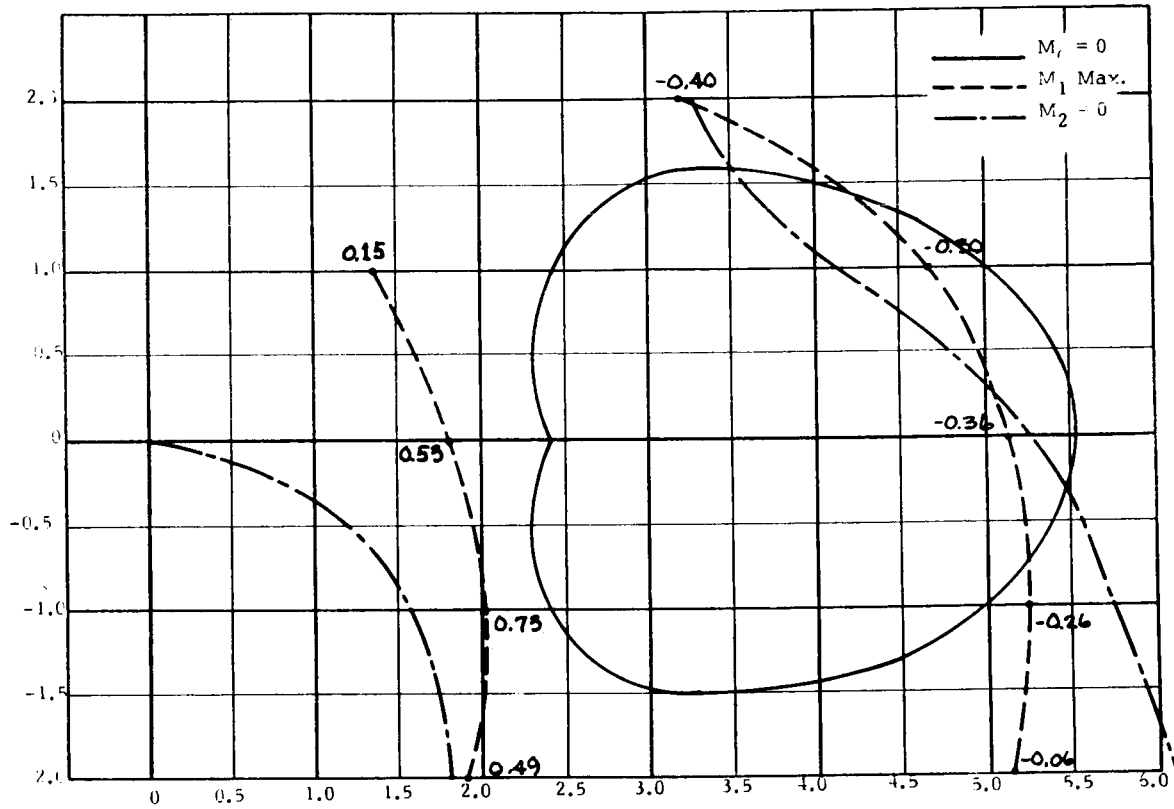


Figure 1-5—Zeros of  $M_0$  and  $M_2$  as a function of  $R$  and  $A$  with  $B = 0$  and the maximum value of  $M_1$  for each value of  $R$  and  $A$ .

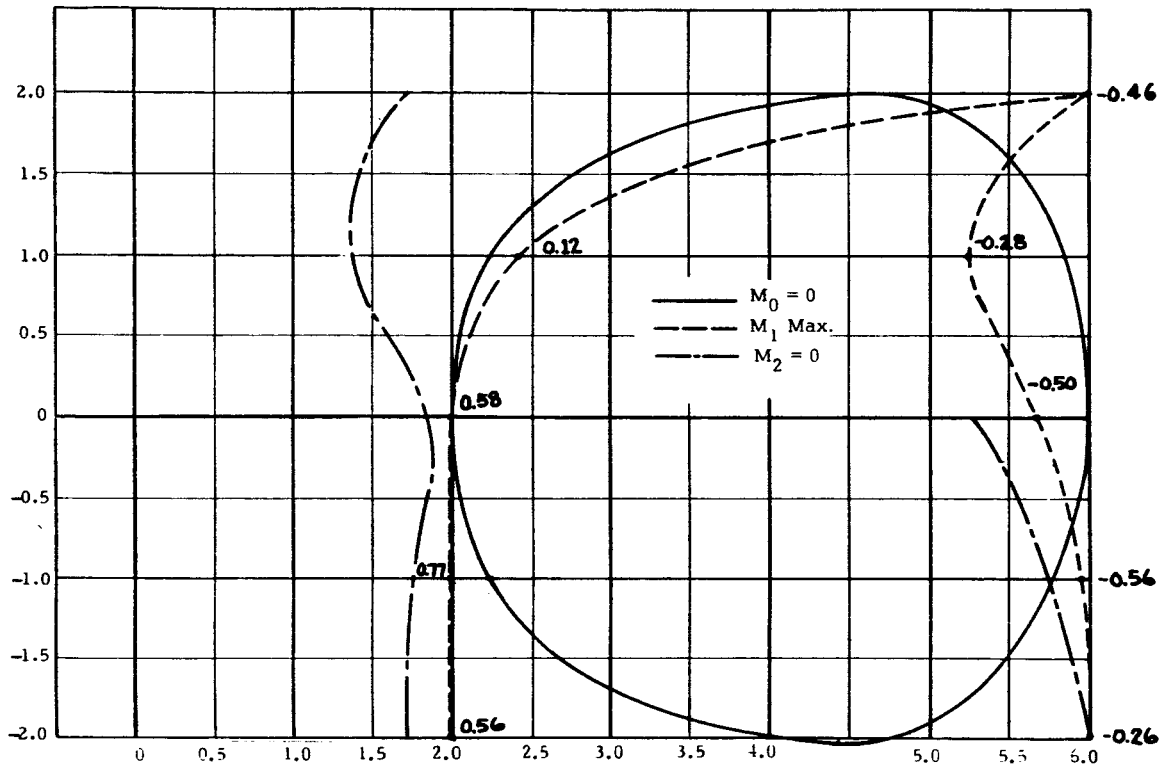


Figure 1-6—Zeros of  $M_0$  and  $M_2$  as a function of  $R$  and  $A$  with  $B = 1$  and the maximum value of  $M_1$  for each value of  $R$  and  $A$ .

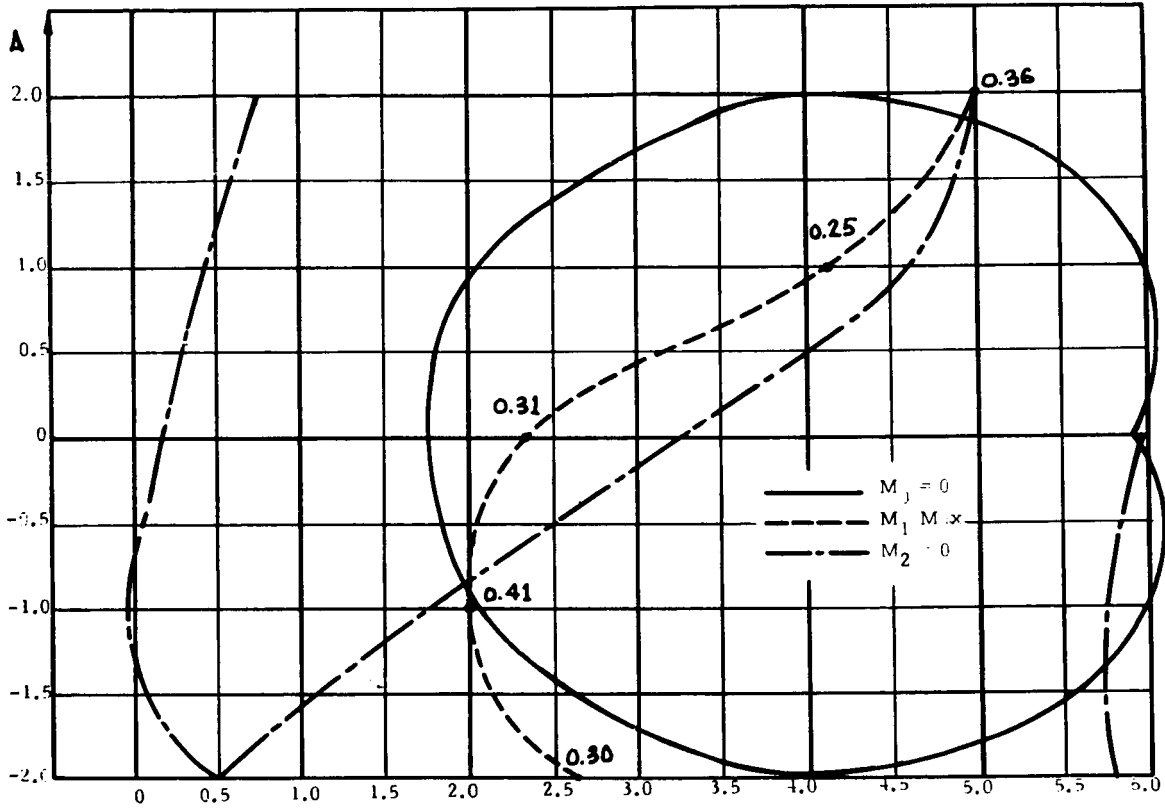


Figure 1-7-Zeros of  $M_0$  and  $M_2$  as a function of  $R$  and  $A$  with  $B = 2$  and the maximum value of  $M_1$  for each value of  $R$  and  $A$ .

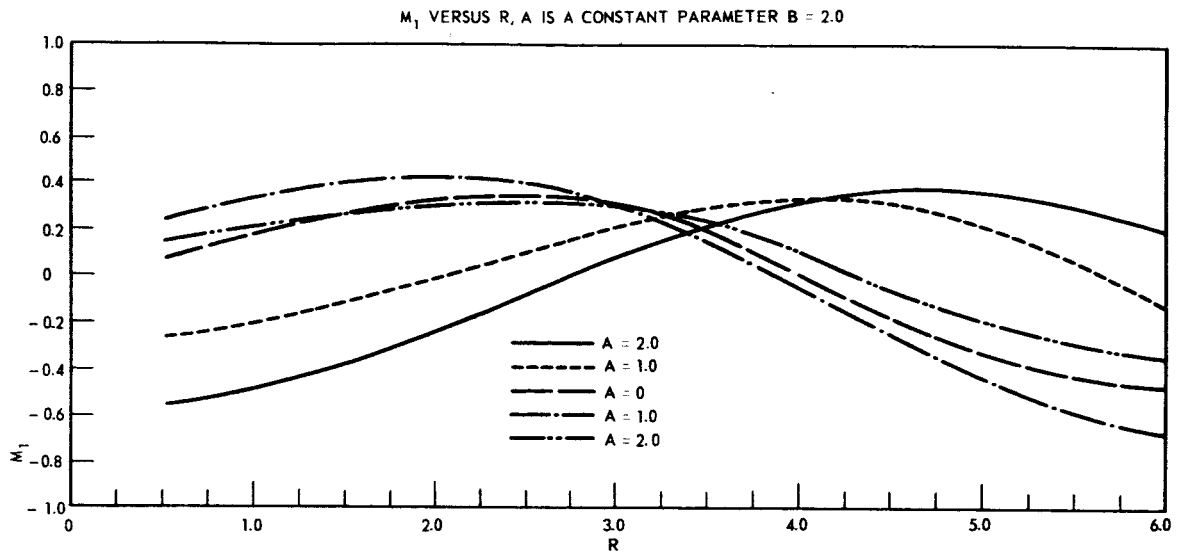


Figure I-8—Computed values of  $M_1$  for values of R and A with B = 2.0.

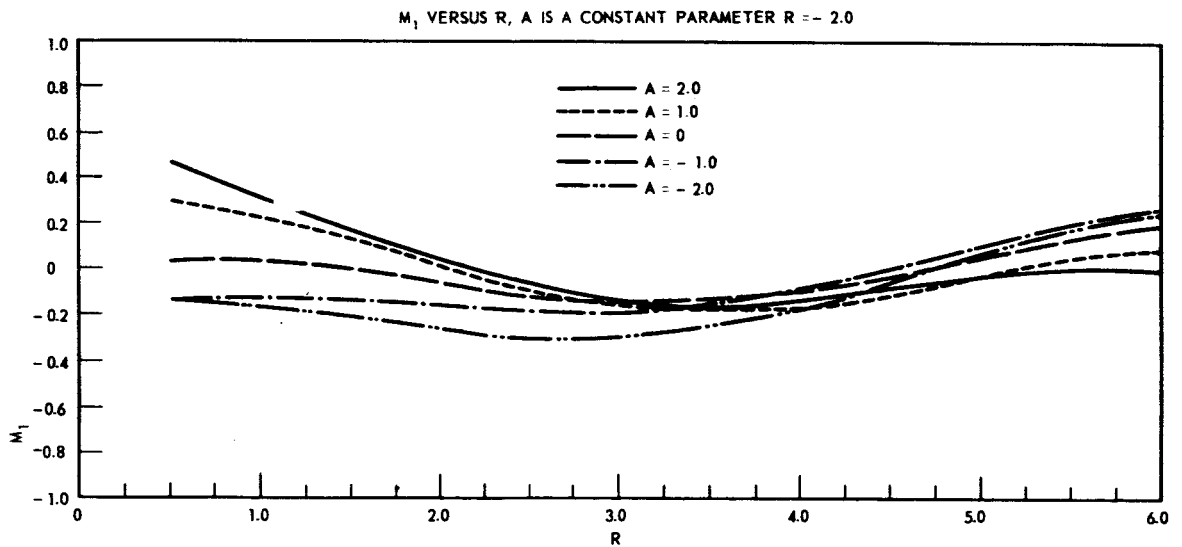


Figure I-9—Computed values of  $M_1$  for values of R and A with B = -2.0

## 1.5 APPENDIX II-TRAVELING-WAVE TUBE AMPLIFIER TEST METHODS

The tests performed on the TWT were described above. The test setups are described in this appendix. Setups shown are those used for measuring VSWR, saturated power output, small signal gain and phase characteristics of the TWT.

The setup for measuring VSWR versus frequency is shown in Figure II-1. Reflectometer output is fed to the Y-axis of the record and the X-axis is fed with the sweeper voltage output.

Saturated power output is measured using the setup shown in Figure II-2. The TWT is saturated at each frequency and the output power recorded. This is a point-by-point measurement.

Figure II-3 shows the setup used for measuring small-signal gain. The system is calibrated using the sweeper output. Both attenuators are set at zero, and this is the uppermost calibration line on the small-signal-gain versus frequency plots. Successive calibrated lines are plotted by setting either attenuator, normally in 5-db steps. The sweeper output is then fed to the TWT and the input attenuator is set at 30 db. Thus, the uppermost calibration curve represents 30-db gain.

To measure the TWT phase characteristics, a phase bridge is used. The setup is shown in Figure II-4. Phase variation with voltage was referenced to the synchronous voltage of the TWT, this being the voltage of maximum small-signal gain. The helix voltage was varied on the plus and minus side of synchronism, and the phase change was measured by balancing the phase bridge. Phase-versus- $P_{in}$  characteristics were determined similarly; in this instance the input power was varied. The tube was operated at synchronous voltage for the latter measurement.

Noise figure was measured by two methods; using an automatic noise-figure meter and the Y-factor method. The two setups are shown in Figures II-5 and II-6. When using the automatic-noise-figure meter method, the signal generator is set at the desired frequency where the noise figure is to be measured. The noise figure is then read on the meter.

The Y-factor method requires calculation of the noise figure. This is determined from

$$\text{N.F.} = 10 \log \left( \frac{T_2}{T_0} - 1 \right) - 10 \log (Y - 1)$$

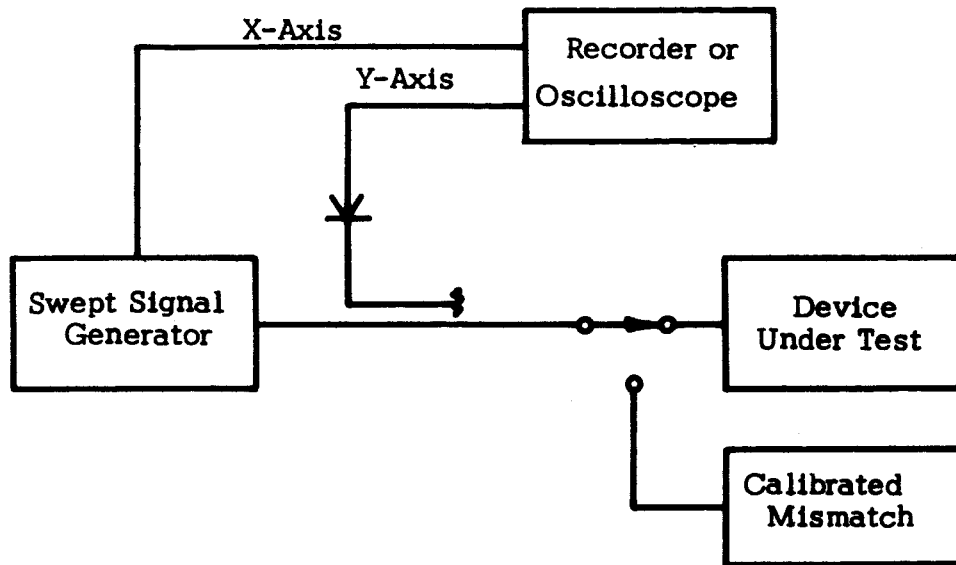


Figure II-1-VSWR test setup.

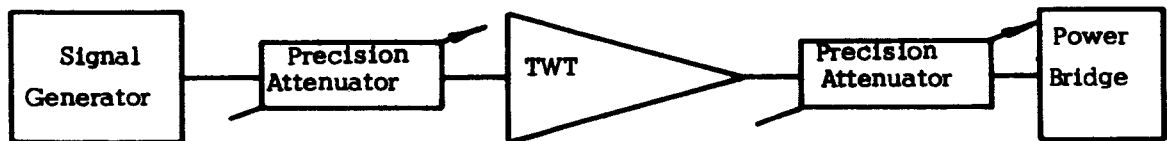


Figure II-2-Saturated power output test setup.

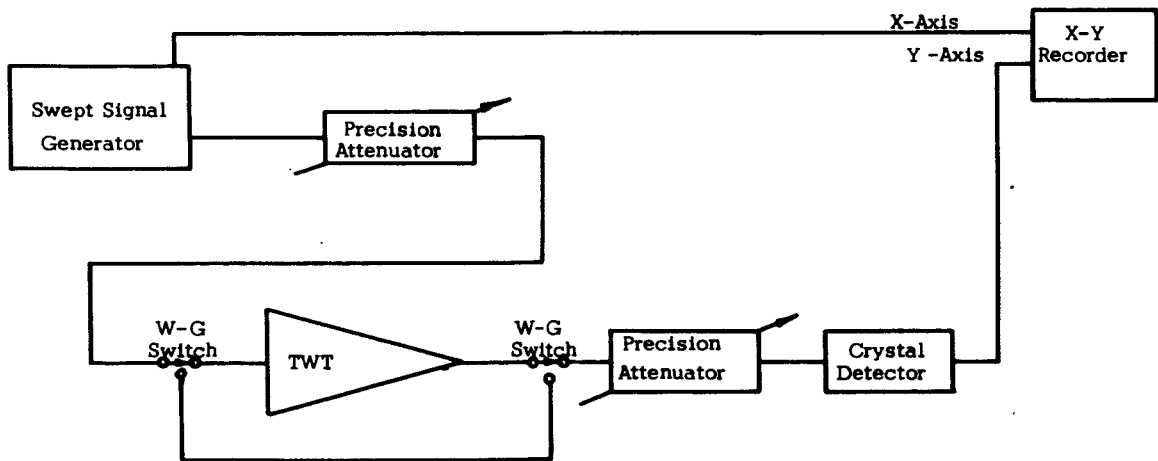


Figure II-3-Test setup for measuring small-signal gain.

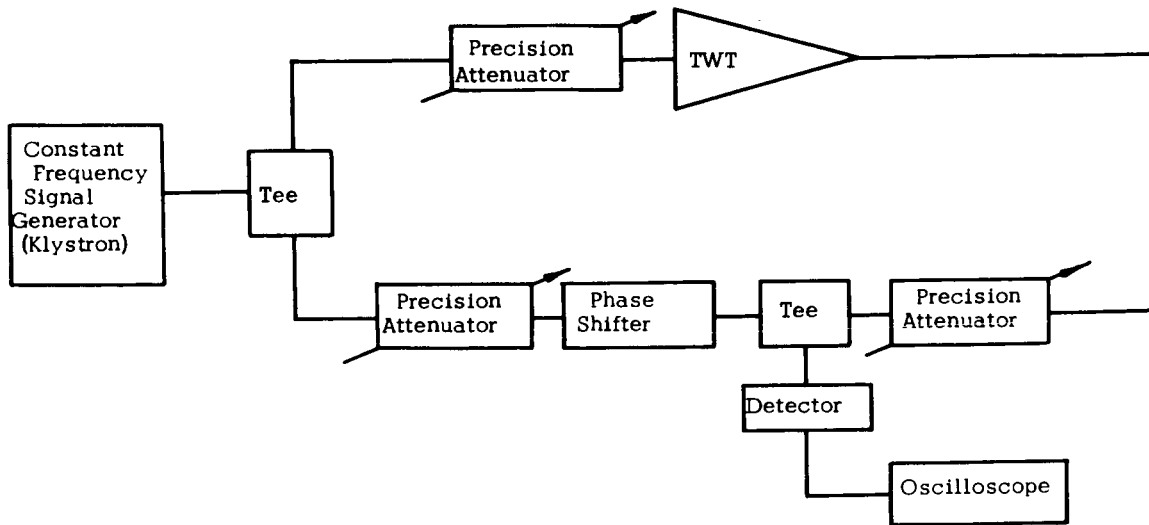


Figure II-4—Setup for measuring TWT phase characteristics.

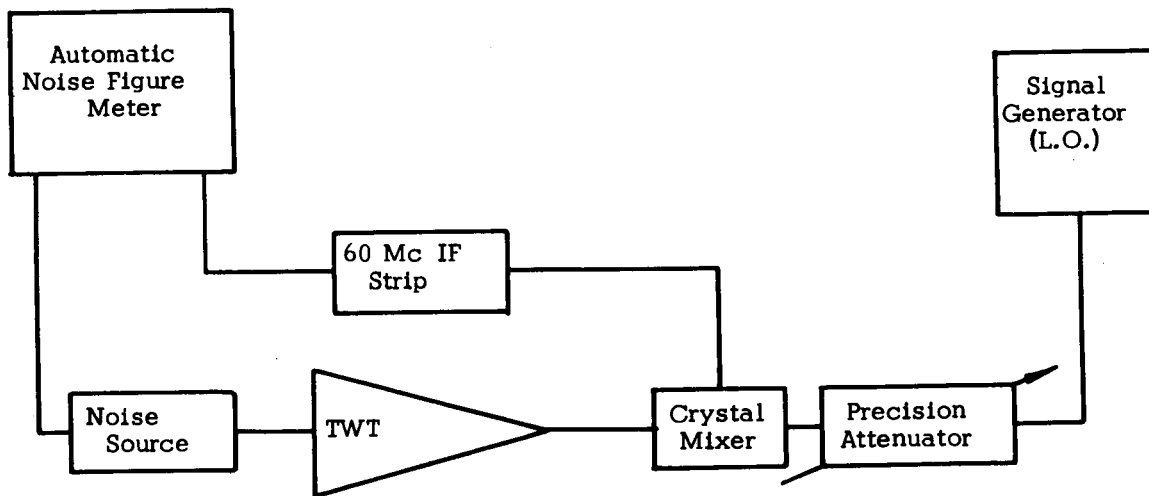


Figure II-5—Setup for measuring noise figure (automatic).



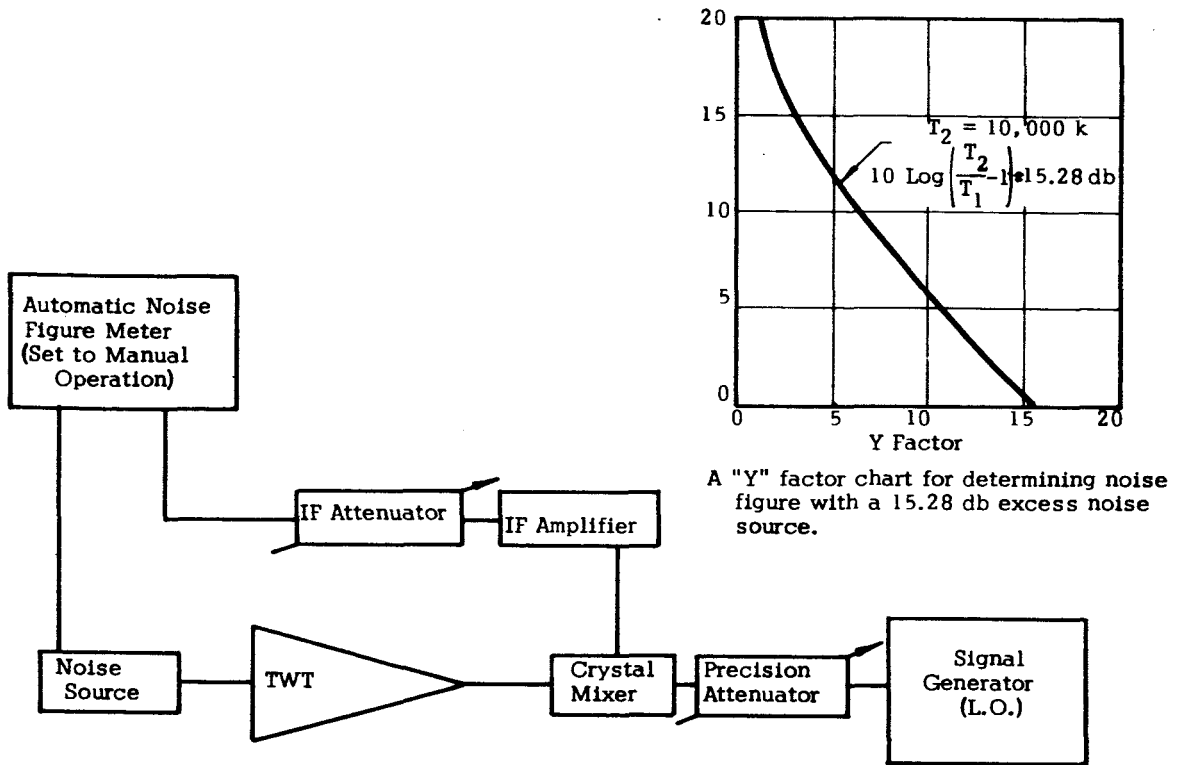


Figure II-6—Noise figure measurement setup ("Y factor" method).

For the noise source used,  $10 \log (T_2/T_0 - 1)$  equals 15.2 db. To determine Y, the IF attenuator setting is taken with the noise source on and off. This is then entered in the accompanying chart and the noise figure may be determined.

The FM-to-AM distortion was measured from the small-signal-gain characteristics. By determining the gain change for frequency change, the FM-to-AM distortion may be calculated at any frequency, this being the slope of the small-signal-gain characteristics.

The experimental setup shown in Figure II-7 was used to evaluate both conversion gain and sideband suppression. The spectrum analyzer is calibrated without the TWT. The sidebands are then all measured with reference to the carrier level out of the TWT when no modulation voltage is applied. Factors which introduce errors are the frequency response of the spectrum analyzer and the filter losses.

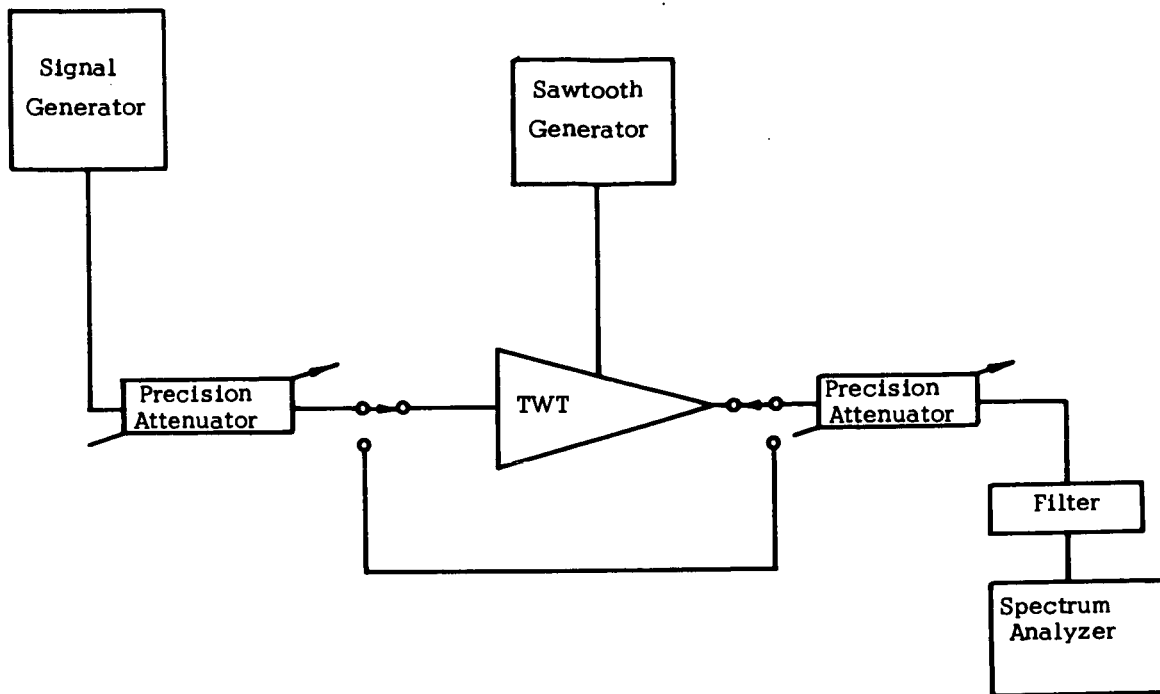


Figure II-7-Gain and suppression test setup.

## 1.6 APPENDIX III-RE-ENTRANT AMPLIFIER TEST METHODS

Re-entrant-amplifier gain was measured with the setup shown in Figure III-1. The system is calibrated at the output frequency, in this case being 6000 Mc/sec. With the input frequency at 5940 Mc, the filters and TWT are connected and system gain is measured. The filter and cable losses must be considered when calculating actual gain.

Echo-effect measurements were performed using the test setup shown in Figure III-2. The delay line was included between the TWT and  $f_1$  filter to stretch out the echo to give sufficient persistence after the termination of the input pulse for determining its amplitude. Delay-line and filter losses must be considered in calculating echo amplitude.

A block diagram of the setup used for FM to AM distortion is shown in Figure III-3. Due to the narrow bandwidth of the filters, the frequency deviation was limited to 25 Mc. The small deviation prevented generation of AM within the signal generator. By calibrating the spectrum analyzer and using it instead of a detector, all sidebands could be seen at once and the amplitude deviation from the center frequency could be determined immediately. Factors which introduce errors are the frequency response of the spectrum analyzer, and filter bandwidth.

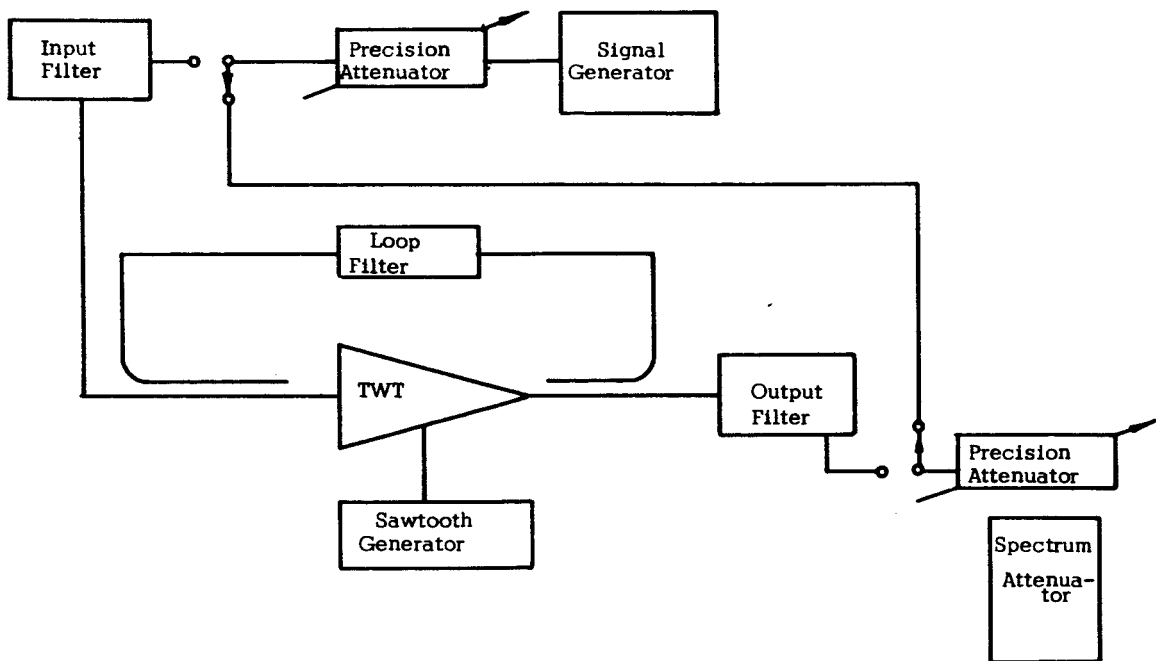


Figure III-1-Re-entrant amplifier gain measurement setup.

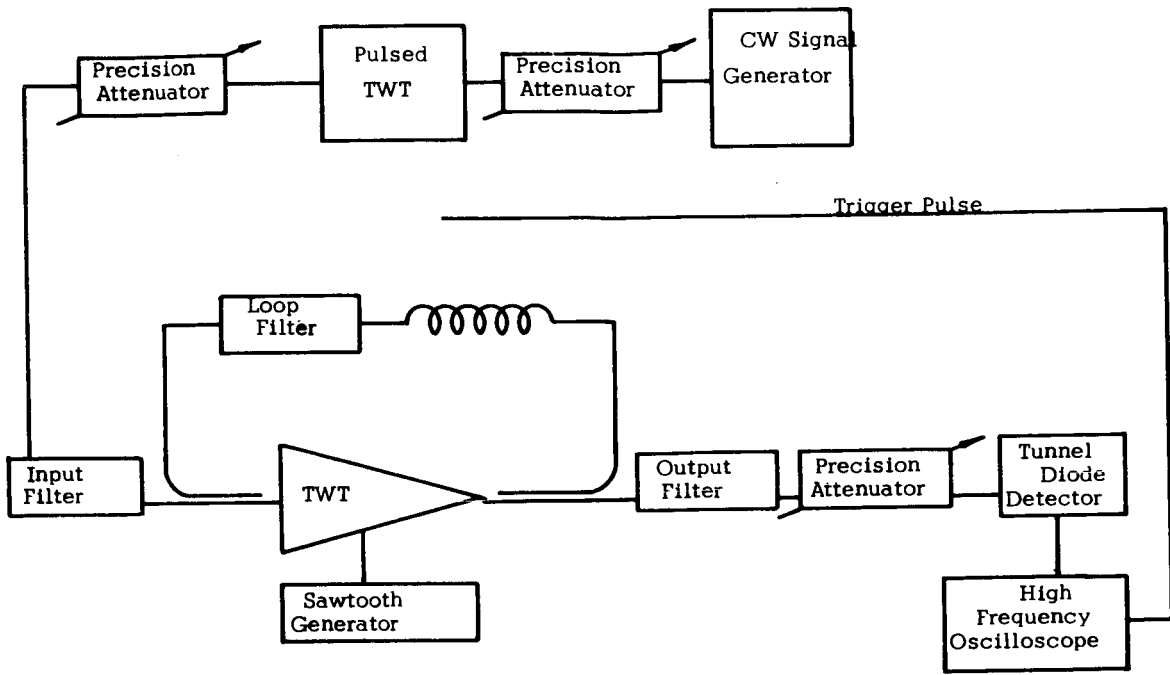


Figure III-2—Setup for measuring echo effects.

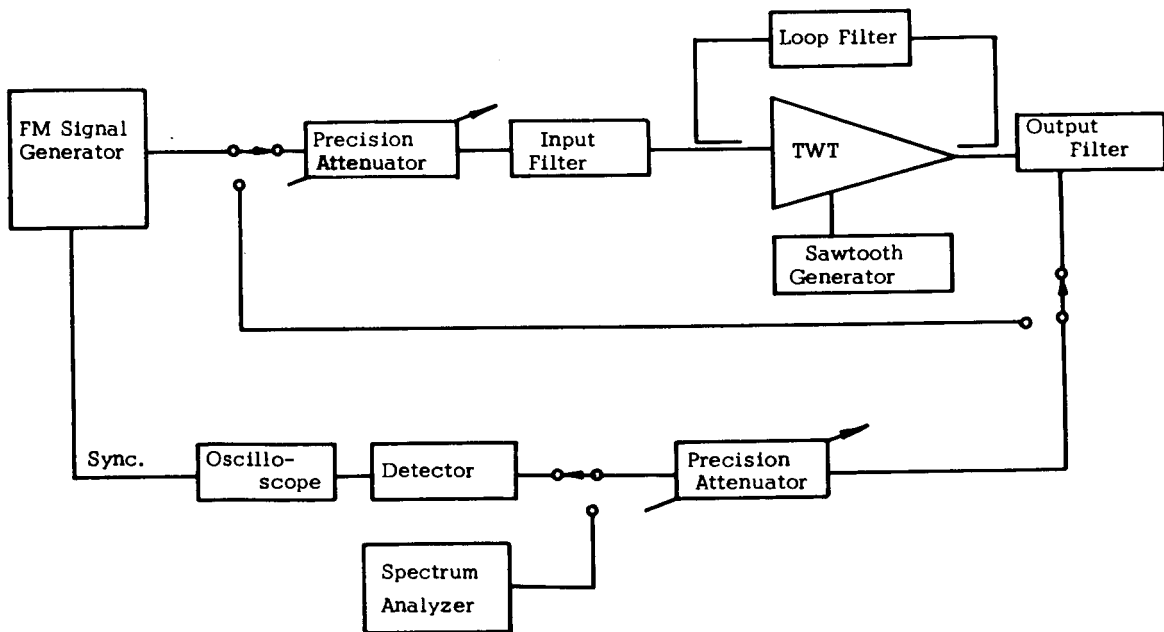


Figure III-3—FM to AM distortion measurement block diagram.

AM to PM distortion was not measured since no test procedure could be conceived for this measurement. The difficulty in this case is that the input and output frequencies are at different frequencies.

Noise-figure measurements were made using an automatic noise-figure meter. The test setup is shown in Figure III-4. The noise figure was also measured by the "Y" factor method described in Appendix I.

The test setup shown in Figure III-5 was used for evaluating intermodulation distortion. The two signal-generator frequencies had to be within 25 Mc because the filter bandpass is only 29 Mc. Resulting sideband levels were measured on the spectrum analyzer.

Re-entrant-amplifier gain and intermodulation-distortion tests were performed over a range of power input levels to determine the amplifier dynamic range.

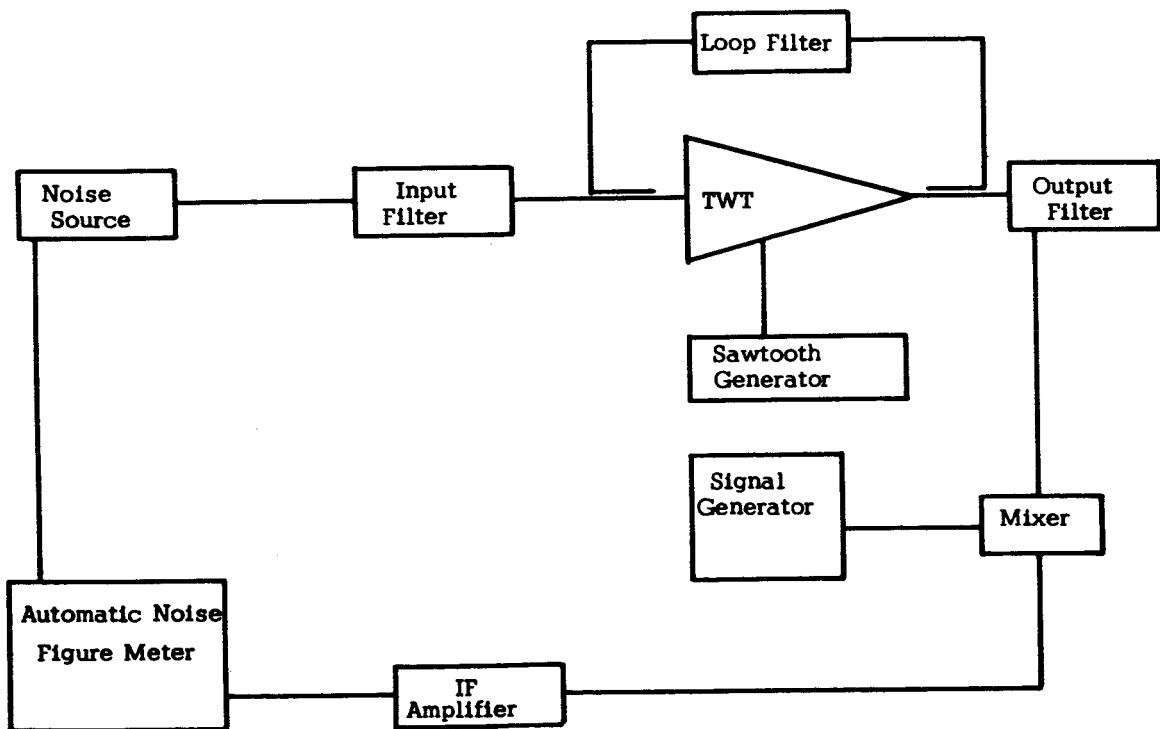


Figure III-4—Test setup to measure noise figure.

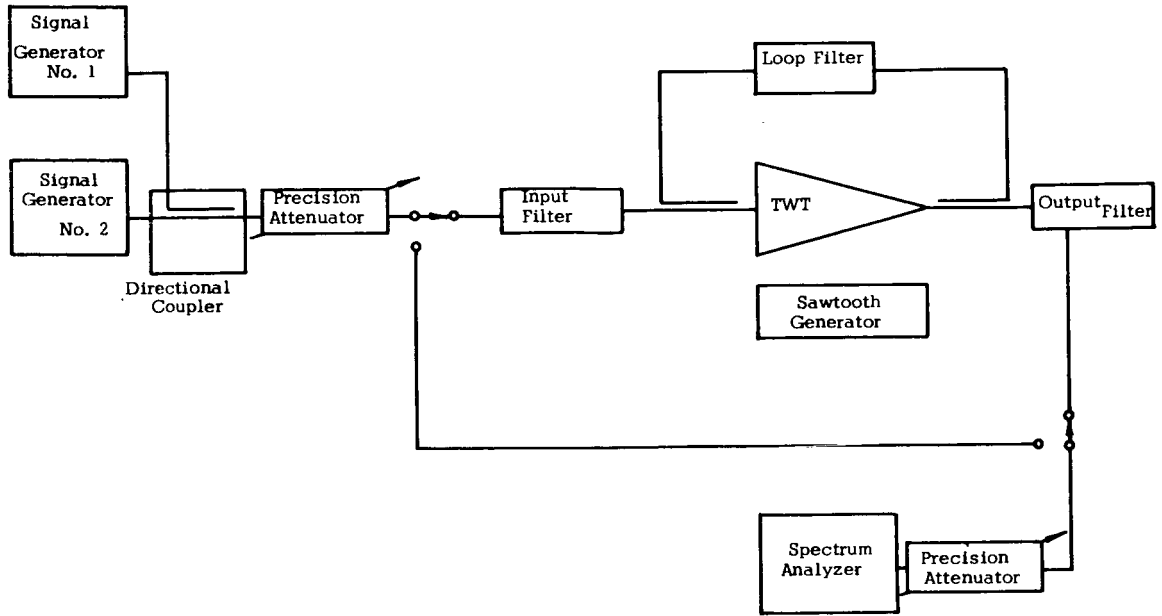


Figure III-5—Intermodulation distortion test setup.

SECTION 2  
GSFC COMMENTS

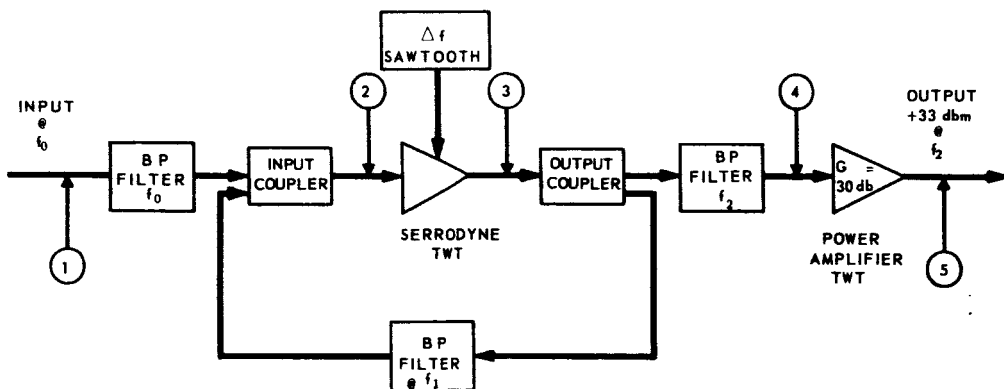
2.1 NOTES ON TEXT OF MEC REPORT

The following comments on the MEC final report by the sponsoring personnel at Goddard Space Flight Center are intended to further clarify and underscore certain aspects of the study. In the opinion of the GSFC reviewing personnel, these notes will lead to a more precise understanding of the serrodyne re-entrant amplifier system.

G1 (Abstract) – The MEC report was not consistent in its description of the 'harmonics' of the 30 Mc sinusoid used in the serrodyne modulator. To prevent possible confusion, the text was changed, where necessary, to conform to the following standard nomenclature;

FUNDAMENTAL      → 30 Mc  
SECOND HARMONIC → 60 Mc  
THIRD HARMONIC    → 90 Mc

G2 (page 8) – The system defined by NASA and mentioned in this sentence does not define a 1 milliwatt desired sideband output, as implied in the text. The system defined by NASA is shown below.



The input is at frequency  $f_0$ . After the first pass through the serrodyne TWT, the desired sideband at frequency  $f_1$  is re-entered through the input coupler, thus the desired sideband is at  $f_2$  for the second pass through the serrodyne TWT.

For a +33dbm  $f_2$  output level (point ⑤), the required level of  $f_2$  at point ④ is +3dbm, hence the required level at the output of the serrodyne TWT (point ③) will be +3dbm plus the losses of the output coupler and bandpass filter at  $f_2$ . Therefore a 2 milliwatt output at the desired sideband is the minimum that could be utilized, and, assuming a coupler and filter loss of 3db, a 4 milliwatt output would be a more practical design level for the serrodyne TWT.

G3 (page 18) -  $M_n$  is the relative level of the  $n^{\text{th}}$  sideband referenced to the output level with no serrodyne modulation present. The desired component, the first upper sideband, is therefore designated as  $M_1$ .

G4 (page 24) - For the three frequency modulation measurements discussed in this section the desired output component is the first lower sideband ( $f_{-1}$ ).

G5 (page 26) - The interfering sideband under discussion in this paragraph was generated by the first pass of the carrier (5970 Mc) through the serrodyne TWT. This frequency, at 5940 Mc was of sufficient level to pass through the loop filter and become shifted upward by the second pass through the TWT to 5970 Mc and appears at the output.

## 2.2 SUMMARY OF RESULTS OF MEC STUDY PROGRAM

Figure 2.2.1 summarizes the experimental results of the 3 serrodyne techniques and the mixer tube. Figure 2.2.2 outlines the performance characteristics of the serrodyne tube delivered to NASA. Figure 2.2.3 shows the serrodyne characteristics of the delivered tube for the operating characteristics listed in Figure 2.2.2.

The results of the MEC study have shown that, in general, gun-modulation of the TWT produces the best sideband suppression, but the presence of high (25% peak-to-peak) AM limits the maximum frequency shift attainable. The introduction of three frequencies to a drift tube and a split helix has minimized the AM present, but sideband suppression was not as great as that afforded by the gun modulation approach.



Method of Serrodyne Modulation	Frequency Shift In Mc	Maximum Measured Sideband Suppression		Translation Loss	
		Of Carrier	Of Second Sideband	Theoretical	Measured
Fundamental (30 Mc) and Second Harmonic (60 Mc) Impressed on TWT Gun	30	26db	26db	9.4 db	12 <sup>(2)</sup>
Fundamental (30 Mc), Second <sup>(1)</sup> (60 Mc), and Third (90 Mc) Harmonic Impressed on TWT Gun	30	42	36	5.4	12 <sup>(2)</sup>
30 Mc Impressed on Drift Tube, <sup>(1)</sup> 60 Mc Impressed on Input Helix 90 Mc Impressed on Output Helix	30	18	20	5.4	12
TWT Mixer	2,000	ND	ND	30db Gain	10db Gain

(1) Modulation Voltages in Ratio of 7:1:1

ND - Not Determined

(2) 25% P to P Incidental AM Present

Figure 2.2.1-Summary of Serrodyne Techniques

Frequency of Operation	6000	Mc
Saturated Power Output	26.5	dbm
Small Signal Gain (No Serrodyne Mod.)	32.5	db
Noise Figure	33	db
<b>Operating Conditions</b>	<b><u>Voltage</u></b>	<b><u>Current</u></b>
Heater	6.4 v	.235 A
Grid	-6.8 v	0
Anode	655 v	0
Cathode	-1214 v	9.9 mA
Helix (Ground)	0 v	4 mA
Collector	0 v	5.9 mA

Figure 2.2.2--Performance Characteristics of Delivered Serrodyne Traveling Wave Tube

Limitations imposed by sawtooth generation and modulation impression for all of the transit time techniques investigated were found to prevent the frequency shifts necessary for satellite communications transponders, even with the employment of a re-entrant loop.

The preliminary investigation of the mixer TWT, although not in the original scope of the study, has shown that this technique may offer the required frequency shift and suppression characteristics necessary for the communications transponder. Further study, however, will be required to further define the characteristics of the TWT mixer and optimize the conversion efficiency.

### 2.3 REVIEW OF THE RE-ENTRANT SERRODYNE TWT COMMUNICATIONS SATELLITE TRANSPONDER

This section presents a discussion of the communications satellite transponder and indicates some of the considerations of the system for which the MEC study program was initiated.

The primary function of an active communications satellite involves the reception, amplification and re-transmission of information-bearing radio frequency signals between two or more ground terminals. The signal received at the satellite must be translated to a different carrier frequency before satellite re-transmission to prevent interaction between the input and output signals. The satellite equipment for performing these functions is termed a transponder or a repeater.

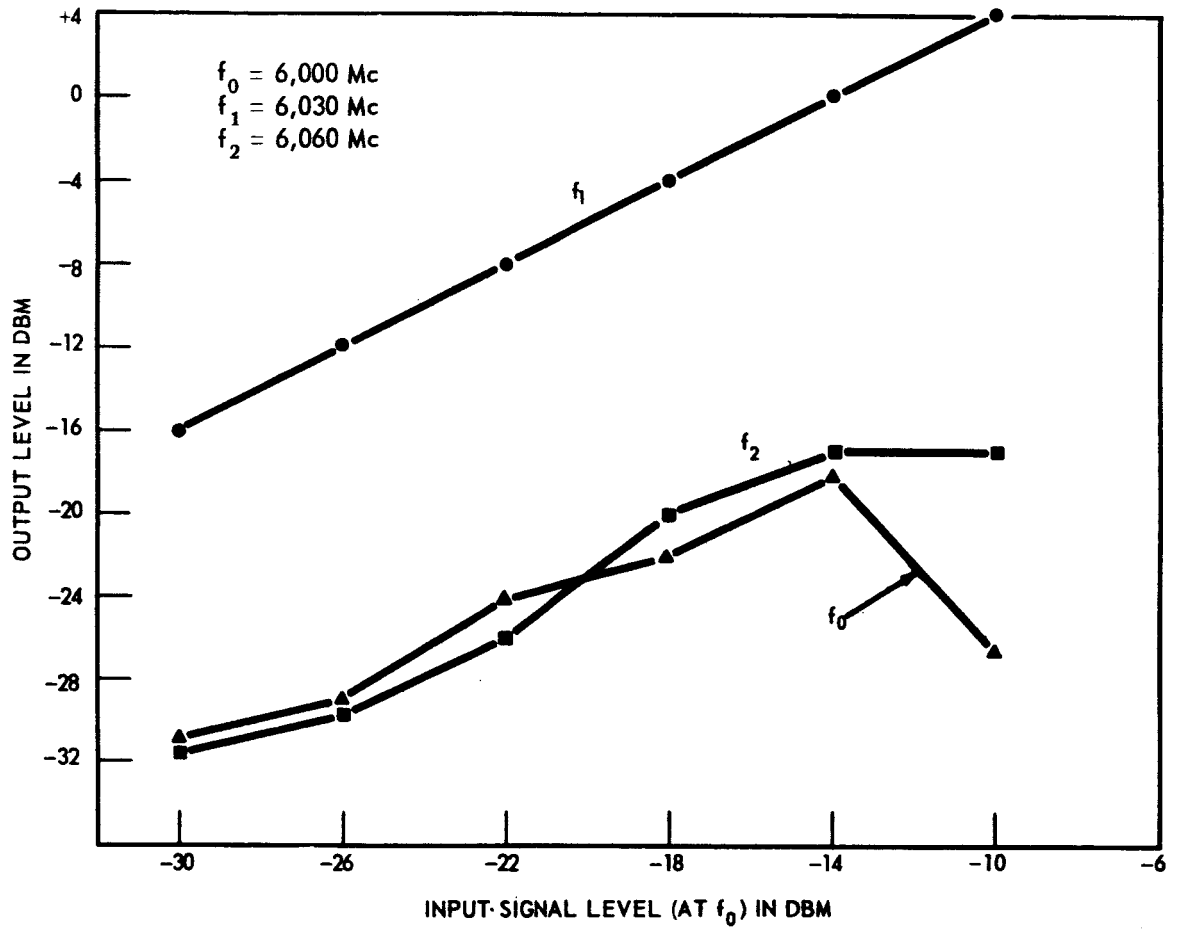


Figure 2.2.3—Serrodyne Output versus input characteristics for delivered TWT serrodyne system.

Conventional techniques for obtaining frequency conversion and amplification require the received signal at the satellite to be reduced to an intermediate frequency for amplification and then translated to a new radio carrier frequency for further amplification and retransmission. Figure 2.3.1 shows a typical frequency translation satellite transponder system.

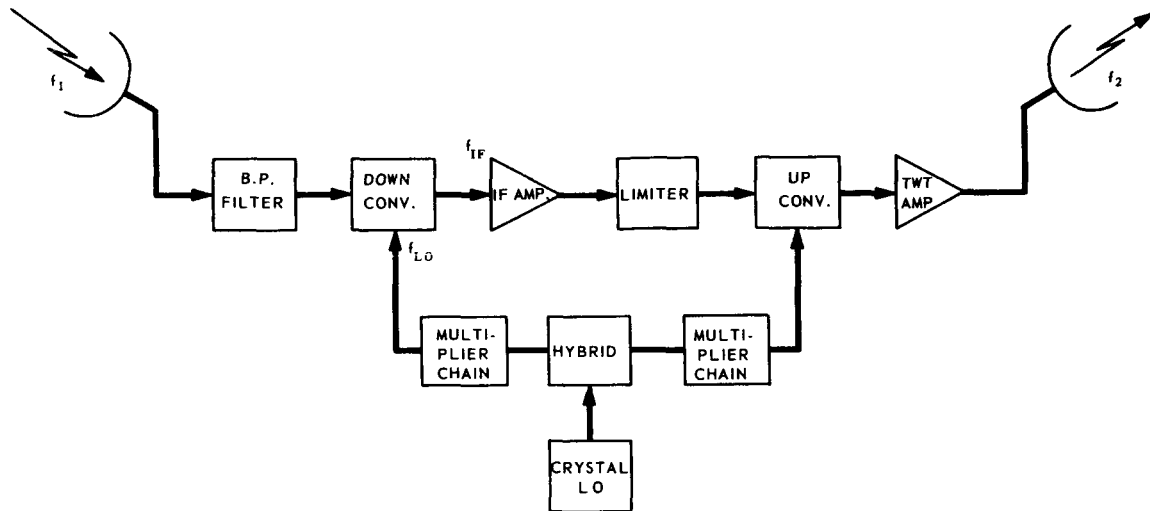


Figure 2.3.1—Frequency translation satellite transponder.

The received signal at  $f_1$  is down converted to  $f_{IF}$  and most of the amplification occurs at this frequency. After limiting, the signal is up converted to and is amplified in the traveling wave tube to obtain the necessary transmission power.

A modulation conversion transponder utilizes similar frequency translation techniques but in addition employs a modulation conversion scheme to convert the uplink modulation to a different form for downlink transmission. The modulation conversion is accomplished in the IF portion of the transponder.

Present communications satellite transponder frequency conversions range from 6-7 KMC for the received signal to below 100 Mc for the IF back to 2-4 KMC for transmission. The received signals for communication transponders are at the -120 dbw level, converted and re-transmitted at the +3 dbw (2-25 watt) level.

Investigations have shown that traveling wave tubes (TWT's) can be employed to convert directly from one radio frequency to another with sufficient amplification that IF conversion, amplification, detection and re-modulation are not required. This simplifies satellite transponders considerably, netting many advantages.

The most promising method for accomplishing the conversion and amplification objectives appears to be the use of TWT's in a re-entrant mode. In this mode of operation, a signal is applied to the TWT, amplified; shifted in frequency; and re-fed at the new frequency back into the same tube for further amplification. In the serrodyne re-entrant amplifier, the serrodyne characteristics of the TWT are utilized to obtain the frequency displacement and amplification. This system is diagrammed in Figure 2.3.2.

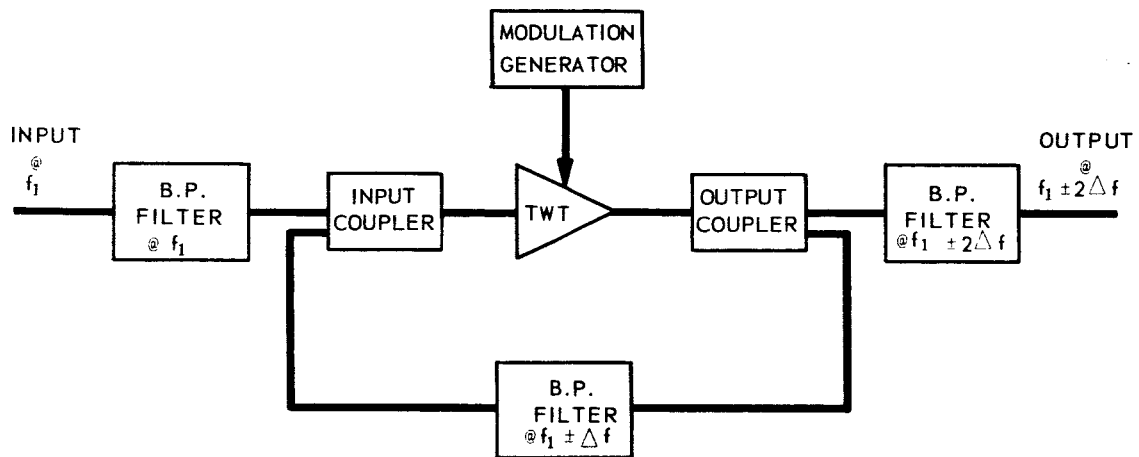


Figure 2.3.2—Serrodyne re-entrant TWT amplifier.

The frequency shift in the TWT is accomplished by a transit time modulation effect. The transit time delay of a TWT is a near linear function of the voltage impressed on the helix of the TWT. If the helix D.C. voltage is modulated with a signal, the TWT, effectively, phase modulates the carrier of RF signal. When the modulating signal is a sine wave the resultant RF signal has many sidebands, both positive and negative. When the amplitude of the modulation is adjusted for a phase deviation of  $2.4$  radians the carrier disappears and all of the energy is in the sidebands. This technique is called synchronizing.

If the modulating signal is a linear sawtooth adjusted to deviate the phase  $2\pi$  radians, all the sideband and the carrier are suppressed with the exception of one of the 1st sidebands. The slope of the sawtooth determines which sideband (+ or -) remains. This is serrodyne and is effectively termed single sideband, suppressed carrier. The deviation of the sideband is equal to the fundamental of the modulating sawtooth signal. If the amplitude of the modulating sawtooth were increased so as to increase the phase deviation to  $4\pi$  radians, the deviation of the sideband would be equal to twice the fundamental of the modulating sawtooth. In general terms, if the modulation deviates the phase by  $2N\pi$  radians, then the sideband is displaced by  $N$  times the fundamental frequency of the modulation.

The degree of suppression of the carrier and unwanted sidebands is affected by the flyback time of the sawtooth, the linearity of the sawtooth as well as certain of the helix characteristics.

The MEC study program was initiated to determine; the optimum methods of modulation impression to the TWT structure; the upper limit of linear serrodyne for a TWT; and the necessary modulation generation circuitry for the serrodyne amplifier.

#### 2.4 REFERENCES

The following is a list of additional sources of information on the traveling-wave tube serrodyne amplifier and re-entrant transponder systems.

1. Cumming, Raymond C., The Serrodyne Frequency Translator, Proc. of the IRE, February 1957, p. 175-186.
2. Traveling Wave Tube Re-Entrant Amplifier Serrodyne System, W. K. Allen, L. J. Ippolito, D. A. Nace, NASA Technical Note D-2149, June 1964.
3. Traveling Wave Tube Simplifies Microwave Relay, NASA Technical Brief G5-10127, May 1965.
4. System Study of a Direct R. F. to R. F. Re-Entrant Traveling Wave Tube Communications Satellite Transponder, L. J. Ippolito, NASA/GSFC X-625-65-48, March 1965.
5. Evaluation of Commercial Traveling Wave Tubes for Applications in Direct R. F. to R. F. Transponders, I. C. Prillaman, NASA/GSFC X-625-65-46, March 1965.
6. Study of an R. F. to R. F. Satellite Transponder, W. H. Allen, L. J. Ippolito, I. C. Prillaman, NASA/GSFC X-625-65-41, February 1965.